UNIVERSITA' DEGLI STUDI DI NAPOLI "FEDERICO II"

DOTTORATO DI RICERCA
IN
"SCIENZA DEL FARMACO"
XXIII CICLO 2007-2010

Bioactive Marine Natural Products: Isolation, Structure Elucidation and Synthesis

Dott.ssa Cristina Perinu

Tutor	Coordinatore
Prof. A. Mangoni	Prof.ssa M. V. D'Auria

TABLE OF CONTENTS

ABSTRACT

Marine sponges are a rich source of bioactive compounds which play an important role as protection against predators, overgrowing space competitors, invading microorganisms, and others. Over the past three decades, several biologically active secondary metabolites have been isolated from marine sponges and used to design and develop new therapeutic agents. The work described in this thesis addresses this research topic: the aim is to identify new chemical structures from marine organisms to be used as leads or scaffolds for the elaboration of new drugs.

In particular, this PhD thesis consists of two main research activities:

- ✓ Isolation and structural determination of new bioactive metabolites from marine sponges (*Tedania ignis*, *Pseudaxinella flava* and *Plakortis simplex*);
- ✓ Synthesis of an analogue of simplexide, a glycolipid with an important immunoregulatory role.

The results obtained from the chemical and pharmacological characterization of the new bioactive metabolites from marine sponges are here summarized:

1. *Tedania ignis:* three new metabolites having interesting pharmacological activity were isolated. One of them is tedanol, a new brominated and sulfated pimarane diterpene. The structure was elucidated by mass spectroscopy and extensive NMR studies (including spectral simulation), and its absolute configuration was determined using the Mosher method. Tedanol showed a potent anti-inflammatory activity evaluated *in vivo* in a mouse model of inflammation. The anti-inflammatory activity was coupled with a strong inhibition of COX-2 expression, inhibition of cellular infiltration measured as

mieloperoxidase (MPO) levels, and inhibition of iNOS expression. These features make tedanol a promising template for the development of new anti-inflammatory molecules with low gastrointestinal toxicity. Further interesting metabolites extracted from *Tedania ignis* are tedarene A and tedarene B, two new cyclic diarylheptanoids, diaryl ether and diphenyl types respectively. The structure elucidation of the two compounds required Dynamic NMR experiments, molecular modelling studies and quantum mechanical calculations. Each compound exists as a mixture of two conformers in slow equilibrium. Moreover, tedarene A is biologically active: *in vitro* it showed an interesting inhibition of NO_2^- production in LPS stimulated cells.

2. *Pseudoaxinella flava:* one new diterpene isonitrile and three known analogues were isolated from this sponge. Their chemical structures are closely related but differ in the number and position of the isonitrile functional groups and double bonds. The *in vitro* anticancer activity of these compounds was assayed in human cancer cell lines using the MTT colorimetric assay and quantitative videomicroscopy. The compounds with one isonitrile functional group exerted their anticancer activity through non-apoptotic cytotoxic effects. On the other hand, the compounds with two isonitrile functional groups demonstrated to mediate anticancer activity through cytostatic effects. These results identify diterpene isonitriles as potential hits in anti-cancer drug discovery.
3. *Plakortis simplex:* the chemical analysis of an Indonesian specimen has been undertaken. In spite of the geographical distance, the glycolipidic content was very similar to that of Caribbean specimens. However, the Indonesian *P. simplex* also contained a new glycolipid, plakohopanoid, which is made of a mannosil inositol unit esterified by a C_{32} hopanoic acid. Actually, C_{32} hopanoic

acids are currently believed to be geohopanoids because mostly present in sediments and are considered diagenetic products. This finding in a marine organism is worthy of note because shows that also a biogenetic pathway can lead to hopanoic acids.

The second line of research concerns a project focused on the synthesis of an analogue of simplexide, a glycolipid isolated from the Caribbean sponge *Plakortis simplex* in the year 1999. The simplexide showed to be a potent stimulus for the production of cytokines and chemokines, with interesting perspectives to be used in cancer and autoimmune diseases. In order to better understand the mechanism of action on immune system, the synthesis of a simpler analogue, having only a sugar in the saccharide chain, was carried out. Several synthetic approaches were applied, focusing on β-glycosilation step. The reactions were performed using conventional and microwave heating. Although the yields need further optimizations, the amount of the analogue of simplexide obtained so far will be tested on human blood monocytes.

Breve descrizione del lavoro di tesi e dei risultati

La natura rappresenta una grande risorsa di metaboliti secondari con spiccato interesse terapeutico. Più della metà dei principi attivi dei farmaci correntemente in uso, sono prodotti naturali o derivati. In particolare, negli ultimi decenni dagli organismi marini sono stati isolati migliaia di nuovi composti, con interessanti strutture chimiche e attività farmacologiche tali da svolgere un ruolo sempre più importante nella ricerca biomedica e drug discovery. In quest'ambito si inserisce l'attività di ricerca di questo lavoro di tesi, il cui obiettivo principale è consistito nell'individuazione di nuove molecole bioattive da spugne marine al fine di ottenere 'lead-compounds' per la progettazione di nuovi farmaci.

In particolare, sono stati affrontati due aspetti della ricerca sui prodotti naturali marini:

✓ Isolamento e determinazione strutturale di composti bioattivi da poriferi: *Tedania ignis*, *Pseudaxinella flava* e *Plakortis simplex*.

✓ Sintesi di un analogo del simplexide, un glicolipide con interessanti proprietà immunoregolatorie, nell'ambito di un più ampio progetto diretto alla drug discovery da prodotti naturali.

L'analisi chimica e farmacologica dei metaboliti secondari isolati dagli organismi marini ha portato ai seguenti risultati:

1. Dalla spugna caraibica *Tedania ignis* sono stati isolati tre nuovi metaboliti con interessanti proprietà farmacologiche. Il primo composto isolato è stato il tedanolo, un nuovo bromoditerpene solfato a scheletro pimaranico. La struttura è stata determinata mediante spettrometria di massa e spettroscopia NMR, che ha richiesto anche l'ausilio di simulazioni, mentre per la configurazione

assoluta ci si è avvalsi del metodo di Mosher. Da studi *in vivo* si è osservato che il tedanolo è in grado di ridurre in maniera significativa l'edema indotto da carragenina. L'attività antiinfiammatoria è associata all'inibizione dell'espressione della COX-2 e della iNOS, e alla riduzione dei livelli di mieloperossidasi. La selettività d'azione per le COX-2 e la buona idrofilia rendono questo composto un promettente lead compound nella ricerca di farmaci ad attività antiinfiammatoria con bassa tossicità gastrointestinale.

Dallo stesso organismo sono stati isolati anche il tedarene A e il tedarene B, due nuovi diarileptanoidi ciclici, che rappresentano il primo esempio di questa classe di composti nell'ambiente marino. Essi sono costituiti da uno scheletro 1,7-difenileptanoico, i cui due anelli benzenici sono legati in modo da formare un ciclo mediante un ponte etereo (tedarene A) o mediante legame diretto (tedarene B). La determinazione strutturale delle due molecole, apparentemente semplice, ha in realtà richiesto anche esperimenti NMR a temperatura variabile (Dynamic NMR), studi di molecular modelling e calcoli quantomeccanici. È stato dimostrato che i tedareni A e B esistono entrambi come miscele di due conformeri in lento equilibrio. Inoltre, saggi farmacologici *in vitro* hanno dimostrato che il tedarane A è in grado di inibire il rilascio di nitriti in cellule macrofagiche LPS stimolate, mentre il tedarene B è inattivo.

2. Lo studio del contenuto metabolico della *Pseudaxinella flava* ha portato all'isolamento di quattro diterpeni isonitrilici con scheletro amphilectanico, tre dei quali già riportati in letteratura. Differiscono principalmente per il numero e la posizione delle funzioni isonitrile e per la presenza o meno di doppi legami

sulla catena laterale. I quattro composti sono stati saggiati *in vitro* su linee cellulari tumorali umane mediante saggi colorimetrici MTT e metodi di quantitative videomicroscopy. E' risultato che i composti contenenti una sola funzione isonitrilica esercitano la loro attività antitumorale mediante un effetto citotossico non apoptotico, mentre quelli con due funzioni isonitriliche mediante un effetto citostatico. Ne consegue che questi diterpeni isonitrili costituiscono dei potenziali leads nella ricerca di farmaci antitumorali.

3. Per quanto riguarda la *Plakortis simplex,* è stata studiata la composizione glicolipidica di un esemplare indonesiano, mettendola a confronto con quella degli esemplari caraibici, già studiati approfonditamente sotto questo punto di vista. Nonostante la distanza geografica, la composizione glicolipidica è risultata pressoché identica nelle due spugne. Tuttavia, la *P. simplex* indonesiana contiene anche un nuovo glicolipide, il plakohopanoide, che è costituito da un mannosilinositolo esterificato da un acido opanoico C_{32}. Quest'ultimo è ritrovato normalmente nei sedimenti, ed è comunemente definito geo-opanoide in quanto è ritenuto un prodotto di degradazione abiotica degli opanoidi presenti nei batteri. La sua presenza in *P. simplex* suggerisce l'esistenza di una via biogenetica che conduce alla formazione dell'acido opanoico C_{32}.

La seconda linea di ricerca ha riguardato invece la sintesi di un analogo del simplexide, un glicolipide atipico isolato dalla spugna caraibica *Plakortis simplex* nel 1999. Saggi farmacologici hanno dimostrato che il simplexide stimola la produzione di citochine e chemochine, e se ne ipotizza l'uso in terapia per la cura

di malattie autoimmuni e del cancro. Al fine di indagare in dettaglio sul meccanismo d'azione è stata esaminata la possibilità di sintetizzare un analogo semplificato, in cui la porzione saccaridica è ridotta ad un solo zucchero. Sono stati utilizzati diversi approcci sintetici, focalizzando l'attenzione sullo step di β-glicosilazione. Le reazioni sono state condotte applicando sia il riscaldamento convenzionale sia il riscaldamento per irraggiamento di potenza a microonde. Nonostante le rese di reazione necessitino ulteriori ottimizzazioni, l'analogo sintetico del simplexide è stato ottenuto in quantità tali da poter essere sottoposto a saggi immunologici.

”When someone seeks, then it happens all to easily
that his eye will see only the thing he is seeking,
that he cannot find anything, cannot let anything in,
because he is always thinking of that thing he seeks,
because he has a goal, because he is possessed by the goal.
Seeking means: have a goal. But finding means:
being free, being open, having no goal,,

”Quando un uomo cerca, accade facilmente che il suo
occhio veda soltanto la cosa che cerca,
che egli non sia capace di trovare niente,
di lasciare entrare niente in sé, perché pensa
solo e sempre a ciò che cerca, perché ha uno scopo,
perché è posseduto dallo scopo. Cercare significa:
avere uno scopo. Trovare invece vuol dire:
essere liberi, restare aperti, non avere alcuno scopo,,

Hermann Hesse

INTRODUCTION

Natural products have been considered an important source of drugs since ancient times and they are the major component of the drugs currently used to treat human disease.[1]

In particular, marine natural products coming from the ocean are playing an increasingly important role in biomedical research and drug discovery.

More than 70 % of globe's surface is covered by oceans and life on Earth has its origin in the sea. In certain marine ecosystems, experts have estimated that the biological diversity is higher than in tropical forests.[2] Among marine organisms, the chance of finding bioactive compounds is remarkably higher in some invertebrates, like corals, tunicates, and sponges. Many of these compounds are involved in their chemical defense, which is essential for the survival of sessile organism, often lacking any physical defense from their predators. Therefore they have developed the ability to synthesize toxic compounds or to obtain them from marine symbiotic organisms.

Natural products released into the water are rapidly diluted and, therefore, they need to be highly potent to have any effect. For this reason, and because of the diversity of organisms in the marine environment, it is increasingly recognized that a huge number of marine natural products could be developed into drugs.

---

[1] Mayer, A. M. S. et al., *Trends in Pharmacological Sciences*, June **2010,** 31, 6, 255-265

[2] Burkhard Haefner, DDT Vol.8, No. 12 June **2003**

However, even when showing interesting and specific pharmacological activities, natural compounds isolated from marine organisms rarely raise the interest of pharmaceutical companies because it is difficult to obtain them in sufficient amounts for clinical use.

The supply or manufacture of quantities of compounds, with interesting and specific pharmacological activities, from marine sources to ensure a sustainable supply for clinical use is a bottleneck.[3] Sponges and their microbial fauna are largely unculturable, and rare compounds must be extracted and purified from specimens collected by hand using scuba diving or sometimes with submersibles equipped with robotic arms. Apart from the high price of these techniques, the problem is to conciliate development dynamics necessary for man and protection of the marine environment and biodiversity. Oceans are showing increasing signs of overexploitation and degradation, resulting in loss of both productivity and biodiversity. Thus, the urgent need for protection of biodiversity is, at molecular level, a need for protection of the chemical diversity, that consists of a variety of natural compounds not yet identified and characterized.

Due to the remarkable properties of marine natural compounds, the interest remains high so that can drive innovative methods for their supply: a multidisciplinary approach to drug discovery, involving the generation of molecular diversity from natural product sources, combined with total and combinatorial synthetic methodologies, and including the manipulation of biosynthetic pathways (combinatorial biosynthesis), provides the best

[3] Molinski, F. T.; Dalisay, D. S.; Lievens, S. L. and Saludes, J. P., *Nature Reviews Drug Discovery*, (January **2009**)8, 69-85

solution to the current productivity crisis of the scientific community involved in drug discovery and development.

As matter of fact, 30% of the 1184 New Chemical Entities, which cover all diseases, countries and sources in the years 1981-2006, are totally synthetic drugs, often found by random screening or/and modification of an existing agent (see Figure 1). [4]

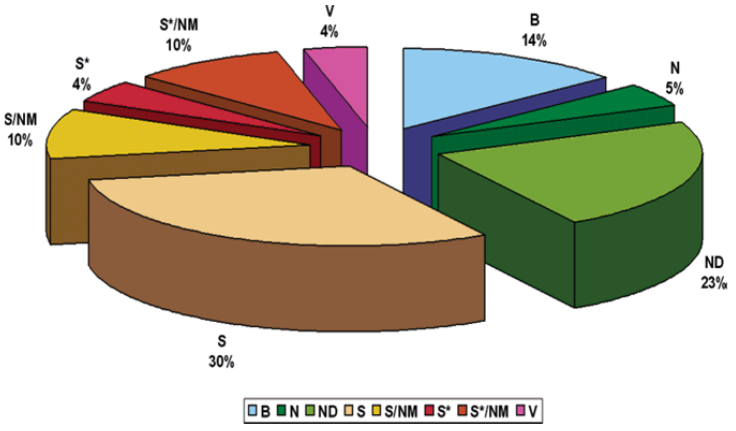

"B" Biological - **"N"** Natural product - **"ND"** Derived from a natural product, usually a semisynthetic modification - **"S"** Totally synthetic drug, often found by random screening/modification of an existing agent - **"S*"** Made by total synthesis, but the pharmacophore is/was from a natural product - **"V"** Vaccine - **"NM"** Natural product Mimic.

Figure 1: All New Chemical Entities organized by source (01/1981-06/2006).

A good example is represented by *Cytarabine* (Cytosar-U®, Depocyt®), a synthetic pyrimidine nucleoside, which was developed from spongothymidine, a nucleoside originally isolated from the Caribbean sponge *Tethya crypta*.

Caribbean marine sponges are well-known to produce a large array of new chemical structures with promising anti-cancer, anti-inflammatory, immunomodulating and anti-bacterial properties.

[4] Newman, D. J. and Cragg., G. M.; *J. Nat. Prod.*, **2007**, 70, 461-477

My research project focused on the study of the chemistry of these colorful animals living in the tropical oceans as a source of new structures to be used as leads and scaffolds for the elaboration of new drugs.

This PhD thesis reports the results obtained working at the Department of Chemistry of Natural Products, Faculty of Pharmacy, University of Naples "Federico II", in collaboration with the research group of Professor Alfonso Mangoni, who has multi-year experience in this research field.

The largest part of the research activities focused on the "core activity" of natural product chemistry, i.e. isolation and structure elucidation of new bioactive compounds from different specimens of Porifera, and their symbiotic microorganisms.

A second line of research focused on the synthesis of an analogue of simplexide, a glycolipid isolated from the Caribbean sponge *Plakortis simplex*.[5] This compound showed interesting perspectives to be used in cancer and autoimmune diseases. In order to have a better understanding of the mechanism of action on immune system, the possibility to synthesize an analogue has been investigated. This work was done as a part of a project aiming at the drug discovery from natural products.

Therefore, the results of the three year research work can be summarized in two main sections:

- ✓ Discovery of new bioactive compounds from marine sponges, such as *Tedania ignis, Pseudaxinella flava, Plakortis simplex*.

[5] Costantino V., Fattorusso E., Mangoni A., Di Rosa M., Ianaro A., *Bioorg .Med. Chem. Let.t* **1999**, 9, 271–276

- ✓ Synthesis of an analogue of simplexide, a glycolipid with an important immunoregulatory role.

Chapter 1

Porifera

Porifera, commonly known as sponges, are the simplest form of multicellular animals, just up from protozoans and down from cnidarians (stinging-celled like corals and anemones) in most taxonomic schemes. They don't have tissues or organs and their cells are unspecialized and quite independent, more like colony than a single animal.

There are about 5,000 identified marine species of sponges. There are a few ambulatory types but almost all are attached permanently to hard or soft substrata. Sponges are found worldwide, in all colors, shapes and sizes. Most sponges live in salt water; only about 150 species live in fresh water.

Their body consists of specialized tube-like cells called porocytes which control channels leading to the interior of mesohyl (ostia).

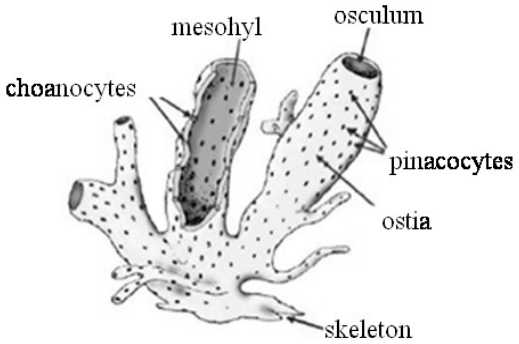

Figure 1.1: A sponge body structure

Mesohyl is the gelatinous matrix within the sponge made of collagen and covered by choanocytes, cylindrical flagellated cells. The outer layer is formed by pinacocytes, plate-like cells which digest food particles too large to enter the ostia. The body is reinforced by the skeleton, collagen fibers and spicules. Calcareous sponges produce spicules made of silica calcium carbonate while the larger class (90%) of Demonspongiae produce a special form of collagen called spongin besides silica spicules. Glass sponges, common in polar water and in the depths of temperate and tropical seas, contain synctia in their structure which enable them to extract food from these resource-poor waters with the minimum effort. Sponges are filters feeders; they obtain nourishment, tiny and floating organic particles, plankton and oxygen from flowing water that they filter through their body.

Water flows into a sponge through porocytes and flows out through oscula, large opening. The flowing water also carries waste products.

The simplest body structure in sponges is a tube or vase shape known as asconoid; in siconoids the body wall is pleated and the pumping capacity is increased; leuconoids contain a network of chambers lined with choanocytes and connected to each other and to the water intakes and outlet by tubes (Figure 1.2).

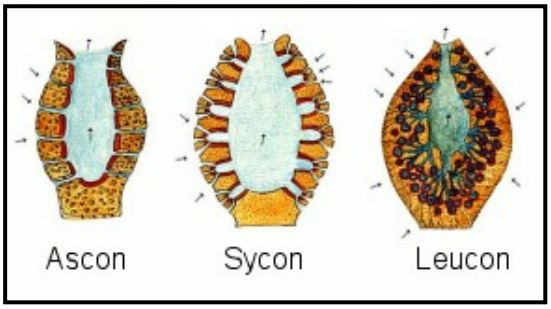

Figure 1.2: Sponge classification: asconoid; siconoids; leuconoids

Most sponges are hermaphrodites (each adult can act as either the female or the male in reproduction). Fertilization is internal in most species; some released sperm randomly float to another sponge with the water current. If a sperm is caught by another sponge's collar cells (choanocytes), fertilization of an egg by the travelling sperm takes place inside the sponge.

The resulting tiny larva is released and is free-swimming; it uses tiny cilia (hairs) to propel itself through the water. The larva eventually settles on the sea floor, becomes sessile and grows into an adult.

Some sponges also reproduce asexually; fragments of their body (buds) are broken off by water currents and carried to another location, where the sponge will grow into a clone of the parent sponge (its DNA is identical to the parent's DNA).

During my PhD thesis, two sponges from Caribbean (*Tedania ignis* and *Pseudaxinella flava*) and one from Indonesian seas (*Plakortis simplex*) were analyzed (Figure 1.3).

Plakortis simplex *Tedania ignis* *Pseudaxinella flava*

Figure 1.3. Sponges discussed in this PhD Thesis

Chapter 2

Methods

2.1 Structural Determination Methods

2.1.1 Mass spectrometry

The first step in the study of a new bioactive compound is the determination of the molecular formula through the high resolution mass spectrometry.

Mass spectrometry is an analytical technique that is used to determine the molecular mass of a compound on the basis of the mass-to-charge ratio (*m*/*z* ratio) of ions produced from the molecules. A very accurate measurement of the molecular mass (high resolution mass spectrometry) can also provide the molecular formula of the molecule under study.

The *source* is the component of the mass spectrometer which produces ions from the molecule, while the *analyzer* measures the mass-to-charge ratio of the ions. There are many different types of sources, as well as of analyzers.

During or after ionization the molecule may fragment, and the mass of the fragments provides information on the structure of the molecule under examination. If the ions do not fragment by themselves, they may be induced to fragment by letting them collide with gas molecules. In this case, a second analyzer is used to measure the mass of the fragments. This is known as tandem mass spectrometry or MS/MS.

Most of compounds described in the following sections were analyzed by ESI mass spectrometry. The ESI source is a widely used technique for polar

and/or charged macromolecules. The sample is dissolved in a volatile solvent like H_2O, MeOH, and CH_3CN; volatile acids, bases or buffers are often added to the solution. This solution is pumped through a charged metal capillary and, in coming out of the capillary, forms a spray. Because of the electric potential of the capillary, each droplet of the spray carries an excess positive or negative charge, and this causes extensive protonation or deprotonation of the molecules of the sample, which become ions. An uncharged carrier gas such as nitrogen is used to help the liquid to nebulize and the neutral solvent in the droplets to evaporate.

As the solvent evaporates, the ionized analyte molecules become closer and closer, until they can escape from the droplet by electrostatic repulsion. For molecules with a high molecular weight, the ions may take more than one proton (up to some tens), and therefore may have multiple charge. Formation of multiply charged ions allows the analysis of high molecular weight molecules such as proteins, because it reduces the *m/z* ratio of the ions, which is therefore easier to measure.

2.1.2 Nuclear Magnetic Resonance

Nuclear Magnetic Resonance Spectroscopy is a powerful analytical method widely used in chemical laboratories and is the most important spectroscopic technique used for structure elucidation of compounds. In addition to standard ^{1}H and ^{13}C NMR spectra, a large use of 2D NMR experiments was made. They are superior to their 1D NMR counterparts both for the shorter acquisition times, and for the easier assignment of nuclei

resonating in crowded regions of the spectra (signal overlapping is much less likely in two dimensions than in one).

The COSY (Correlation SpectroscopY) experiment is one of the simplest and yet most useful 2D NMR experiment. It allows determination of the connectivity of a molecule by identifying which protons are scalarly coupled. In spite of the many modifications which have been proposed along the years, the very basic sequence composed of two $\pi/2$ pulses separated by the evolution period t_1 is still the best choice if one is simply dealing with the presence or the absence of a given coupling, but not with the value of the relevant coupling constant.

The TOCSY (Total Correlation SpectroscopY) experiment is a 2D NMR experiment very useful in the analysis of molecules composed of many separate spin systems, such as oligosaccharides or peptides. The TOCSY spectrum shows correlation peaks between nuclei that may be not directly coupled, but are still within the same spin system. The appearance of a TOCSY spectrum resembles in all aspects a COSY; the difference is that the cross peaks in a COSY result from coupled spins, whereas in the TOCSY spectra they arise from coherence transfer through a chain of spin-spin couplings, and therefore any pair of protons within a spin system may give rise to a peak. The range of the coherence transfer (i.e. through how many couplings the coherence may be transferred) increases with increasing mixing times (Δ), but a mixing time too long may reduce sensitivity.

The HSQC (Heteronuclear Single Quantum Correlation) and HMQC (Heteronuclear Multiple Quantum Correlation) experiment are 2D NMR

heteronuclear correlation experiments, in which only one-bond proton-carbon couplings ($^1J_{CH}$) are observed. In principle, the HSQC experiment is superior to HMQC in terms of selectivity and additionally allows DEPT-style spectral editing. However, the sequence is longer and contains a larger number of π pulses, and is therefore much more sensitive to instrumental imperfections than HMQC.

The HMBC (Heteronuclear Multiple Bond Correlation) experiment is a heteronuclear two-and three-bond ^{1}H-^{13}C correlation experiment; its sequence is less efficient than HSQC because the involved $^{2,3}J_{CH}$ couplings are smaller (3-10Hz). Moreover, while $^1J_{CH}$ are all quite close to each other, $^{2,3}J_{CH}$ can be very different, making impossible to optimize the experiment for all couplings. As a result, in most HMBC spectra not all of the correlation peaks which could be expected from the structure of the molecule are present.

The ROESY (Rotating-frame Overhauser SpectroscopY) experiment is a chemical shift homonuclear correlation which can detect ROEs (Rotating-frame Overhauser Effect). ROE is similar to NOE, being related to dipolar coupling between nuclei, and depending on the geometric distance between the nuclei. While NOE is positive for small molecules and negative for macromolecules, ROE is always positive. Therefore, the ROESY experiment is particularly useful for mid-size molecules, which would show a NOE close to zero. The ROESY sequence is similar to the TOCSY sequence, and unwanted TOCSY correlation peaks may be present in the ROESY spectra. Fortunately, these unwanted peaks can be easily

recognized, because their phase is opposite compared to ROESY correlation peaks. It is important to acquire ROESY spectrum in phase-sensitive mode for a correct interpretation of the spectrum.

2.1.3 Circular Dichroism

Circular dichroic (CD) spectroscopy of optically active compounds is a powerful method for studying the three-dimensional structure of organic molecules, and can provide information on absolute configurations, conformations, reaction mechanisms, etc.

The CD spectroscopy takes advantage of the different absorption shown by chiral compounds of left and right circularly polarized UV/Vis light. In circularly polarized light, the electric field vector rotates about its propagation direction forming a helix in the space while propagating. This helix can be left-handed or right-handed, hence the names left and right circularly polarized light.

At a given wavelength, circular dichroism of a substance is the difference between absorbance of left circularly polarized and right circularly polarized light:

$\Delta A = A_L - A_R$

Since circular dichroism uses asymmetric electromagnetic radiations, it can distinguish between enantiomers. Two enantiomers have the same CD spectra, but with reversed sign.

Of course, in order to show a *differential* absorbance, the molecules needs to absorb the UV/Vis light, and therefore must possess at least one

chromophore. If the molecule does not have a chromophore, this can be introduced using a derivatization reaction.

One of the most important methods to establish the absolute configuration of a molecule is the exciton chirality method. This method is based on the interaction between two chromophores. When two or more strongly absorbing chromophores are located nearby in space and constitute a chiral system, their electric transition moments interact spatially (exciton coupling) and generate a circular dichroism. Because the theoretical basis of exciton coupling are well understood, it is possible to correlate the CD spectrum of an exciton-coupled chromophore system with the spatial orientation of the chromophores, which in turn can be related to the absolute configuration of the molecule. It is important to point out that, unlike for example optical rotation, the exciton chirality method does not require any reference compound to provide the absolute configuration of the molecule under study (if its conformation is known).

2.1.4 Mosher method

An efficient and widespread method used to determinate absolute configuration is based on NMR spectroscopy. This method involves the derivatization of a chiral substrate (A) of unknown absolute stereochemistry, with two enantiomers (*R* and *S*) of a chiral derivatizing reagent (CDR).

The CDR should have a functional group (Z) able to react with the functional group (HX) of the chiral substrate, a strong anisotropic

substituent (i.e. an aromatic ring) and a polar group able to fix a preferential conformation (Figure 2.1).

The proton NMR spectrum of the resulting diastereoisomers are compared in order to obtain a difference in chemical shifts. The chemical shift differences are due to the selective shielding effect of the CDR aryl group on the nuclei linked to the stereogenic carbinol center of the obtained diastereoisomers.

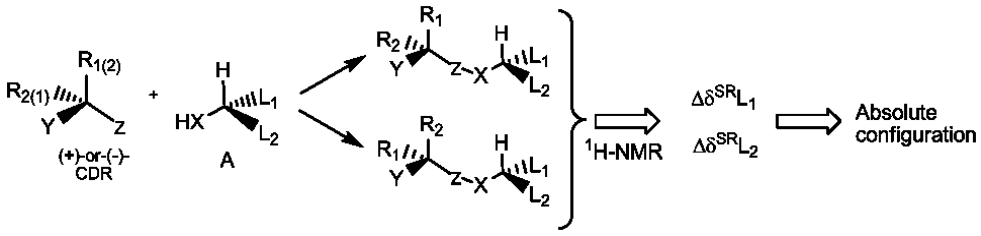

Figure 2.1: General method to define absolute configuration with NMR

The most used chiral derivatizing reagent (CDR) is (S)-(+)- and (R)-(-)-α-methoxy-α-trifluoromethylphenylacetyl chloride [(S)-(+)- and (R)-(-)-MTPA-Cl], also named Mosher's reagent.

On the base of experimental data observed for secondary alcohols of known stereochemistry, Mosher realized that there is a systematic trend of ^{1}H chemical shifts of esters obtained with Mosher's reagent.

This assumption is based on the existence of a preferential conformation in solution, in which the proton of the stereogenic center, the carbonyl of the ester group and the trifluoromethylic group reside on the same plane in anti arrangement (Figure 2.2).

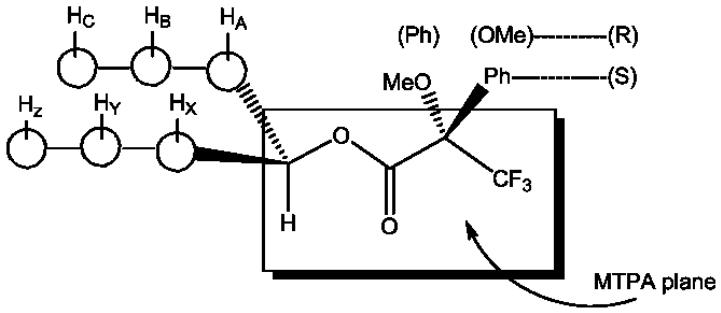

Figure 2.2: Preferential conformation of Mosher ester.

The method involves the resonances assignment of protons adjacent to the stereogenic carbinol center and the chemical shift differences $\Delta\delta_{S-R}$ must be calculated. Using the empirical model reported in the figure 2.3, in which the protons in the left side of the MTPA plane have value $\Delta\delta < 0$, while those in the right side $\Delta\delta > 0$, and applying the priority rules of Cahn et al., the absolute configuration of stereogenic centre is defined.

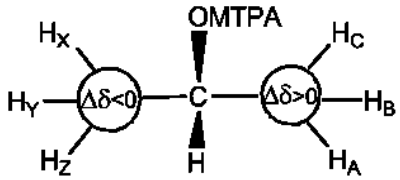

Figure 2.3: Empirical model proposed by Mosher to determine absolute configuration of secondary alcohols.

2.1.5 Computational methods

A lot of experimental techniques give data correlated to the conformation of a molecule, but they don't allow to straightly go up to the conformation.

NMR data allow the determination of relative stereochemistry of organic molecules through the evaluation of coupling constants and the analyses of NOESY or ROESY spectra, which give information about distances of

different protons of molecules. However, the interpretation of experimental data is not always simple, clear and univocal, bothering the exact conformation of a molecule.

Computational chemistry is a branch of chemistry that uses principles of computer science, generating data which complements experimental data on the structures, properties and reactions of substances. It is a discipline based on quantum mechanical principles that allow realistic representation of a 3D structure of a molecule. The calculations are based primarily on Schrödinger's equation and include calculation of electron and charge distributions, molecular geometry in ground and excited states, potential energy surfaces, rate constants for elementary reactions and details of the dynamics of molecular collisions. Computational chemistry is particular useful for determination of properties that are inaccessible experimentally and interpretation of experimental data.

In computational chemistry, energy minimization (also called energy optimization or geometry optimization) methods are used to compute the equilibrium configuration of molecules and solids.

Stable state of molecular systems correspond to global and local minimum on their potential energy surface. Starting from a non-equilibrium molecular geometry, energy minimization employs the mathematical procedure of optimization to move atoms in order to reduce the net forces on the atoms until they become negligible.

The molecular mechanics provides the potential energy of each molecule on the base of the position of the atoms. The potential energy of all system in

molecular mechanics is calculated using force field, which is a function used to describe the potential energy surface of a system of particles.

Force field functions and parameter sets are derived from both experimental data and high-level quantum mechanical calculations.

In energy minimization methods, periodic boundary condition have been allowed to make small systems. A well established algorithm of energy minimization can be an efficient tool for molecular structure optimization.

But it does not include the effect of temperature, and hence the trajectories of atoms during the calculation do not really make any physical sense, i.e. we can only obtain a final state of system that corresponds to a local minimum of potential energy. The conformation resulting from the process of minimization depends on the starting conformation and, therefore, represents the relative minimum closest to the starting conformation. Thus, energy minimization methods allow to know the relative and not absolute minimum of energy.

In order to define the absolute minimum of energy, conformational search (grid search, random search, distance-geometry, simulated annealing) allows to get the favorite conformation of a molecule, which should correspond to the absolute minimum.

Molecular dynamics is a form of computer simulation in which atoms and molecules are able to interact for a period of time by approximations of known physics, giving a view of the motion of the particles. In this way, it is possible to study the transition from one conformation to another.

Concerning semi-empirical method, it indeed makes possible calculations using approximations from experimental data to provide the input into the mathematical models. The comparison, between experimental and theoretical data, enable us to confirm the supposed structure or to choose between two or more structures.

2.2 Microwave assisted synthesis

The use of microwaves as an energy source for chemical reactions and processes has been extensively investigated during recent years. In inorganic chemistry, microwave technology has been used since the late 1970, while it has only been implemented in organic chemistry since mid-1980s. The development of the technology for organic chemistry was slow compared to combinatorial chemistry and computational chemistry.[6] This slow uptake has been principally attributed to its lack of controllability and reproducibility, safety aspects and a generally scarce understanding of the basics of microwave dielectric heating.

Since 1986, when Gedye and Giguere published their first articles in *Tetrahedron Letters* on microwave assisted synthesis in household microwave ovens, there has been a steadily growing interest in this research field. And since mid-1990s the number of publications has increased significantly. The main reasons of this increase include the availability of commercial microwave equipment intended for organic chemistry, the development of solvent-free technique, which has improved the safety

[6] Lidström, P.; Tierney, J.; Wathey, B. and Westman, J. ; *Tetrahedron,* **2001**, 57 , 9225-9283

aspects, and mostly to an increased interest in shorter reaction times. Not only direct microwave heating is able to reduce chemical reaction times from hours to minutes, but it is also known to reduce side reactions, to increase yields and improve reproducibility. Therefore, many academic and industrial research groups are using microwave as a forefront technology for rapid optimization of reactions, for the efficient synthesis of new chemical entities, and for discovering and probing new chemical reactivity. In particular pharmaceutical industry has the need for large sets of novel chemicals with druglike character and structural diversity.

Microwave irradiation[7] is an electromagnetic irradiation in the frequency range of 0.3 to 300 GHz. All domestic ovens or microwave reactors for chemical synthesis operate at a frequency of 2.45 GHz to avoid interference with telecommunication and cellular phone frequencies. The energy of the microwave photon in this frequency region (0.0016 eV) is too low to break chemical bonds and is also lower than the energy of Brownian motion. It is therefore clear that microwaves cannot induce chemical reactions.

Traditionally, organic synthesis is carried out by conductive heating with an external heat source (e.g. oil baths, sand baths or heating jackets). This is a comparatively slow and inefficient method for transferring energy into the system, since it depends on the thermal conductivity of the various materials that must be penetrated. In contrast, in microwave dielectric heating, the microwave irradiation produces efficient internal heating by direct coupling

[7] Kappe, C. O.; *Angew. Chem. Int. Ed*. **2004**, 43, 6250 –6284

of microwave energy with the molecules (solvents, reagents, catalysts) that are present in the reaction mixture.

Microwave-enhanced chemistry is based on the efficient heating of materials by microwave dielectric heating effects. This phenomenon depends on the ability of a material to absorb microwave energy and convert it into heat. There are two major mechanisms for the conversion of electromagnetic energy into heat: Dipolar polarization and ion conduction mechanism (see Figure 2.4).

Irradiation of the sample at microwave frequencies results in the dipoles or ions aligning in the applied electric field. As the applied field oscillates, the dipole or ion field attempts to realign itself with the alternating electric field and, in the process, energy is lost in the form of heat through molecular friction and dielectric loss. The amount of heat generated by this process is directly related to the ability of the matrix to align itself with the frequency of the applied field.

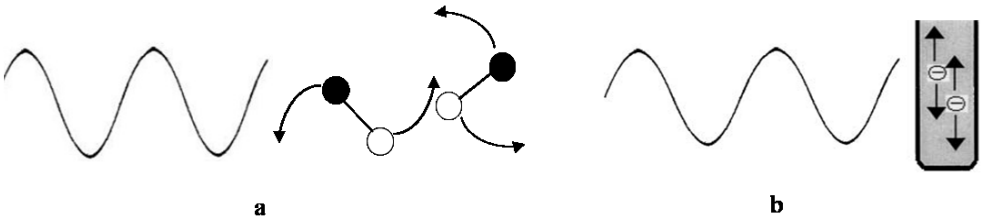

Figure 2.4 a) Dipolar molecules which try to align with an oscillating electric field; **b)** Charged particles in a solution follow the applied electric field.

The heating characteristics of a particular material (e.g. a solvent) under microwave irradiation conditions are dependent on its dielectric properties. However, if two solvents with comparable dielectric constant, ε′, such as ethanol and acetone, are heated at the same radiation power and for the

same period of time, the final temperature will be much higher in ethanol than in acetone. The more efficient a solvent is in coupling with the microwave energy, the faster the temperature of the reaction mixture increases. Microwave energy will reach and bypass the boiling point of most solvents in a matter of seconds, so boiling points become a less important factor in the decision of solvents to be used.

The ability of a specific substances to convert electromagnetic energy into heat at a given frequency and temperature, is determinated by a factor called loss angle, δ:

$$\tan \delta = \varepsilon'' / \varepsilon'$$

where ε′ is the dielectric constant and ε″ is the dielectric loss, which is indicative of the efficiency in converting the absorbed energy into heat. In general, solvents can be classified as high (tan $\delta > 0.5$), medium (tan δ 0.1-0.5) and low (tan $\delta < 0.1$) microwave absorbing.

When microwave irradiations enter a cavity, they are reflected by the walls. The reflections of the waves eventually generate a 3D stationary pattern of standing waves within the cavity, called modes. There are systems in multi-mode cavity and in single-mode cavity. The multi-mode technique consists of different modes to provide a uniform heating, but there is an interaction of each other that creates an area of high and low strength, commonly referred as ‘hot and cold spots’.

The single-mode cavity is sized such that it will propagate one mode of microwave energy. This creates a more homogenous energy distribution and a much higher power density than in multimode cavities.

The microwave equipments used for the synthesis of an analogue of simplexide (see Chapter 7) are the CEM Discover LabMate and Biotage Initiator EXP 8.

The CEM discover LabMate is a flexible single-mode instrument (300 W) that allows batch in open or sealed vessels (20 bar) up to 100 ml of volume. The system also allows the simultaneous cooling of the reaction mixture and the use of fiber-optic temperature probes, which is an accurate but costly and fragile system of temperature measurement (0°C-330°C).

The Biotage Initiator EXP 8 is an automated single-mode (400 W) microwave reactor that incorporates a gripper for the robotic transfer of 8 different types of sealed vessels allowing the processing of sample volumes from 0.2 to 20 ml. There is an external infrared sensor for the measurement of the temperature, which registers a temperature range -40°C to 400°C and is cheaper and less accurate than fiber-optic temperature probes.

Chapter 3

Analysis of the sponge *Tedania ignis* part I

Tedania ignis is a widespread Caribbean sponge, also known as "fire sponge" because it causes a severe rash when handled by humans. Dermatites have also been reported to occur as a consequence of the contact with the sponge tissue,[8] but it has not been determined so far which chemicals cause rash and dermatitis. Previous analyses of Caribbean samples of *T. ignis* led to the isolation of a new atisane derivative,[9] several diketopiperazines,[6,10] and some carbazole and carboline derivatives.[11] Many sponges contain a rich flora of symbiotic bacteria,[12] and *T. ignis* is one of these "high-microbial-abundance sponges". From a *Micrococcus* sp. obtained from the tissue of *T. ignis*, Cardellina et al. have isolated some of the diketopiperazines previously isolated from the sponge[13] along with four new benzothiazoles.[14]

Finally, in 1984 Schimtz's group reported the presence in *T. ignis* of tedanolide,[15] a potent cytotoxic macrolide that has been the target of intensive synthetic efforts. Although re-isolation of tedanolide (Figure 3.1) was one of the reasons for our analysis of *T. ignis*, and in spite of the best

[8] Yaffee, H. S.; Stargardter, F. *Arch. Dermatol.* **1963**, *87*, 601–604.
[9] Schmitz, F. J.; Vanderah, D. J.; Hollenbeak, K. H.; Enwall, C. E. L.; Gopichand, Y. *J. Org. Chem.* **1983**, *48*, 3941–3945.
[10] Dillman, R. L.; Cardellina, J. H. II *J. Nat. Prod.* **1991**, *54*, 1159–1161.
[11] Dillman, R. L.; Cardellina, J. H. II *J. Nat. Prod.* **1991**, *54*, 1056–1061
[12] U. Hentschel, U.; Usher, K.M.; Taylor, M.W. *FEMS Microbiol. Ecol.* **2006**, *55*, 167–77
[13] Stierle, A. C.; Cardellina, J. H. II; Singleton, F. L. *Experientia* **1988**, *44*, 1021.
[14] Stierle, A. A.; Cardellina, J. H. II *Tetrahedron Lett.* **1991**, *32*, 4847–4848.
[15] Schmitz, F. J.; Gunasekera, S. P.; Yalamanchili, G.; Hossain, M. B.; van der Helm, D. *J. Am. Chem. Soc.* **1984,** *106,* 7251–7252.

efforts, we were not able to find any tedanolide in the extracts of the three different specimens of *T. ignis* from Bahamas that we examined.

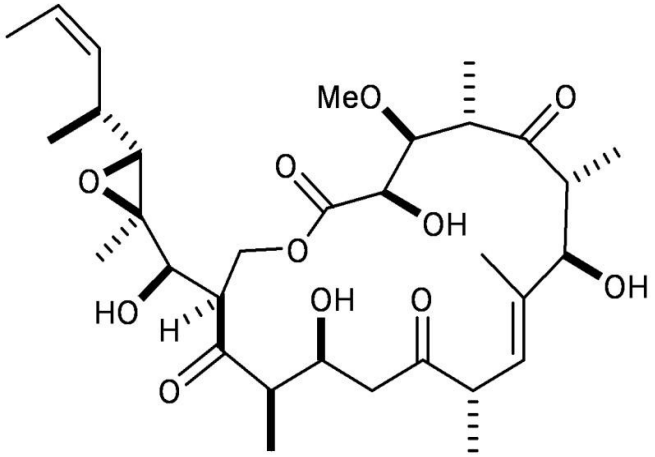

Figure 3.1: Tedanolide; a potent cytotoxic macrolide found in *Tedania ignis*

However, the re-examination of the organic extract of *T. ignis* revealed the presence of a new brominated and sulfated diterpene alcohol having an *ent*-pimarane skeleton (tedanol) and two new cyclic diarylhepatonids (tedarene A and B) (Figure 3.2).

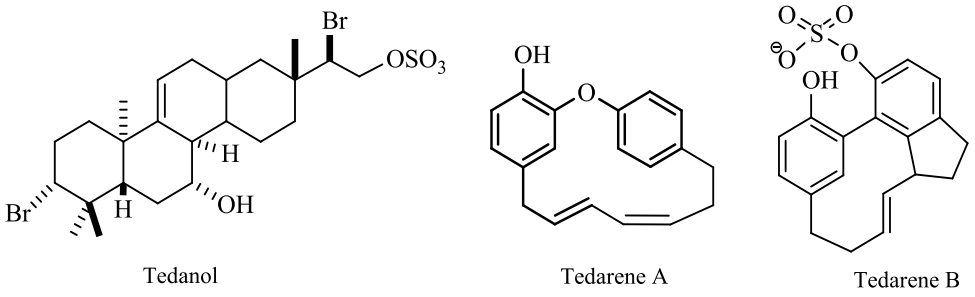

Figure 3.2: The three new compounds isolated from the sponge *Tedania ignis*.

Thus, the first part of the studies on *Tedania ignis* was focused on the isolation, structural determination and pharmacological studies of a new diterpene, the tedanol, which showed a potent anti-inflammatory activity,

evaluated as reduction of the carrageenan-induced mouse paw edema, coupled with a strong inhibition of COX-2 expression.

3.1 Tedanol: a potent anti-inflammatory *ent*-pimarane diterpene

Structure of tedanol was elucidated by mass spectroscopy and extensive NMR studies (including spectral simulation), and its absolute configuration was determined using the Mosher method. Tedanol (Figure 3.3) showed a potent anti-inflammatory activity at 1 mg/kg evaluated *in vivo* in a mouse model of inflammation. After a single intraperitoneal administration, tedanol significantly reduced both the acute (4 h) and subchronic (48 h) phase of the carrageenan-induced paw edema in mice. The anti-inflammatory activity was coupled with a strong inhibition of COX-2 expression, inhibition of cellular infiltration measured as mieloperoxidase (MPO) levels, and inhibition of iNOS expression. These features, together with its solubility in water, make tedanol a promising template for the development of new anti-inflammatory molecules with low gastrointestinal toxicity.

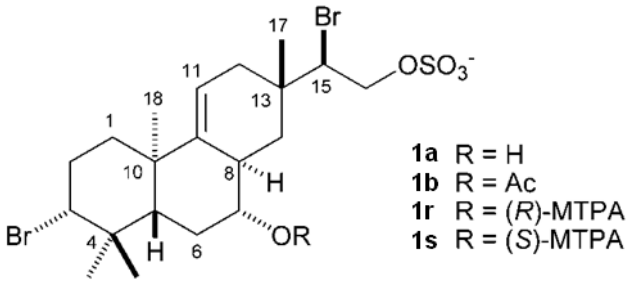

Figure 3.3: Structures of compounds **1a**, **1b**, **1r** and **1s**.

3.2 Isolation and structure elucidation of tedanol

Samples of *Tedania ignis,* collected in the mangroves of Sweeting Cay (Grand Bahama Island) during the 2007 Pawlik expedition, were immediately chopped in small pieces and frozen, then shipped to our laboratory, where the samples were extracted in sequence with MeOH and $CHCl_3$. The MeOH extract was dried and partitioned between water and BuOH, and the combined BuOH and $CHCl_3$ extracts were subjected to reversed-phase column chromatography. The fraction eluted with H_2O/MeOH 2:8 showed to contain tedanol, but we were not able to obtain the compound in the pure form by HPLC only. Instead, pure tedanol (**1a**) (6.5 mg) was obtained by reversed-phase HPLC, followed by preparative TLC using BuOH/AcOH/H_2O (60:15:25) as eluent.

The negative-ion ESI mass spectrum of **1a** showed three M^- molecular ion peaks in the 1:2:1 ratio at *m/z* 545, 543 and 541, suggesting the presence of two bromine atoms in the molecule. A high-resolution measurement performed on the lowest-mass ion at *m*/*z* 541 determined the formula $C_{20}H_{31}Br_2O_5S$ (exp.: 541.0272, calcd. for $C_{20}H_{31}{}^{79}Br_2O_5S$: 541.0258) for this ion.

A preliminary ^1H NMR analysis of compound **1a** showed four methyl singlets between δ 1.13 and δ 1.01 indicatives of a polycyclic diterpene skeleton. The ^{13}C spectrum showed 20 carbon resonances, that were assigned with an HSQC experiment as four CH_3, six CH_2, six CH (one of which is sp^2, δ 115.9, and four linked to heteroatoms, δ 78.3, 70.8, 69.6, and 61.8), and four non-protonated carbon atoms (one of which is sp^2, δ 148.1).

On the basis of the molecular formula and with the evidence of a double bond, it was clear that tedanol is a tricyclic diterpene.

The correlation peaks of the angular methyl groups [δ 1.06 (H_3-17), δ 1.13 (H_3-18), δ 1.01 (H_3-19), δ 1.08 (H_3-20)] in the HMBC spectrum allowed us to delineate two substructures (Figure 3.4, bold bonds), which were connected thanks to the proton-proton vicinal couplings evidenced by the COSY spectrum (Figure 3.4, solid bonds).

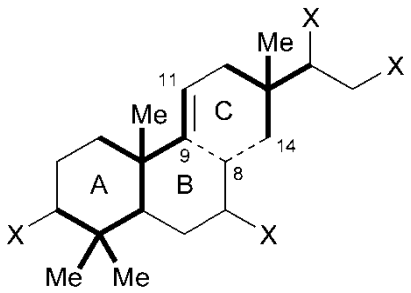

Figure 3.4: Elucidation of the pimarane skeleton of tedanol (**1a**). Part structures determined from HMBC correlations of angular methyl protons are denoted with bold lines, and bond determined from COSY correlations are denoted with solid lines. X's represent heteroatoms.

At this point, a pimarane skeleton was already delineated, except for the C-8/C-14 and C-8/C-9 bonds (Figure 3.4, dashed bonds), connecting ring B with ring C. The bond between C-8 and C-9 was demonstrated by the allylic coupling between H-8 and H-11 and the homoallylic coupling between H-8 and H-12eq evidenced by the COSY spectrum. The coupling between H-8 and the two protons at C-14 could not be evinced from the COSY spectrum because the chemical shifts of H-8 and H-14eq were almost identical, leading to non-first-order multiplets. However, this couplings could be demonstrated by spectral simulation. The subspectrum of the 10-proton spin system comprising all protons on rings B and C was calculated, optimizing

the unknown NMR parameters until the simulated multiplets reproduced accurately the experimental ones.

The results (Figure 3.5) pointed to a 5.9 Hz coupling constant between H-8 and H-14eq and a 10.7 Hz coupling constant between H-8 and H-14ax, and also evidenced a quite large W coupling (3.1 Hz) between H-12eq and H-14eq. In addition, the bond between C-8 and C-14 bond was confirmed by the ROESY correlation peak between H-14ax (δ 1.37) and H-7 (δ 3.02).

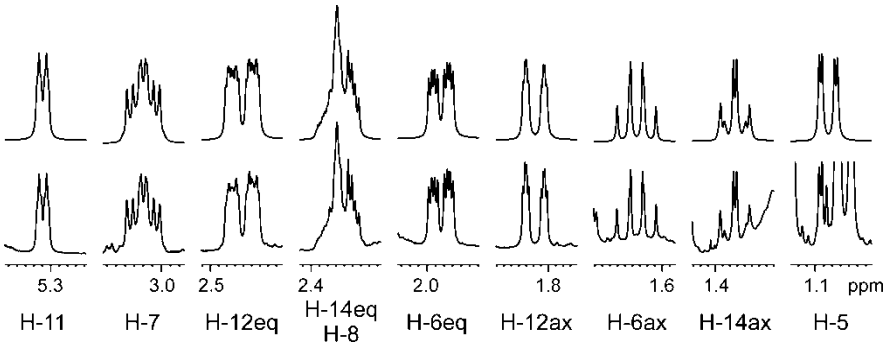

Figure 3.5: Simulated spectrum of the spin system of H-5 through H-14 (upper trace) compared to the experimental spectrum (lower trace). All the signals (including the non-first order multiplets of H8/H14eq and H-14ax) are accurately reproduced. Simulation parameters are: δ(H-5) 1.0846, δ(H-6ax) 1.6345, δ(H-6eq) 1.9834, δ(H-7) 3.0197, δ(H-8) 2.3699, δ(H-11) 5.3095, δ(H-12ax) 1.8184, δ(H-12eq) 2.4609, δ(H-14ax) 1.3731, δ(H-14eq) 2.3593, J(H-5/H-6ax) = 12.7 Hz, J(H-5/H-6eq) = 2.5 Hz, J(H-6ax/H-6eq) = -12.7 Hz, J(H-6ax/H-7) = 11.1 Hz, J(H-6eq/H-7) = 4.7 Hz, J(H-7/H-8) = 9.8 Hz, J(H-8/H-11) = 1.7 Hz, J(H-8/H-12ax) = 3.5 Hz, J(H-8/H-12eq) = 1.6 Hz, J(H-8/H-14ax) = 10.7 Hz, J(H-8/H-14eq) = 5.9 Hz, J(H-11/H-12ax) = 2.0 Hz, J(H-11/H-12eq) = 6.3 Hz, J(H-12ax/H-12eq) = -17.3 Hz, J(H-12eq/H-14eq) =3.1 Hz, J(H-14ax/H-14eq) = –13.9 Hz.

The remaining atoms to be assigned from the molecular formula (two bromine, one sulfur, one hydrogen, and five oxygen atoms) pointed to the presence of one hydroxyl, one sulfate, and two bromide functions linked to

the four deshielded carbon atoms C-3, C-7, C-15 and C-16. Derivatization of 0.6 mg of tedanol with Ac_2O in Py gave the monoacetyl derivative **1b**, which showed a remarkable downfield shift of H-7 from δ 3.02 in the natural compound **1a** to δ 4.39 in the acetate **1b**, thus demonstrating that the hydroxyl function is located at position 7. The two bromine atoms present in the molecular formula were located at C-3 (δ 69.6) and C-15 (δ 61.8), because the chemical shift of these carbon atoms were about 15 ppm lower than those observed in pimaranes oxygenated at these positions,[16] while are close to those observed in a 3,15-dibromoisopimarane from *L. perforata*.[13] Finally, the sulfate group was located at the remaining position 16, thus completing the planar structure of compound **1a**.

3.3 Relative and absolute configuration of tedanol

The relative configuration of the seven stereogenic centers of tedanol was assigned using coupling constant analysis combined with ROESY data. The A/B ring junction was established as *trans* because of the presence of a W long-range coupling between H-5 and H_3-18, indicative of their *anti* relationship. Relative configurations at C-3, C-7 and C-8 were established from the large vicinal coupling constants shown by H-3, H-7, and H-8 (see Table 3.1), indicating that they are all axial. This completed the relative stereochemistry of the *trans*-decaline moiety of the molecule (rings A and B). The ROESY correlation peaks of H-15 with H-8 and H_3-18, indicated that C-15 lies on the same side of the molecule as C-8 and C-18. This

[16] Chen, W.; Tang, W.; Zhang, R.; Lou, L.; Zhao, W. *J. Nat. Prod.* **2007,** *70*, 567–570

determined the relative configuration at C-13, and established that tedanol has the pimarane (or the enantiomeric *ent*-pimarane) skeleton.

The ROESY correlation peak between H-15 and H_3-18 was particularly interesting, because C-15 and C-18 are topologically far in the molecule. Analysis of a molecular model of tedanol easily demonstrated that H-15 and H_3-18 can be in close proximity to each other only if (a) the cyclohexene ring adopts the half-chair conformation such that C-15 is pseudo-axial and C-17 is pseudoequatorial and (b) the conformation around the C-13/C-15 bond is such that H-15 is directed inward of the cyclohexene ring (Figure 3.6). The long-range W coupling between H-15 and H_3-17 observed in the COSY spectrum, indicative of their *anti* relationship, showed that this conformation around the C-13/C-15 bond is indeed largely predominant.

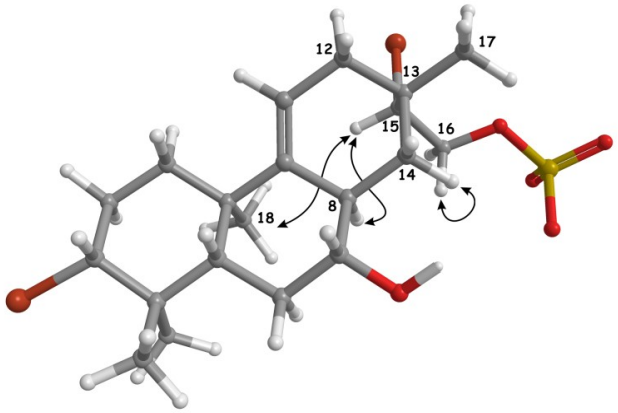

Figure 3.6: ROESY correlations used to determine relative configurations at C-13 and C-15.

The torsional rigidity of the C-13/C-15 bond can be justified by unfavorable steric interactions of either the bromine atom or the $CH_2SO_3^-$ group with H-8 in the two alternative staggered conformations. More importantly, it was the key for the assignment of the relative configuration at C-15. In fact, the

ROESY correlation peak between H-14eq and one of the protons at C-16 indicated that C-14 and C-16 are *gauche* oriented, and this, together with the *anti* relationship between H-15 and C-17, defined the relative configuration at C-15 as depicted in Figure 3.6.

As for the absolute configuration of tedanol, we used Mosher's method,[17] a reliable tool to establish the absolute configuration of secondary alcohols. Tedanol was allowed to react with (*S*)-(+)- and (*R*)-(–)-α-methoxy-α-trifluoromethylphenylacetyl chloride [(*S*)-(+)- and (*R*)-(–)-MTPA-Cl] to give, respectively, the 7-*O*-(*R*)-MTPA and 7-*O*-(*S*)-MTPA esters **1r** and **1s**, whose ^{1}H NMR spectra were acquired and assigned.

According to the Mosher model, the esters adopt a preferential conformation with the eclipsed CF_3 and C=O groups, and the phenyl group has a shielding effect on the neighboring protons. Thus, the observed $\Delta\delta$ values are consistent with the *R* configuration at C-7 (Figure 3.7), and therefore indicate that tedanol has the *ent*-pimarane, and not the pimarane, skeleton.

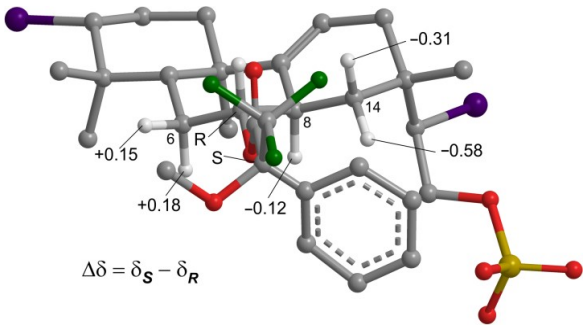

Figure 3.7: Preferred conformation of the (*S*)-MTPA ester of tedanol (**1s**) according to the Mosher model, and observed $\Delta\delta$ of the neighboring protons.

[17] Dale, J.A.; Mosher, H.S. *J. Am. Chem. Soc.* **1993**, *95*, 512; Ohtani, I.; Kusumi, T.; Kashman, Y.; Kakisawa, H. *J. Am. Chem. Soc.* **1991**, *113*, 4092.

3.4 Anti-inflammatory activity of tedanol

The anti-inflammatory activity was evaluated as inhibition of the carrageenan-induced paw edema in mice.[18,19] Intraperitoneal administration of tedanol (0.1-1 mg/kg) to mice 30 minutes before subplanatar carrageenan injection, causes a significant and dose related reduction in edema (Figure 3.8).

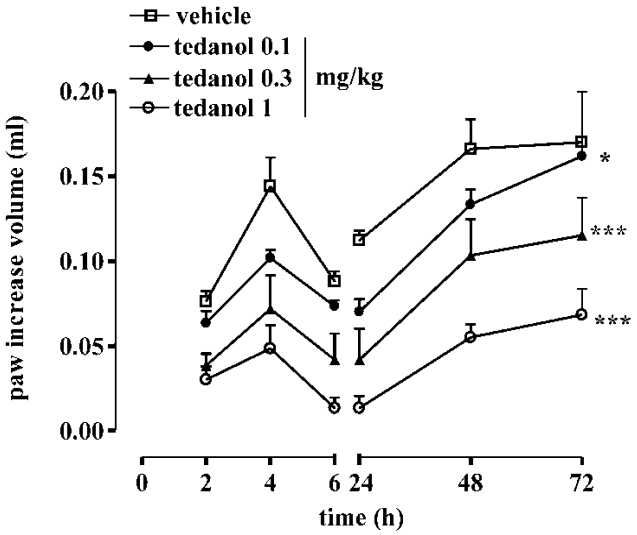

Figure 3.8: Effect of systemic administration of tedanol (0.1-1mg/kg) on carrageenan-induced mouse paw edema (* $p<0.05$; *** $p<0.001$ versus vehicle).

Because edema evaluation gives information relative to inflammatory swelling, due to vascular leakage, but not on cell infiltration, mieloperoxidase (MPO) levels were also measured. MPO evaluation is a widely used indirect index of cell infiltration. The systemic administration of tedanol prior to induction of inflammation (1 mg/kg) significantly inhibits MPO activity at 4 and 48 h after carrageenan injection (Figure 3.9).

[18] Posadas, I.; Bucci, M.; Roviezzo, F.; Rossi, A.; Parente, L.; Sautebin, L.; Cirino, G. *J. Pharmacol.* **2004**, 142(2), 331-338.
[19] M.G. Henriques, M.G.; Silva, P.M.; Martins, M. A.; Flores, C. A.; Cunha, F. Q.; Assreuy-Fiho, J.; Cordeiro, A. *Braz. J. Med. Biol. Res*. **1987**, *20*, 243–249.

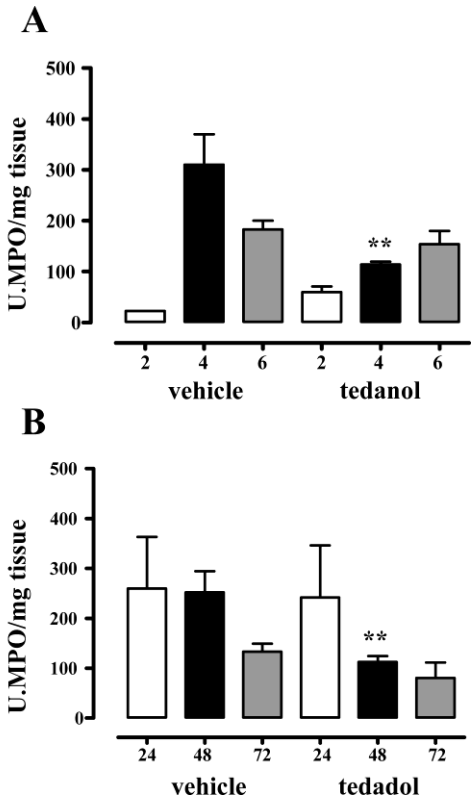

Figure 3.9: MPO evaluation performed on inflamed mouse paws harvested from mice systemically treated with the higher dose of tedanol (1mg/kg)- versus vehicle- treated mice in the first (panel A) and second phase (panel B) of edema (** $p<0.01$ versus vehicle).

In order to further investigate on the mechanism underlying tedanol anti-inflammatory activity, western blot analysis was performed on the paws harvested from mice pretreated with tedanol at the highest dose. Tedanol (1 mg/kg) significantly inhibited COX-2 expression both in the early phase (2 and 4 h) and in the second edema phase (48 and 72 h). Conversely, tedanol did not affect COX-1 expression in the early phase, but significantly inhibited its expression in the second phase. Tedanol pretreatment significantly inhibited iNOS expression at 2 h and 48 h only (Figure 3.10).

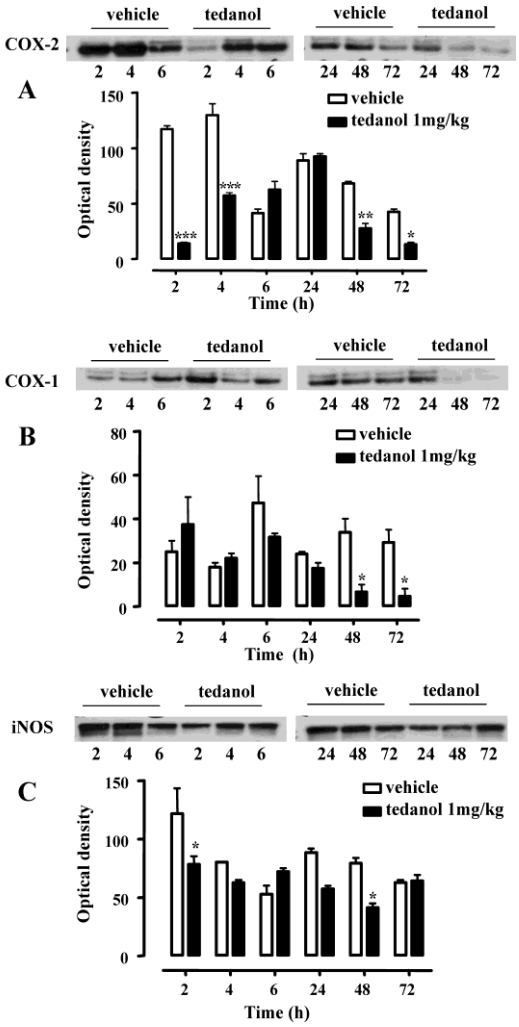

Figure 3.10: Western blot analysis for COX-2 (panel A), COX-1 (panel B) and iNOS (panel C) performed on inflamed mouse paws harvested from tedanol- (1mg/kg) or vehicle-treated mice. The blots are representative of three different experiments reported as densitometry analysis in bar graphs (* $p<0.05$; ** $p<0.01$; *** $p<0.001$ versus vehicle).

These data suggest that tedanol exerts its anti-inflammatory activity by reducing both vascular permeability and cell migration that involves mainly modulation of expression of COX-2 and, to a lesser extent, of COX-1 and iNOS.

3.5 Discussion

The structure of the new diterpene tedanol from *T. ignis* was established as the brominated and sulfated *ent*-pimarane diterpene alcohol **1a**.

To the best of our knowledge this is the first report of an *ent*-pimarane diterpene from a sponge tissue. The known natural metabolites most closely related to tedanol are a dibromoditerpene isolated in 1984 from the alga *Laurencia perforata*[20] and its diacetate from the sponge *Spongia zymocca*,[21] but these are compounds based on an isopimarane rather than an *ent*-pimarane skeleton.[22]

Tedanol turned out to be biologically attractive because it showed a potent anti-inflammatory activity. Another diterpene with the pimarane skeleton, acanthoic acid,[23] which is present in the Korean plant *Acanthopanax koreanum* traditionally used in popular medicine for the cure of rheumatism, has been shown to possess *in vitro* COX-2 inhibitory activity.[24,25] However, no data are available to date on the *in vivo* anti-inflammatory activity of this compound or other natural pimarane diterpenes. Indeed, *in vivo* anti-inflammatory activity requires, in addition to COX-2 inhibition, a favorable pharmacokinetic profile and lack of toxicity. In the present study, we demonstrated that tedanol does possess *in vivo* anti-inflammatory activity.

---

[20] Gonzalez, A. G.; Ciccio, J. F.; Rivera, A. P.; Martin, J. D. *J. Org. Chem.* **1985**, *50*, 1261-1264.

[21] Guella, G.; Mancini, I; Pietra, F. *Comp. Biochem. Physiol.* **1992**, *103B*, 1019–1023.

[22] Although in Ref. and in all the subsequent literature (including Ref.) the compound is described as an isopimarane (i.e. 13-epi-pimarane), the structural drawing on the paper shows the stereochemistry of a pimarane. Because the stereochemical assignment was only based on analogy with known compounds, the actual stereochemistry at C-13 of the bromoditerpene from *L. perforata* remains undetermined.

[23] Kim, Y. H.; Chung, B. S.; Sankawa, U. *J. Nat. Prod.* **1988**, *51*, 1080–1083.

[24] Suh, Y. G.; Kim, Y. H.; Park, M. H.; Choi, Y. H.; Lee, H. K.; Moon, J. Y.; Min, K. H.; Shin, D. Y.; Jung, J. K.; Park, O. H.; Jeon, R. O.; Park, H. S.; Kang, S. A. *Bioorg. Med. Chem. Lett.* **2001**, *11*, 559-562.

[25] Suh, Y. G.; Lee, K. O.; Moon, S. H.; Seo, S. Y.; Lee, Y. S.; Kim, S. H.; Paek, S. M.; Kim, Y. H.; Lee, Y. S.; Jeong, J. M.; Lee, S. J.; Kim, S. G. *Bioorg. Med. Chem. Lett.* **2004**, *14*, 3487–3490.

After a single intraperitoneal administration, tedanol significantly reduced both the acute (4 h) and subchronic (48 h) phase of the carrageenan-induced paw edema in mice. The anti-inflammatory activity was coupled with a strong inhibition of COX-2 expression, inhibition of cellular infiltration measured as mieloperoxidase (MPO) levels, and inhibition of iNOS expression. These features and its solubility in water, not frequently encountered among natural diterpenes, make tedanol a promising lead compound for the development of new anti-inflammatory molecules with low gastrointestinal toxicity.

3.6 Experimental Section

General experimental procedures

High-resolution ESI-MS spectra were performed on a Bruker APEX II FT-ICR mass spectrometer. ESI MS experiments were performed on a Applied Biosystem API 2000 triple-quadrupole mass spectrometer. The spectra were recorded by infusion into the ESI source using MeOH as the solvent. Optical rotations were measured at 589 nm on a Perkin-Elmer 192 polarimeter using a 10-cm microcell. ^{1}H and ^{13}C NMR spectra were determined on Varian UnityInova spectrometers at 500 and 700 MHz; chemical shifts were referenced to the residual solvent signal (CD_3OD: δ_H = 3.31, δ_C =49.0). For an accurate measurement of the coupling constants, the one-dimensional ^{1}H NMR spectra were transformed at 128 K points (digital resolution: 0.05 Hz). Homonuclear ^{1}H connectivities were determined by COSY experiments. Through-space ^{1}H connectivities were evidenced using a ROESY experiment with a mixing time of 450 ms. The reverse single-quantum heteronuclear correlation (HSQC) spectra were optimized for an average $^{1}J_{CH}$ of 145 Hz. The multiple-bond heteronuclear correlation (HMBC) experiments were optimized for a $^{3}J_{CH}$ of 8 Hz. Spectral simulations were performed using Bruker's NMRSIM program. High performance liquid chromatographies (HPLC) were achieved on a Varian Prostar 210 apparatus equipped with an Varian 350 refractive index detector.

Collection, extraction and isolation

Specimens of *Tedania ignis* were collected in the Mangroves of Sweeting Cay (Grand Bahama Island) during the 2007 Pawlik expedition. They were frozen immediately after collection and kept frozen until extraction. The sponge (58 g of dry weight after extraction) was homogenized and extracted with MeOH (5 × 1 L) and then with $CHCl_3$ (2 × 1 L). The MeOH extracts were partitioned between H_2O and *n*-BuOH, and the BuOH layer was combined with the $CHCl_3$ extract and concentrated *in vacuo*. The organic extract (12.8 g) was chromatographed on a column packed with RP-18 silica gel. A fraction eluted with MeOH/H_2O 8:2 (195 mg) was subjected to HPLC separation on an RP-18 column [MeOH/H_2O (7:3)], thus affording a fraction (6.5 mg) mainly composed of compound **1a**. Final purification was achieved by preparative TLC (SiO_2, 20 × 20 cm, 0.5 mm thick) using BuOH/AcOH/H_2O (60:15:25) as eluent, which gave 3.1 mg of pure tedanol **1a**.

Tedanol (1a): Colorless amorphous solid, $[\alpha]_D^{25}$ = +6 (*c* = 0.1 in MeOH); HRESIMS (negative ion mode, MeOH) 541.0272 (M^-, $C_{20}H_{31}{}^{79}Br^{81}BrO_5S$ gives 541.0258); ESIMS (negative ion mode, MeOH) *m/z* 543, 541 e 539 (M^-); ^{1}H- and ^{13}C-NMR: Table 3.1.

Tedanol 7-*O*-Acetate (1b): Tedanol **1a** (0.6 mg) was dissolved in 500 µl of pyridine and 500 µl of acetic anhydride were added. The reaction was allowed to proceed for 18 h at room temperature, and the reaction mixture

was then dried under vacuum, giving 0.6 mg of tedanol 7-*O*-acetate (**1b**): colorless amorphous solid; ^{1}H-NMR (CD_3OD): δ 5.39 (1H, br. d, J = 6.3 Hz, H-11), 4.45 (1H, dd, J = 11.6 and 4.1 Hz, H-16a), 4.39 (1H, ddd, J = 10.8, 10.6, and 4.7 Hz, H-7), 4.36 (1H, dd, J = 8.2 and 4.1 Hz, -), 4.20 (1H, dd, J = 11.6 and 8.2 Hz, H-16b), 4.04 (1H, dd, J = 12.7 and 4.2 Hz, H-3), 2.66 (1H, m, H-8), 2.46 (1H, br. d, J = 17.4 Hz, H-12eq), 2.29 (1H, m, H-2ax), 2.17 (2H, overlapped, H-2ax and H-14eq) , 2.03 (1H, ddd, J = 12.5, 4.6 and 2.5 Hz, H-6eq), 1.84 (1H, ddd, J = 17.4, 3.5, and 2.2 Hz, H-12ax), 1.72 (2H, overlapped, H-1eq and H-6ax), 1.58 (1H, ddd, 13.3, 13.4 and 3.6 Hz, H1ax), 1.31 (1H, m, H-14ax), 1.160 (3H, s, H_3-18), 1.16 (1H, dd, J = 12.8 and 2.5 Hz, H-5), 1.055 (3H, s, H_3-20), 1.046 (3H, s, H_3-17), 0.998 (3H, s, H_3-19).

MTPA derivatization of tedanol.

Tedanol (0.4 mg) was dissolved in 500 µl of pyridine, and (*S*)-(+)-MTPA chloride (10 µl) was added. The reaction was allowed to proceed for 18 h at room temperature, and the reaction mixture was then dried under vacuum, giving, the 7-*O*-(*R*)-MTPA ester **1r**. The same procedure, using (*R*)-(–)-MTPA chloride, gave the 7-*O*-(*S*)-MTPA ester **1s**.

Tedanol 7-*O*-(*R*)-MTPA ester (1r): Colorless solid; ^{1}H-NMR (CD_3OD): δ 5.42 (1H, br. d, J = 6.3 Hz, H-11), 4.62 (1H, ddd, J = 10.9, 10.9, and 4.7 Hz, H-7), 4.36 (1H, dd, J = 11.6 and 3.1 Hz, H-16a), 4.33 (1H, dd, J = 9.0 and 3.1 Hz, H-15), 4.11 (1H, dd, J = 11.6 and 9.0 Hz, H-16b), 4.05 (1H, dd,

J = 12.6 and 4.2 Hz, H-3), 2.70 (1H, m, H-8), 2.47 (1H, br. d, *J* = 17.4 Hz, H-12eq), 2.26 (1H, dddd, *J* = 13.3, 13.3, 13.3, and 3.2 Hz, H-2ax), 2.17 (1H, dddd, *J* = 13.7, 3.9, 3.9, and 3.9 Hz, H-2eq), 2.01 (1H, ddd, *J* = 12.1, 4.6, and 2.4 Hz, H-6eq), 1.95 (1H, ddd, *J* = 13.8, 5.9, and 3.1 Hz, H-14eq), 1.85 (1H, ddd, *J* = 17.4, 3.1, and 2.4 Hz, H-12ax), 1.71 (1H, ddd, *J* = 13.4, 3.4, and 3.4 Hz, H-1eq), 1.62 (quartet, *J* = 12.2 Hz, H-6ax), 1.59 (1H, m, H-1ax) , 1.34 (1H, *J* = 13.8 and 10.7 Hz, H-14ax), 1.20 (1H, dd, *J* = 12.7 and 2.3 Hz, H-5), 1.11 (3H, s, H_3-18), 1.06 (3H, s, H_3-20), 1.00 (3H, s, H_3-17), 0.94 (3H, s, H_3-19).

Tedanol 7-*O*-(*S*)-MTPA ester (1s): Colorless solid; ^{1}H-NMR (CD_3OD): δ 5.37 (1H, br. d, *J* = 6.3 Hz, H-11), 4.52 (1H, ddd, *J* = 10.9, 10.9, and 4.7 Hz, H-7), 4.22 (1H, dd, *J* = 9.8 and 2.7 Hz, H-15), 4.04 (2H, overlapped, H-3 and H-16a), 3.88 (1H, dd, *J* = 11.9 and 9.8 Hz, H-16b), 2.57 (1H, m, H-8), 2.42 (1H, br. d, *J* = 17.4 Hz, H-12eq), 2.27 (1H, dddd, *J* = 13.3, 13.3, 13.3, and 3.2 Hz, H-2ax), 2.17 (2H, overlapped, H-2eq and H-6eq), 1.80 (1H, quartet, *J* = 12.1 Hz, H-6ax), 1.77 (1H, ddd, *J* = 17.4, 3.3, and 2.4 Hz, H-12ax), 1.70 (1H, ddd, *J* = 13.4, 3.4, and 3.4 Hz, H-1eq), 1.57 (1H, ddd, *J* = 13.4, 13.4, and 3.5 Hz, H-1ax) , 1.37 (1H, m, H-14eq), 1.21 (1H, dd, *J* = 12.7 and 2.4 Hz, H-5), 1.13 (3H, s, H_3-18), 1.09 (3H, s, H_3-20), 1.03 (1H, *J* = 13.9 and 10.9 Hz, H-14ax), 1.00 (3H, s, H_3-19), 0.85 (3H, s, H_3-17).

Table 3.1: ^{1}H and ^{13}C NMR data of tedanol **1a** (CD_3OD).

Position		δ_H [mult., *J* (Hz)]	δ_C [mult.]
1	ax	1.55 (ddd, 13.5, 13.3, 3.6)	39.6 (CH_2)
	eq	1.70 (ddd, 13.3, 3.6, 3.4)	
2	ax	2.27 (dddd, 13.6, 13.5, 12.7, 3.4)	32.4 (CH_2)
	eq	2.16 (dddd, 13.6, 4.2, 3.6, 3.6)	
3		4.02 (dd, 12.7, 4.2)	69.6 (CH)
4		-	40.8 (C)
5		1.08 (dd, 12.7, 2.5)	51.6 (CH)
6	ax	1.62 (ddd, 12.7, 12.7, 11.1)	33.8 (CH_2)
	eq	1.98 (ddd, 12.7, 4.7, 2.5)	
7		3.02 (ddd, 11.2, 9.7, 4.7)	78.3 (CH)
8		2.37 (dddddd, 10.7, 9.8, 5.9, 3.5, 1.7, 1.6)[a]	40.3 (CH)
9		-	148.1 (C)
10		-	40.1 (C)
11		5.31(ddd, 6.3, 2.0, 1.7)	115.9 (CH)
12	ax	1.82 (ddd,17.3, 3.5, 2.0)	39.7 (CH_2)
	eq	2.46 (ddd, 17.3, 6.3, 3.1, 1.6)	
13		-	36.7 (C)
14	ax	1.37(dd, 13.9, 10.7)[a]	39.4 (CH_2)
	eq	2.36 (ddd, 13,9, 5.9, 3.1)[a]	
15		4.37 (dd, 8.9, 3.4)	61.8 (CH)
16	a	4.49 (dd,11.8, 3.4)	70.8 (CH_2)
	b	4.19 (dd, 11.8, 8.9)	
17		1.06 (s)	24.6 (CH_3)
18		1.13 (s)	21.7 (CH_3)
19		1.01 (s)	18.7 (CH_3)
20		1.08 (s)	30.9 (CH_3)

Non-first-order multiplet, coupling constants determined by spectral simulation (see text and Figure13).

Mouse paw edema

Male CD-1 mice weighing 23-27 g were separated in groups (n = 6) and lightly anesthetized with enflurane. Each group of animals received subplantar injection of 50 µl of carrageenan 1% w/v. Paw volume was measured using a hydroplethismometer specially modified for small volumes (Ugo Basile, Milan, Italy) immediately before the subplantar injection and 2, 4,6, 24, 48 or 72h thereafter. The increase in paw volume was evaluated as difference between the paw volume at each time point and the basal paw volume. In another set of experiments, CD-1 were subjected to a previous intraperitoneal injection of tedanol **1a** (200 µl of water solution, 0.1–1 mg/kg), and after 30 minutes each group of animals received subplantar injection of 50 µl of carrageenan. Data are expressed as mean ± s.e. mean. The level of statistical significance was determined by two-way analysis of variance (ANOVA) followed by Bonferroni's test for multiple comparisons, using the GraphPad Prism software.

Western blot

Carragenan-injected paws from CD-1 mice sacrificed at 2, 4, 6 24, 48 and 72 hours were homogenised in a 10 mM HEPES pH 7.4 buffer containing saccharose (0.32M), EDTA (100µM), dithiothreitol (1 mM), phenylmethylsulfonyl fluoride (1 mg/ml) and leupeptin (10 µg/ml) using a Polytron homogenizer (3 cycles of 10 seconds at maximum speed). After centrifugation at 3000 rpm for 15 min, protein supernatant content was measured by Bradford reagent, and protein concentration was adjust at 30

μg. Protein samples were loaded on 10% PAGE-SDS and transferred onto nitrocellulose membranes for 45 min at 250 mA. Membranes were blocked in PBS-Tween 20 (0.1%) containing 5% non-fat milk and 0.1% BSA for 30 min at 4°C. Membranes were washed with PBS-Tween 20 (0.1%) at 5 min intervals for 30 min, and incubated with anti-COX-1, anti-COX-2, anti-iNOS, and anti-eNOS overnight at 4°C. Blots were washed with PBS-Tween 20 (0.1%) at 5 min intervals for 30 min and incubated with HRP-anti-rabbit IgG (1:20000) for 2 h at 4°C. The immunoreactive bands were visualized using an enhanced chemiluminiscence system (ECL; Amersham, USA).

MPO measurement

Mice from different groups were sacrificed with CO_2 at 2, 4, 6 24, 48 and 72 hours after carrageenan injection. Injected paws were cut, weighted and homogenated in 1 ml of HTAB buffer using a Polytron homogenizer (2 cycles of 10 seconds at maximum speed). After centrifugation of homogenates at 10000 rpm for 2 minutes, supernatant fractions were assayed for MPO activity using the method described by Bradley et al..[26] Briefly, samples were mixed with phosphate buffer containing 1mM *O*-dianisidine dihydrochloride and 0.001% hydrogen peroxide in a microtiter plate reader. Absorbance was measured at 450 nm taking three reading at 30 seconds intervals. Units of MPO were calculated considering that 1 U. MPO

[26] Posadas, I.; Terencio, M.C.; Guillén, I.; Ferrándiz, M. L.; Coloma, J.; Payá, M.; Alcaraz, M. J. *Naunyn-Schmied. Arch. Pharmacol*. **2000**, *361*, 98–106

= 1 μmol H_2O_2 split , and 1 μmol H_2O_2 gives a change in absorbance of 1.13 $\times 10^{-2}$ nm/min.

3.7 NMR data

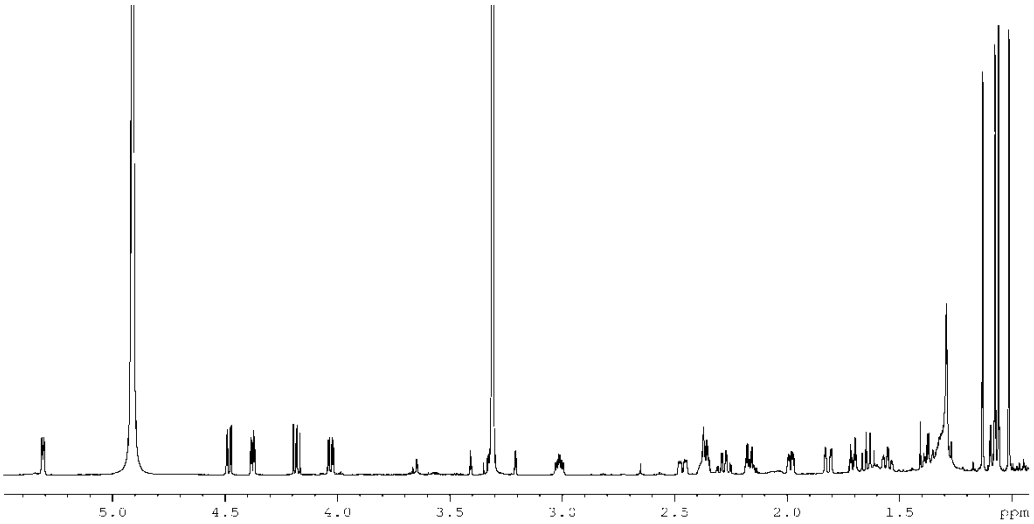

^{1}H NMR spectrum (700 MHz, CD_3OD) of tedanol (**1a**)

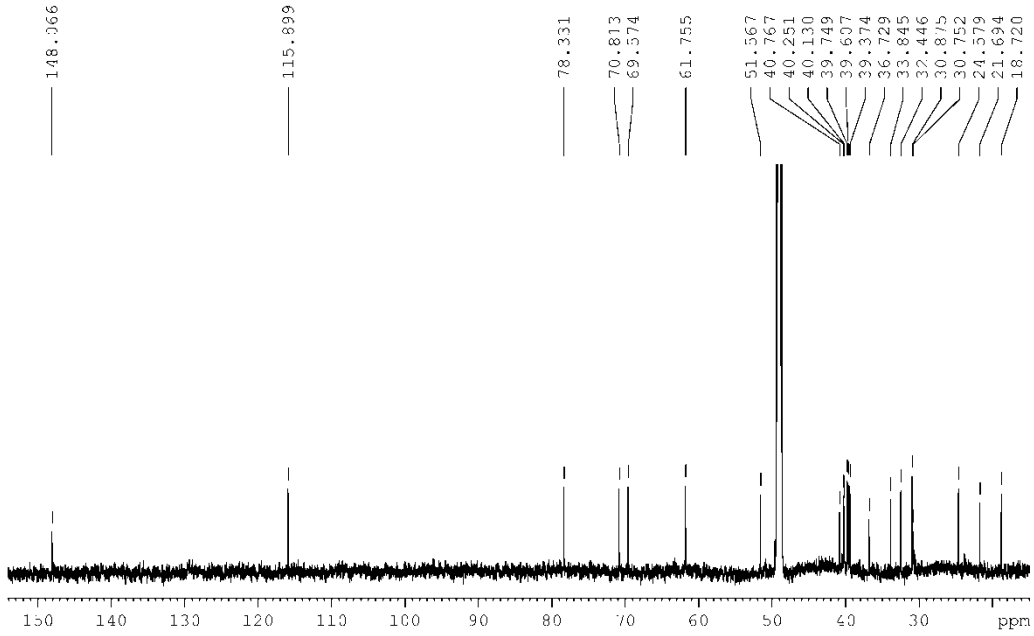

^{13}C NMR spectrum (125 MHz, CD_3OD) of tedanol (**1a**)

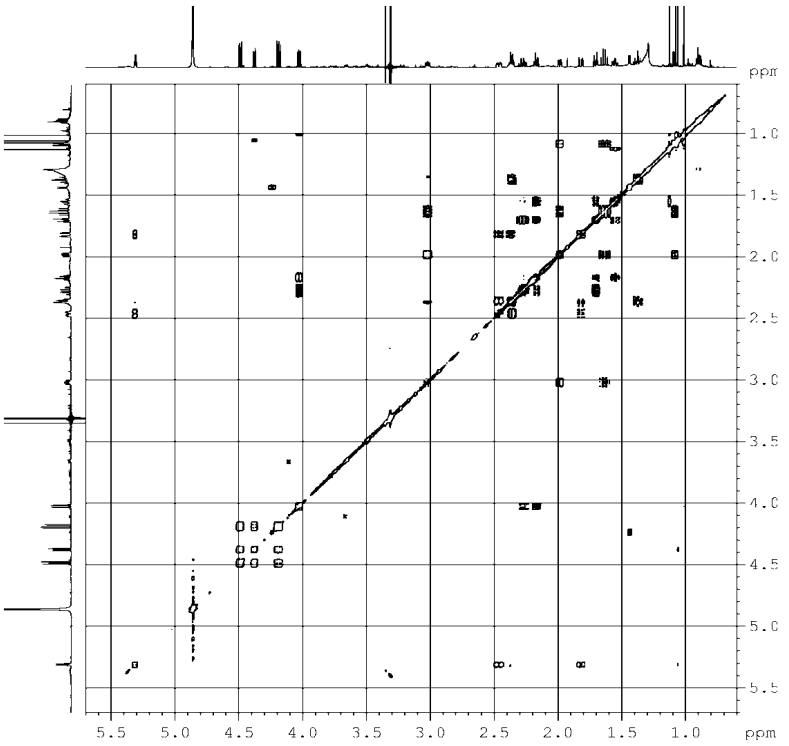

COSY spectrum (500 MHz, CD_3OD) of tedanol (**1a**)

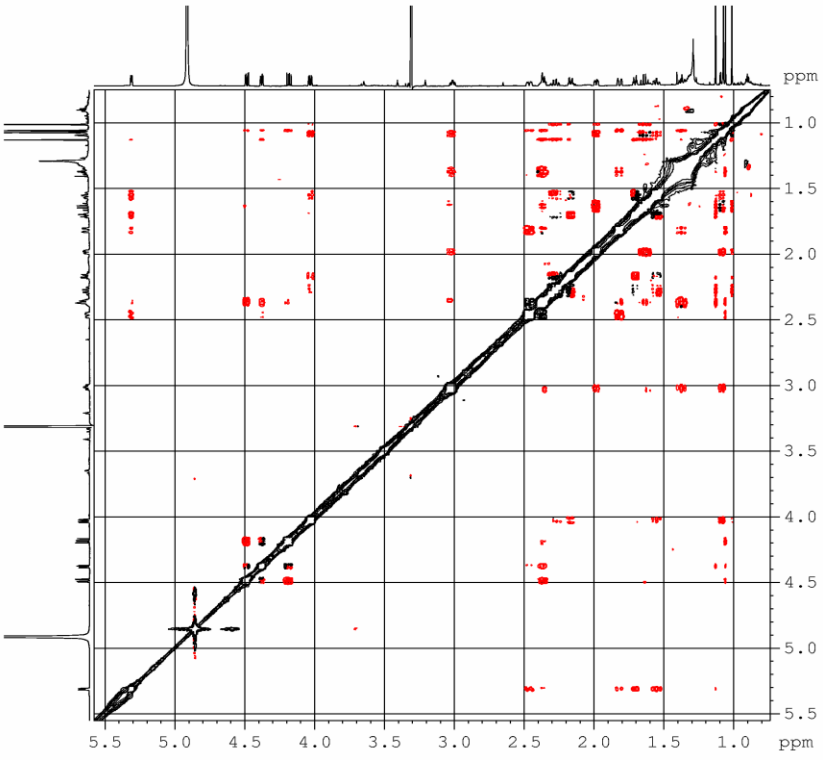

ROESY spectrum (500 MHz, CD_3OD) of tedanol (**1a**)

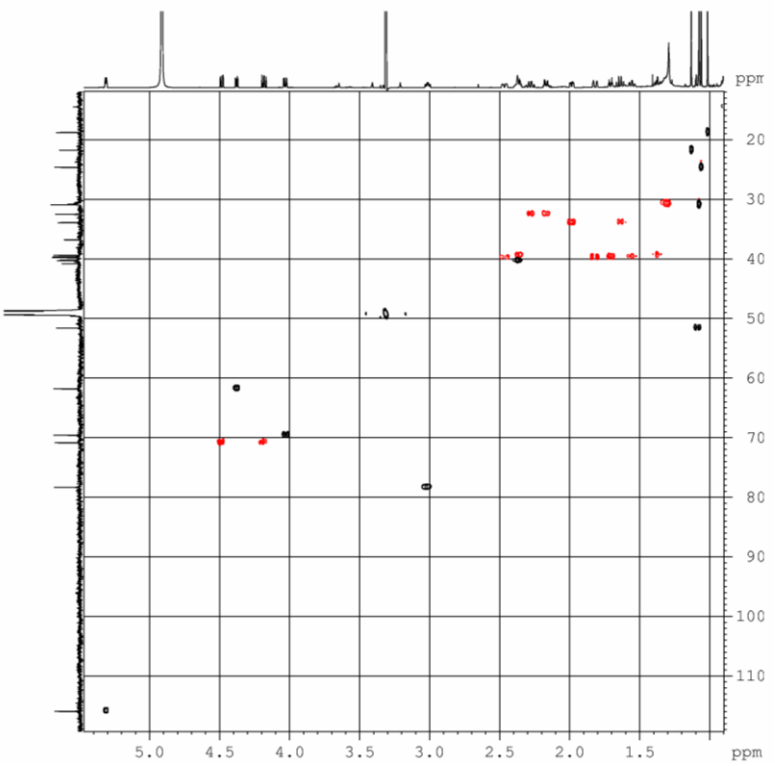

HSQC spectrum (500 MHz, CD_3OD) of tedanol (**1a**)

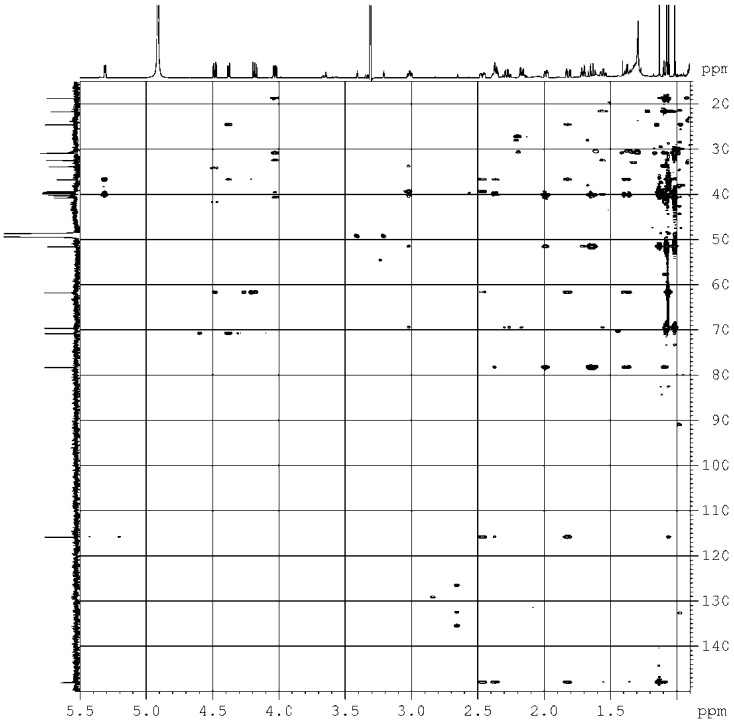

HMBC spectrum (700 MHz, CD_3OD) of tedanol (**1a**)

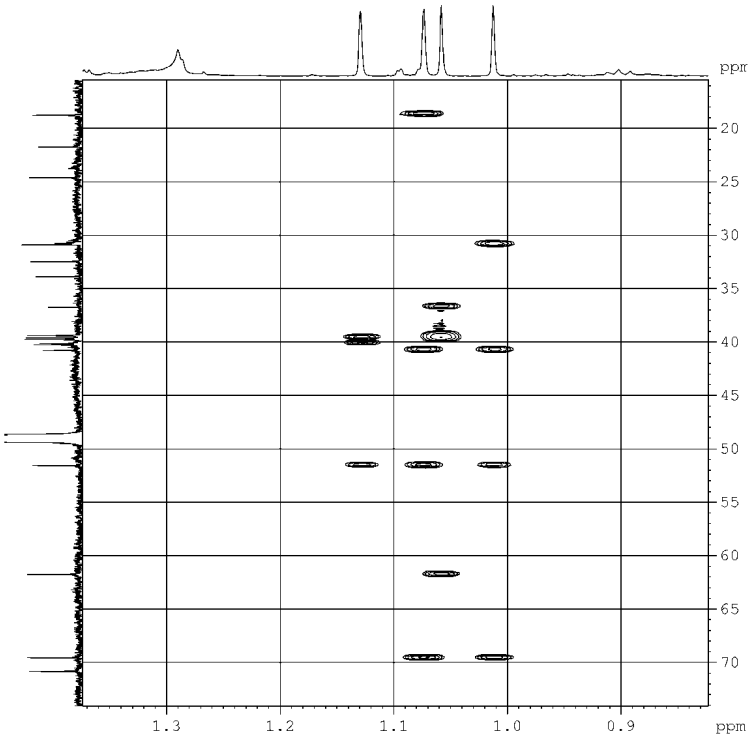

HMBC spectrum (700 MHz, CD_3OD, methyl region) of tedanol (**1a**)

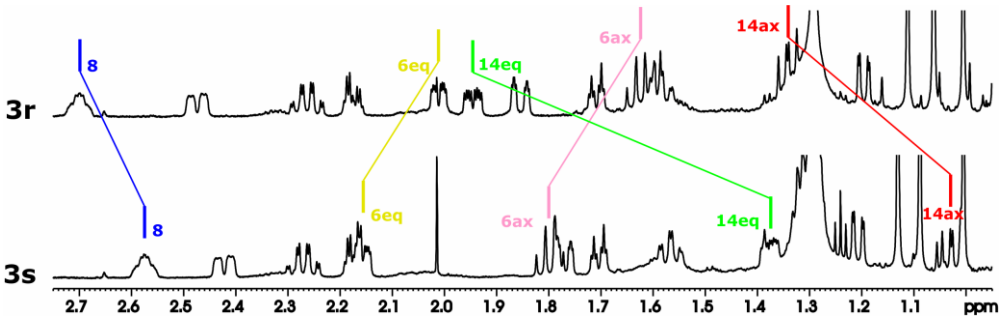

^{1}H NMR spectra (700 MHz, CD_3OD) of tedanol MTPA derivatives **1r** and **1s**

Chapter 4

Analysis of the sponge *Tedania ignis* part II

In addition to tedanol (see Chapter 3), from the sponge *Tedania ignis* two novel compounds named tedarene A and tedarene B, belonging to a class of diarylheptanoids, were isolated.

Diarylheptanoids (DHs) are a class of natural products mainly found in terrestrial plants of the families Betulaceae, Aceraceae, Myricaceae, Zingiberaceae and Dioscoreaceae. The structure of this class of compounds is based on 1,7-diphenyleptane skeleton and they are classified in linear and cyclic types. The latter are formed from the corresponding linear type by phenolic oxidative coupling, either C–C coupling leading to *meta*, *meta*-bridged biaryls, or C–O coupling leading to bridged biaryl ethers.[27] The linear diarylheptanoids are widely spread, while the cyclic types are rare, and especially the biaryl ether types are scarcely found in nature.

These compounds are particularly interesting because they have been reported to possess various biological activities, including leishmanicidal and antiprotozoal, antitumor, antioxidant, anti-ischemic, anti-inflammatory.[28] Recently, the Myricanins and the Acerosides, cyclic diarylheptanoids isolated from the roots of *Myrica nana* and the stem bark

[27] Henley-Smith, P.; Whiting, D. A.; Wood A. F. *J. Chem. Soc., Perkin Trans. 1*, **1980**, 614–622.
[28] Takahashi, M.; Fuchino, H.; Sekita, S.; Satake, M. *Phytother. Res.* **2004**, *18*, 573–578.

of *Acer nikoense* respectively, showed inhibitory effects against nitric oxide production.[29]

Tedarene A and tedarene B are two cyclic diaryheptanoids, diaryl ether and diphenyl types respectively. Considering the inhibitory effects against nitric oxide production already reported for compounds belonging to this class, the potential inhibitory activity on iNOS was investigated testing both compounds.

4.1 New cyclic diarylheptanoids: tedarene A and B

To the best of our knowledge, tedarene A (**1**) and B (**2**) represent the first diarylheptanoids reported from marine organisms. The two compounds differ mainly for the type of cyclization. Tedarene A has the two phenyl rings linked through C–O linkage, while tedarene B presents a C–C linkage leading to *meta*, *meta*-bridged biaryls. Moreover, in tedarene B there is an additional five-membered ring and a sulfate group (Figure 4.1).

Tedarene A and B turned out to be very interesting for their structures which required Dynamic NMR experiments, molecular dynamics studies and quantum mechanical calculations.

Their inhibitory effects against nitric oxide production in lipopolysaccharides activated macrophages were investigated. Tedarene A showed a significant inhibition of NO_2^- production, while tedarene B was inactive.

[29] Wang, J.; Dong, S.; Wang, Y.; Lu, Q.; Zhong, H.; Du, G.; Zhang, L.; Cheng, Y., *Bioorganic & Medicinal Chemistry,* **2008**, *16*, 8510–8515.

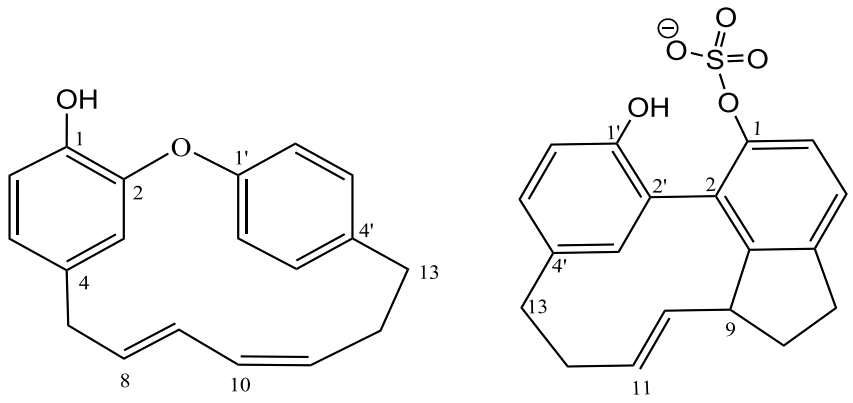

Figure 4.1: Structures of compounds **1** and **2**

4.2 Isolation of tedarene A and B

Samples of *Tedania ignis* were collected in the mangroves of Sweeting Cay (Grand Bahamas Island) during the 2007 Pawlik expedition. Freshly specimens were frozen on site, transferred to our lab in Naples (Italy) over dry ice and kept at –20 °C until the extraction. The sponge was chopped while still frozen and extracted in sequence with MeOH and $CHCl_3$. The MeOH extract was partitioned between water and *n*-BuOH, and the BuOH and $CHCl_3$ extracts were combined and subjected to reversed-phase column chromatography. The fraction eluted with H_2O/MeOH 2:8 contained a mixture of DHs. Reversed-phase HPLC of this fraction (RP-18, MeOH-H_2O 7:3) gave partially purified tedarene A (**1**) and B (**2**)

Pure compound **1** was obtained by HPLC on silica column using as eluent *n*-hexane-isopropanol 95:5. Instead, compound **2** was subjected to an analytical reversed-phase HPLC (MeOH-H_2O 1:1), followed by HPLC on PFP column (MeOH-H_2O 1:1), reaching pure form.

4.3 Structure determination of tedarene A

The positive-ion ESI mass spectrum of tedarene A (**1**) showed an intense pseudomolecular ion peak $[M+Na]^+$ at *m/z* 301. A high resolution mass measurement (*m/z* 301.1205) accounted for the molecular formula $C_{19}H_{18}O_2Na$.

A preliminary ^1H NMR analysis of compound **1** showed characteristic signals of aromatic (δ 6.5-7.5) and olefinic (δ 5-6) protons.

A COSY (CD_3OD, 20 °C) experiment led to the identification of a conjugated diene system between C-8 and C-11, with two methylenes at both ends. The configuration of the double bond at the position 8 was determined as *trans* (*J* = 15,1 Hz between H-8 and H-9), while the configuration at the position 10 was defined as *cis* (*J* = 11 Hz between H-10 and H-11).

The double doublet centered at δ 6.52 (*J* = 7.8 Hz and 1.2 Hz), the doublet at δ 6.64 (*J* = 7.8 Hz) and the broaden signal at δ 5.37 (anomalous chemical shift for an aromatic proton) were assigned to H-5, H-6 and H-3 respectively, and were demonstrative of the 1,2,4-trisubstituted benzene ring. The chemical shifts of C-1 (δ 151.5) and C-2 (δ 154.0) suggested the possible link of these carbons to oxygen atoms.

HMBC correlations of H_2-7 (δ 2.96) with C-3 (δ 117.6) and C-5 (δ 121.5) showed the connection between the carbon C-7 of alkyl chain and the carbon C-4 of benzene ring, confirmed by the long range coupling between methylene protons H_2-7 (δ 2.96) and aromatic protons H-3 (δ 5.37) and H-5 (δ 6.5) in the COSY spectrum.

In mono- and two-dimensional NMR experiments performed at room temperature, signals of ring B and of the attached methylene group (C-13) were very broad, enough to be confused with the base line of the ^{1}H-NMR spectrum, thus preventing the elucidation of this part of molecule. One of the possible explanations of these very broad signals is an equilibrium between two conformers, at an interconversion rate at which coalescence of exchanging proton signals occurs.

Generally speaking, a molecule can undergo fluxional processes by interchanging two or more sites. If the exchange rate is much faster than NMR time scale, the two (or more) different groups will appear at an average chemical shift. In contrast, if the exchange rate is much slower than NMR time scale, separate NMR signals are obtained. The exchange rate depends on the energy barrier between the conformers and on the temperature.

The well known example of undecadeuterocyclohexane is often used to demonstrate the equilibrium between the two chair conformations of cyclohexane. At very low temperature (less than –70 °C), the equilibrium between the two chair conformations of cyclohexane is very slow (slow exchange limit) and two lines appear, one for the equatorial hydrogen and one for the axial hydrogen. At higher temperature (–50 °C and above) the equilibrium is fast (fast exchange limit) and one averaged signal is observed. At intermediate temperature, the exchange rate is comparable to NMR time scale. In this conditions, the two signals coalesce and very broad lines are observed (Figure 4.2).

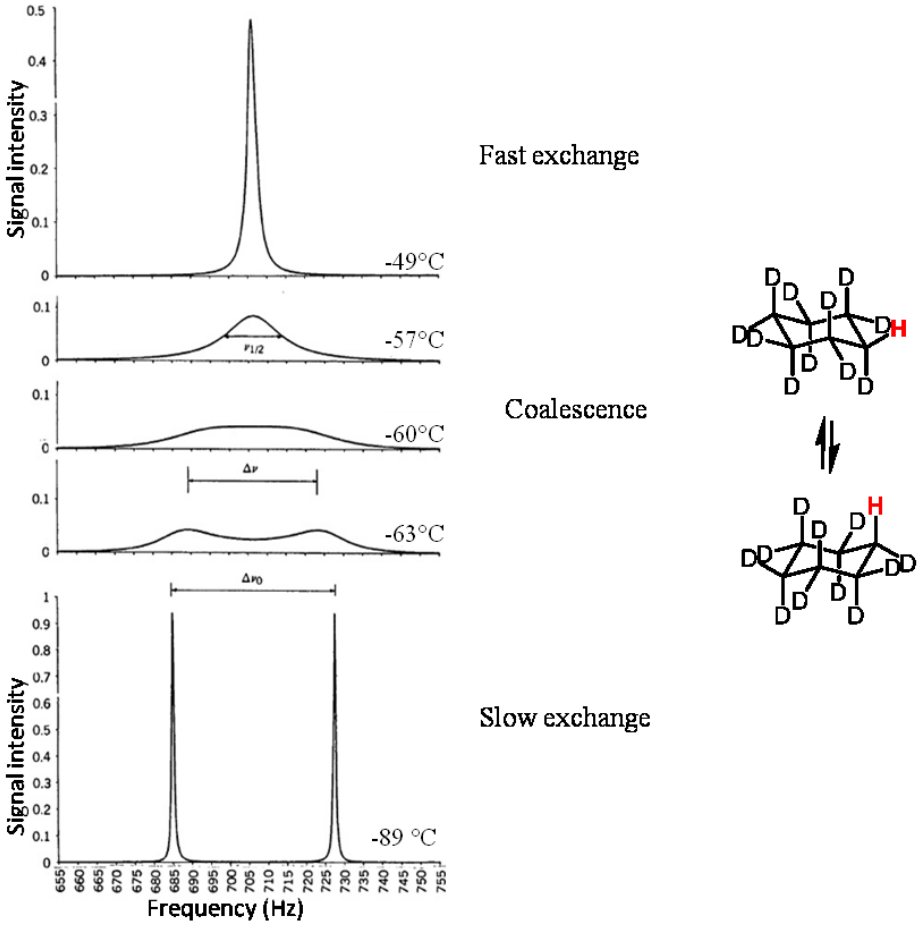

Figure 4.2: The NMR lineshape for exchange between two equally populated sites.

This is what was observed at room temperature in the ^{1}H and ^{13}C NMR spectra of tedarene A (**1**). Therefore, in order to complete the structure elucidation of compound **1**, NMR experiments at low and high temperatures were performed.

In ^{1}H-NMR experiments carried out at –40 °C, the molecule was in the slow exchange limit, resulting in sharp signals for all protons (Figure 4.3). In the low-field region, four additional well-defined signals appeared [H-2′ (δ 7.06), H-3′ (δ 7.38), H5′ (δ 7.08), H-6′ (δ 6.81)], while in the high-field

region two additional signals appeared at δ 3.06 and 2.52 (H-13a and H-13b, respectively).

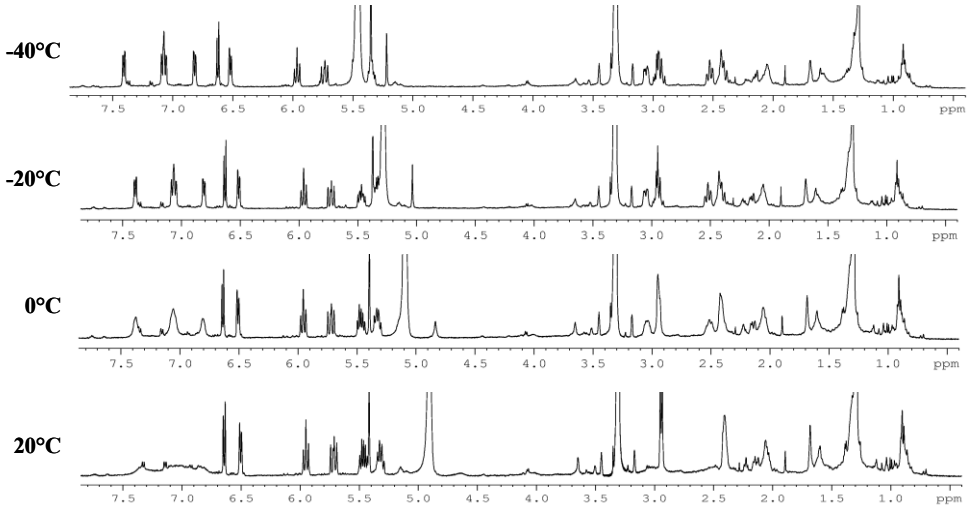

Figure 4.3: ^{1}H-NMR spectra at low temperatures of compound **1** in CD_3OD

A similar behavior was shown by with the ^{13}C spectrum. At -40 °C, four carbon signals at δ 123.8, δ 125.6, δ 131.5, δ 133.3 appeared, which had been completely undetectable in the spectrum recorded at room temperature. They were assigned to C-6′, C-2′, C-5′ and C-3′ respectively (Figure 4.4).

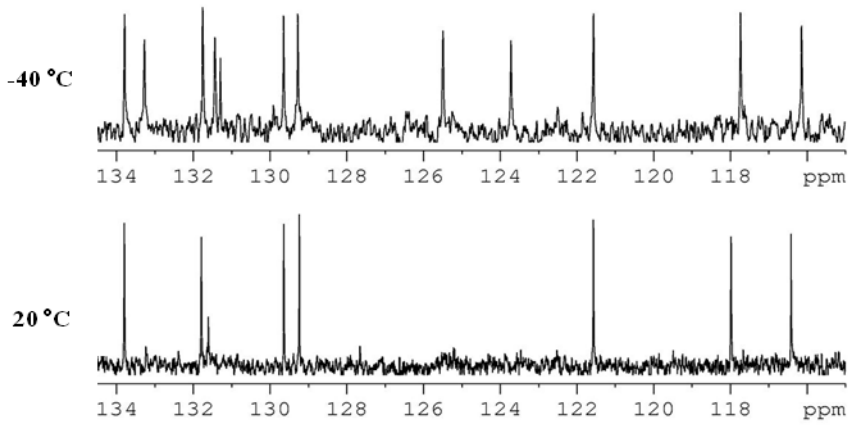

Figure 4.4: ^{13}C NMR spectra at -40 °C and 20 °C in low field region (CD_3OD).

The presence of a *para*-disubstitute aromatic ring was established by means of a COSY experiment recorded at –40°C: H-2′ (J = 8.3 Hz and 1.9 Hz) and

H-3′ (*J* = 8.3 Hz and 1.5 Hz) are in the *ortho* position, as well as H-5′ (*J* = 8.3 Hz and 1.3 Hz) and H-6′ (*J* = 8.3 Hz and 1.9 Hz). The COSY also displayed the coupling between H_2-12 (δ 2.41) and the protons H-13a (δ 3.06) and H-13b (δ 2.52). In the HMBC spectrum (recorded at –23°C because this temperature can be kept for a longer time on our NMR spectrometer) H-13a (δ 3.06) showed correlations peaks with the C-3′ (δ 131.5), C-4′ (δ 140.9), C-5′ (δ 133.3) and C-11 (δ 129.4), which allowed to connect the alkyl chain to the second aromatic system (ring B).

The ^{13}C NMR spectrum exhibited signals for three carbons linked to oxygen at δ 151.5, δ 154.0 and δ 156.3 (C-1, C-2 and C-1′, respectively). The presence of only two oxygen atoms in the molecular formula suggested the connection of the two rings through an ether bridge. The ROESY experiment showed a correlation peak between H-3 (δ 5.37) and H-6′ (δ 6.81). This allowed us to locate the biaryl ether bridge between C-2 and C-1′, and not between C-1 and C-1′, because the latter linkage would have made geometrically impossible the spatial proximity of the two protons.

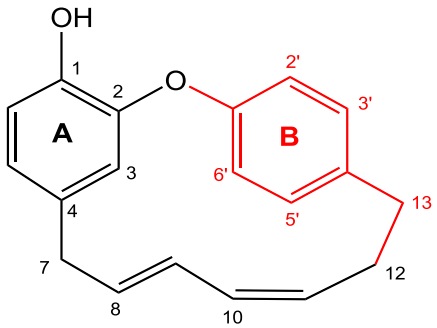

Figure 4.5: Full structure of tedarene A (**1**). Part structure determined from NMR experiments at room temperature is drawn in **black**, and part structure from NMR experiments at low temperature is drawn in **red**.

The full structure of tedarene A (**1**) was thus defined (Figure 4.5). To get further evidence of the conformational equilibrium, and to get insight on its nature, NMR experiments at high temperatures were also performed (Figure 4.6).

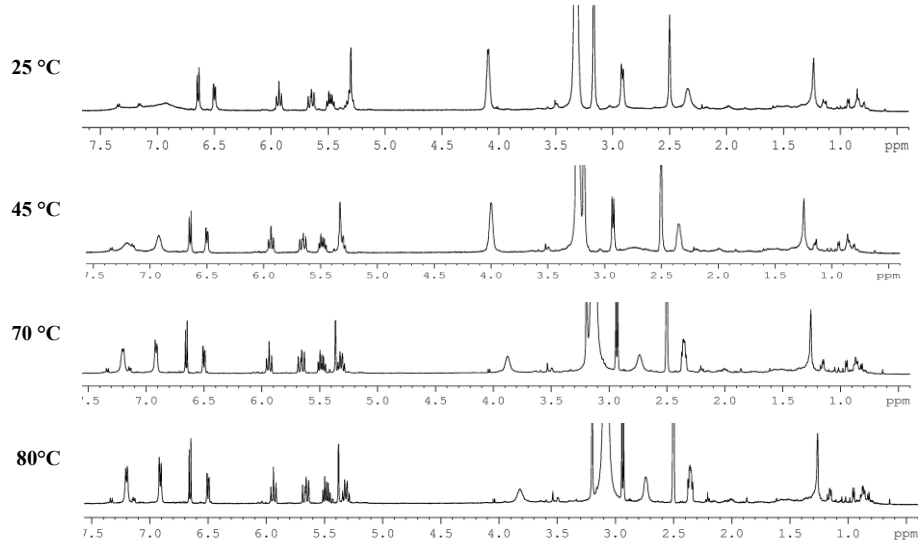

Figure 4.6: ^{1}H-NMR spectra at high temperatures of tedarene A (**1**) in DMSO-d_6

In the experiment recorded at +80 °C (DMSO-d_6), only sharp signals were observed; for each of the three methylene groups, the two protons were equivalent and gave rise to single signals, as H2′/H-6′ (δ 6.91) and H-3′/H-5′ (δ 7.20) did. This means that, at this temperature, the conformational equilibrium is fast, and the chemical shifts are averaged.

In contrast, in the experiment recorded at -40 °C (CD_3OD), each of the three methylene groups showed two diastereotopic protons. In addition, H-2′ and H-3′ resonated at chemical shifts different from those of the apparently symmetric H-6′ and H-5′, respectively.

In summary, all three methylene groups have diastereomeric protons, which should not happen in a planar molecule such as tedarene A, and indeed does

not happen at high temperature; each pair of diatereotopic protons exchange their chemical shift when the conformation change occurs. The same applies to the apparently symmetric para-disubstituted benzene ring (Figure 4.7). Although at room temperature the protons of ring B and methylene groups coalesce, most protons and carbons in the molecule do not. The chemical shift of the latter nuclei, therefore, does not change upon conformational change.

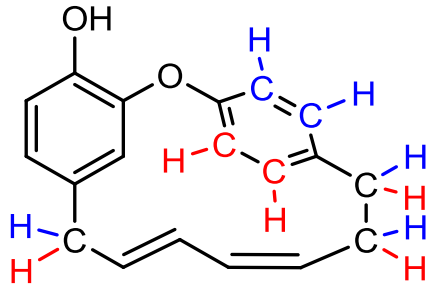

Figure 4.7: Apparently symmetric protons (blue and red) of compound **1**.

On the whole, these results are a clear indication that, while structure **1** appears non-chiral, compound **1** exists in two slowly interconvertible chiral (because methylene protons are diastereomeric) and enantiomeric (because many protons keep their chemical shift) conformers.

A conformational analysis performed in the MM2 force field using the Chem3D software showed indeed that there are only two reasonable conformations for tedarene A, and they are enantiomeric to each other (Figure 4.8).

The two conformations are in agreement with data obtained from the ROESY spectrum, recorded at –40°C. The spectrum showed intense correlation peaks of H-3 (δ 5.37) with H-9 (δ 5.71), and of H-5′ (δ 7.08) with H-13b (δ 2.52) and H-12 (δ 2.41).

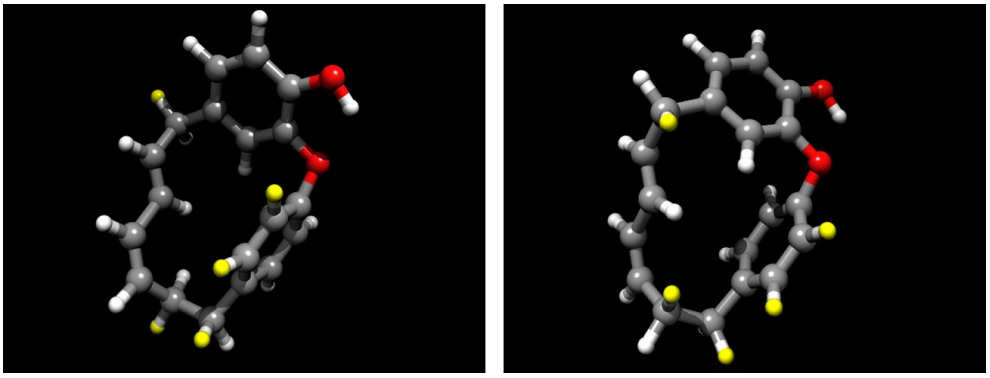

Figure 4.8: The two conformations in agreement with experimental ROESY correlation peaks.

The reason why the chemical shift of the proton H-3 (δ 5.37) is abnormally low for an arylic proton is also explained by these conformers. In fact, in both conformers H-3 is located just on the top of ring B, and is therefore strongly shielded by its ring current.

Tedarene A (**1**) exists in two chiral enatiomeric conformers in slow equilibrium, and this kind of molecules is not rare in nature. In most cases, however, this equilibrium is much faster than NMR time scale, so the NMR spectrum exhibits averaged chemical shifts and coupling constants. In the case of tedarene A (**1**) the interconversion between conformers is hindered by the cyclic strain of its cyclophane structure, causing a relatively high energy barrier between the two conformers. At room temperature the exchange rate is such that the ^{1}H and ^{13}C spectra of the molecule are the coalescence region, hiding some of the signals in the spectrum.

This phenomenon, together with the fact that it involves only some of the signals in the NMR spectra, made the structural elucidation of this apparently simple molecule a challenging problem, and shows that a clear

comprehension of dynamic processes in NMR may be important in the structure elucidation of natural products.

4.4 Structure determination of tedarene B

The negative-ion ESI mass spectrum of compound **2** (Figure 4.1) showed a M^- molecular ion peak at 357 *m/z* (100%), with isotopic peaks at 358 *m/z* (about 24%) and 359 *m/z* (about 3.8%). A high-resolution measurement on the ion at *m/z* 357 (*m/z* 357.0796) determined the formula $C_{19}H_{17}O_5S$ (calcd. 357.0802).

Two set of signals were present in the ^1H and ^{13}C NMR spectra of tedarene B (**2**), showing it to exist as a mixture of two conformers in slow equilibrium (half-life of days). The ratio of 4:1 between the two conformers was established by integration of the ^1H-NMR spectrum. In the following discussion, the most abundant conformer is called major conformer, while the other is named minor conformer.

The ^1H-NMR spectrum recorded just after purification contained only signals of the main conformer. However, after few days at room temperature the signals of minor conformer appeared again. Thus, even though the interconversion is slow on the NMR time scale, it is still fast enough not to allow separate structural studies.

^1H- and ^{13}C-NMR signals of the major conformers were studied and assigned first (Table 4.2). Analysis of COSY spectrum and chemical shifts, combined with calculation of coupling constant, allowed to identify two aromatic rings. The doublet at δ 6.08 (H-3′, J = 2.1 Hz) and at δ 6.80 (H-6′, J

= 8.1 Hz), and the double doublet at δ 6.96 (H-5′, J = 8.1 Hz and 2.1 Hz) were suggestive of 1,2,4-trisubstituted benzene (ring A), while the signals resonating at δ 7.20 (H-5, J = 8.3 Hz) and at δ 7.46 (H-6, J = 8.3 Hz and 1.0 Hz) were assigned to ring B, a 1,2,3,4-tetrasubstituted benzene. The relevant sp^2 carbon atoms C-3' (δ 145.1), C-5' (δ 129.2), C6' (δ 118.3), C-5 (δ 125.4) and C-6 (δ 120.5) were assigned by means of a HSQC experiment.

In addition, the chemical shift of the methine sp^2 carbon atoms C-11 (δ 126.0) and C-10 (δ 140.6) were demonstrative of the presence of a double bond. HSQC correlations have shown their connection to H-11 (δ 5.34) and to H-10, respectively. The latter resonated at 3.86 ppm, a very shielded chemical shift for an olefinic proton. The configuration of the double bond was defined as *trans* on the base of the large coupling constant (16.6 Hz) between H-10 and H-11.

Taking into account the molecular formula, two more insaturations needed to be assigned. By means of COSY and HMBC correlations, the aliphatic chain C-7/C-13 was defined, whose ends were bound to the benzene rings.

Specifically, the proton H-7α at δ 2.86 showed HMBC correlations with C-3 (δ 150.4), C-4 (δ 142.5), C-5 (δ 125.4), C-8 (δ 32.9) and C-9 (δ 48.3). In the ROESY spectrum, an intense correlation peak between H-7α (δ 2.86) and H-5 (δ 7.20) suggested the bond of C-7 with C-4 (H-5 is ortho position), and this was confirmed by the long range coupling between H-7α and H-5 observed in the COSY spectrum.

HMBC interactions of H-13α (δ 2.88) with C-3' (δ 145.1), C-4' (δ 131.9) and C-5' (δ 129.2) were demonstrative of the link between C-13 and C-4′.

Moreover, HMBC spectrum evidenced correlations peaks of H-8 (δ 1.98) with C-3 (δ 150.4) and C-4 (δ 142.5), and of H-9 (δ 3.35) with C-3, which supported a further link of aliphatic chain to the benzene ring B: the carbon C-9 and C-3 are linked, giving rise to a further five terms ring.

Finally, HMBC interaction of H-3' (δ 6.08) with C-2 (δ 130.8) proved the link of C-2 to C-2′, showing that tedarene B is a cyclic diarylheptanoid originated by C-C coupling of the two benzene rings.

The last two quaternary carbons were assigned to C1 and C1′. According to their chemical shifts and to molecular formula, they must be bound to one hydroxyl and one sulfate groups. The hydroxyl group was located at position C-1′ on the base of the chemical shift of proton H-6′ (δ 6.8) at ortho position, while the sulfate group was assigned to C-1, because the vicinal proton resonated at a higher chemical shift (H-6, δ 7.46).

The structure of minor conformer was determined in a similar way, and all the signals in the ^{1}H and ^{13}C NMR were assigned. The main difference between the two conformers is the chemical shifts of the olefinic protons. In the minor conformer, H-10 resonated at 5.11 ppm, while it was H-11 to resonate at an abnormally low chemical shift (δ 3.96). Even for this conformer the configuration of the double bond was defined as *trans* (J = 15.6 Hz) (Figure 4.9).

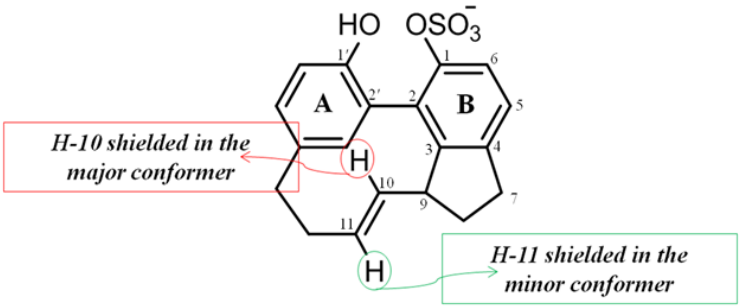

Figure 4.9: Main difference between major and minor conformers of compound **2**.

The nature of the two conformers was investigated by means of Rotating-frame Overhauser Effect (ROE) measurements and conformational analyses. These latter were carried out by means of molecular mechanics studies in the CVFF force field using the molecular modeling program Insight II. A high temperature molecular dynamics simulation was carried out to explore the conformational space of tedarene B. The temperature of the simulation was kept very high (2000 K) to overcome the high energy barrier between the conformers evidenced by their very slow interconversion. The simulation was 100 ns long, and 200 structures were obtained by saving the coordinated every 500 ps. The obtained structure were allowed to relax at 300 K for 10 ps and then minimized. Analysis of the structures obtained in this way showed that four reasonable conformations for tedarene B (**2**) are possible (Figure 4.10 ***a-d***).

Flipping of the double bond is the main difference between ***a*** and ***b*** and between ***c*** and ***d*** (H-9 and H-10 are *syn* in ***a*** and ***d***, *anti* in ***b*** and ***c***), while conformations ***a*** and ***b*** differ from ***c*** and ***d*** for the relative orientation of the phenyl rings, leading to an opposite helicity of the diphenyl system in the two groups of conformations.

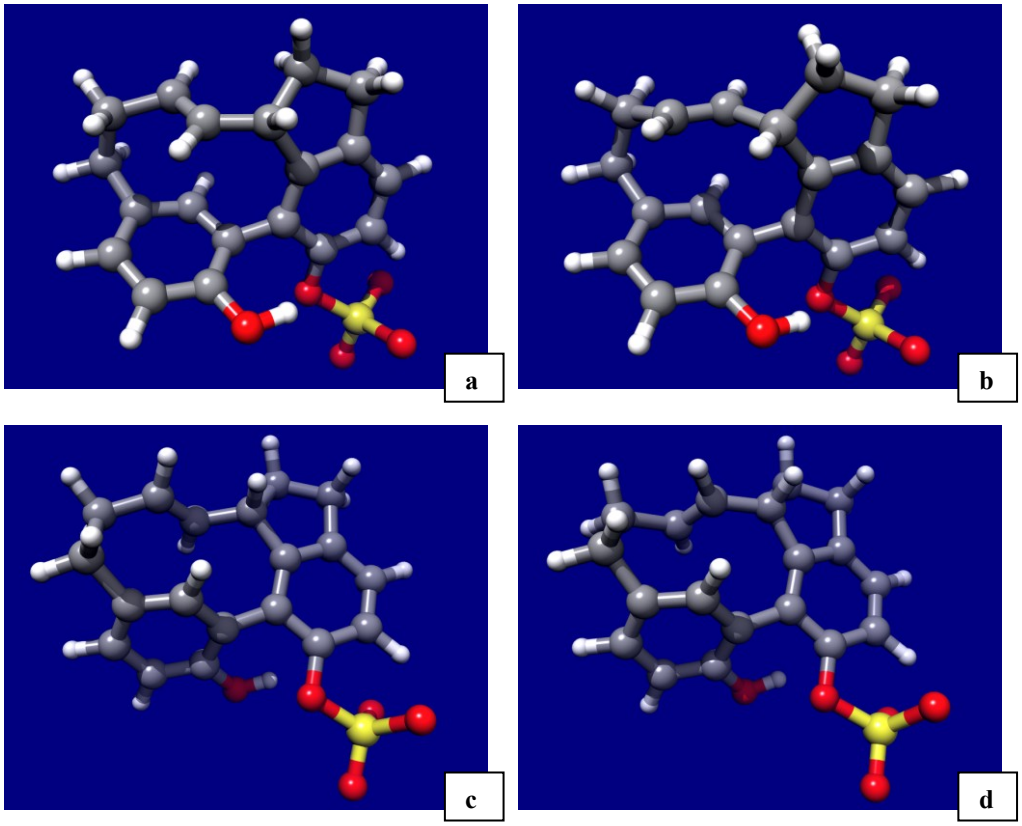

Figure 4.10: The four possible conformations ***a-d*** of tedarene B (**2**)

In conformations ***a*** and ***c***, H-10 lies in the shielding cone of phenyl ring A. Therefore, this proton is expected to be strongly shielded, as observed in the major conformer of compound **2**. Several ROESY correlations peaks between protons of the major conformer [namely H-10 (δ 3.86) with H-9 (δ 3.35) and H-12α (δ 2.48), and H-11 (δ 5.34) with H-3' (δ 6.08), H-8α (δ 2.17), and H-12β (δ 1.49)] were fully accounted for by conformation ***a***, but not by conformation ***c***, showing that the conformation ***a*** is the actual conformation of the major conformer of tedarene B (Figure 4.11).

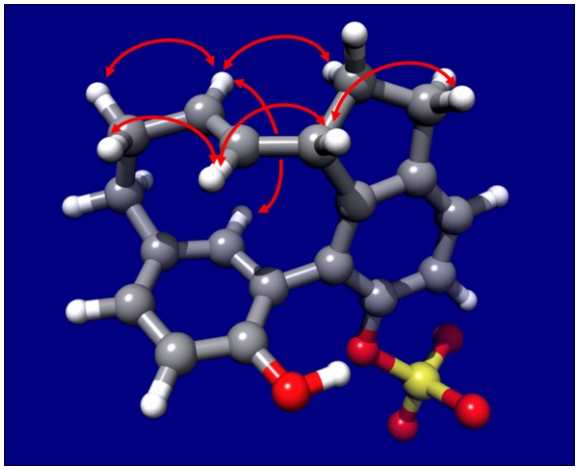

Figure 4.11: Conformation of the major conformer of tedarene B (**2**) in agreement with experimental ROESY correlations.

In contrast, in conformations ***b*** and ***d*** the proton H-11 is shielded, as observed in the minor conformer of compound **2**. The ROESY correlation peaks between the signals of the minor conformer [H-11 (δ 3.96) with H-12α (δ 2.31) and H-9 (δ 3.25), and H-10 (δ 5.11) with H-12 β (δ 2.29) and H-3' (δ 6.56)] can only be accounted for by conformation ***b***, which is therefore the minor conformation of compound **2** (Figure 4.12).

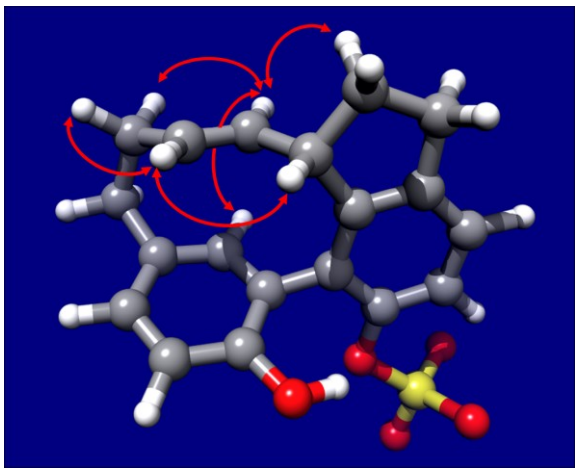

Figure 4.12: Conformation of the minor conformer of tedarene B (**2**) in agreement with experimental ROESY correlations.

Tedarene B (**2**) is optically active ($[\alpha]_D^{25}$ +33) in that it contains the stereogenic carbon C-9. Its absolute configuration was determined by circular dichroism measurement. A search in the literature showed that no CD was available of a compound close enough to tedarene B as to be used as a model compound. Therefore, the CD spectrum of tedarene B was predicted theoretically by quantum mechanics using the Gaussian 03 software. We used density functional theory (DFT) metods, with the B3LYP functional and the 6-31G* basis set. The calculations were carried out on the *S* enantiomer. The geometry of conformers ***a*** and ***b*** was optimized, and then the CD spectrum was calculated for each conformer. The software SpecDis version 1.45 (T. Bruhn, Y. Hemberger, A. Schaumlöffel, G. Bringmann, SpecDis, Version 1.45, University of Wuerzburg, Germany, 2009) was used to produce a CD curve from the rotational strength values of electronic transitions provided by the Gaussian calculations.

The CD spectrum of tedarene B mainly originates from the interaction between the two phenyl rings. Therefore the two conformers ***a*** and ***b***, that have the same helicity of diphenyl system, showed very similar CD spectra. The calculated CD spectrum to be compared with the experimental spectrum was obtained as the mean of the CD spectra calculated for the two conformers, weighed by their relative abundance as determined by ^{1}H NMR (Figure 4.13a).

Even though the relative intensity and the maxima of the three bands are somehow different, the predicted spectrum has the same general aspect of the experimental spectrum (Figure 4.13b), with the same sign for each of the

three bands. Therefore, tedarene B has the same *S* absolute configuration as the models used for calculations (Figure 4.14).

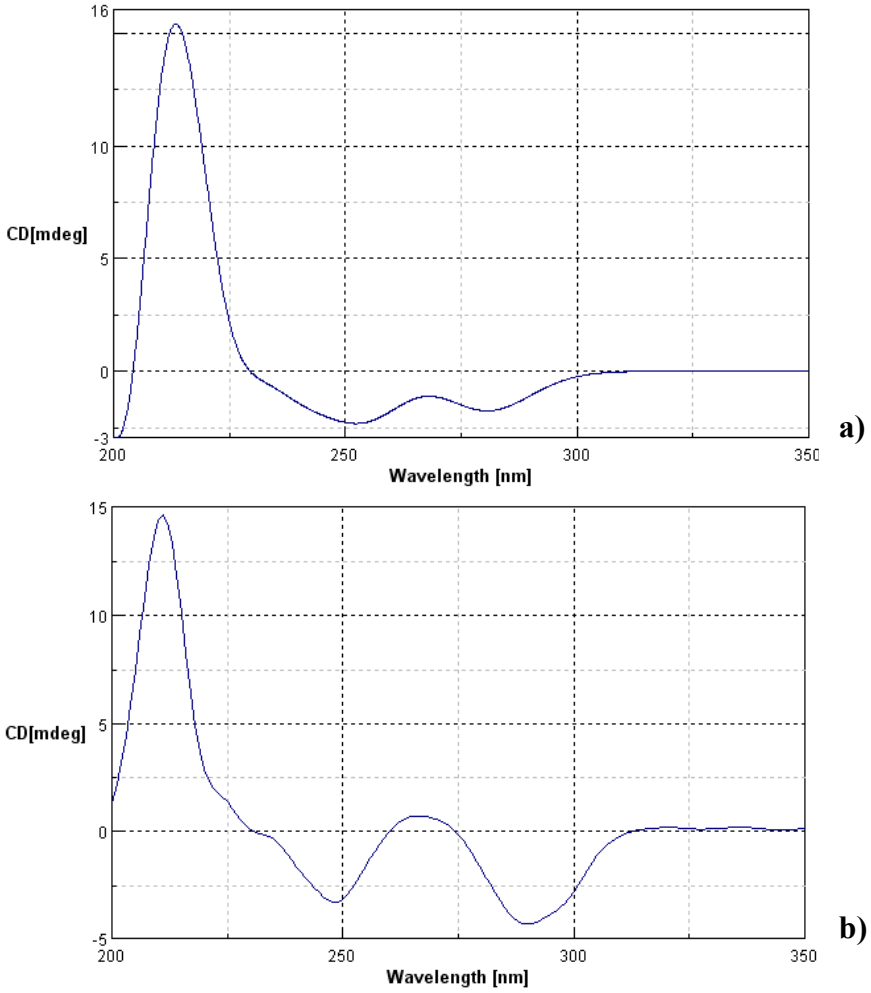

Figure 4.13: a) Calculated CD spectrum for S enantiomers; **b)** Measured CD spectrum of tedarene B (**2**).

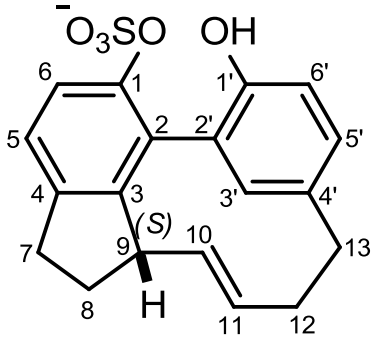

Figure 4.14: The *S* enantiomer of tedarene B (**2**).

4.5 Inhibition of NO_2^- production

Nitric oxide (NO), a short lived mediator, is an important messenger molecule involved in many physiological and pathological processes within the human body both beneficial and detrimental.[30] Appropriate levels of NO production are important in protecting an organ such as the liver from ischemic damage. However sustained levels of NO production result in direct tissue toxicity and contribute to the vascular collapse associated with septic shock, whereas chronic expression of NO is associated with various carcinomas and inflammatory conditions including juvenile diabetes, multiple sclerosis, arthritis and ulcerative colitis.

Nitric oxide (NO) is synthesized by a family of enzymes termed NO-synthase (NOS). Two types of NOS are recognised: constitutive isoforms (endothelial NOS and neuronal NOS) and an inducible isoform, for which mRNA translation and protein synthesis are required. Inducible NOS (iNOS) is regulated by inflammatory mediators (LPS, cytokines), and the excessive production of NO by iNOS is implicated in the pathogenesis of the inflammatory response. We measured the production of NO_2^- (a stable metabolite of NO) as a parameter of macrophages activation and iNOS induction. Unstimulated J774 cells generated undetectable (<5 nmol/mL) amounts of NO_2^-. Stimulation of the cells with LPS (1 μg/mL) for 24 h produced a dose-dependent release of NO_2^- (20 ± 0.3 nmol/mL). When the cells were incubated with different concentrations (3-10-30 μM) of tedarene A (**1**), a significant ($p < 0.001$) inhibition of NO_2^- production was observed

[30] Hou, Y.C.; Janczuk, A.; Wang, P.G., *Current pharmaceutical design* , **1999**, 5 (6), 417–41

at the concentrations of 10 and 30 μM. On the other hand, tedarene B was inactive and, on the contrary, seems to increase slightly but not significantly the LPS response (Figure 4.15).

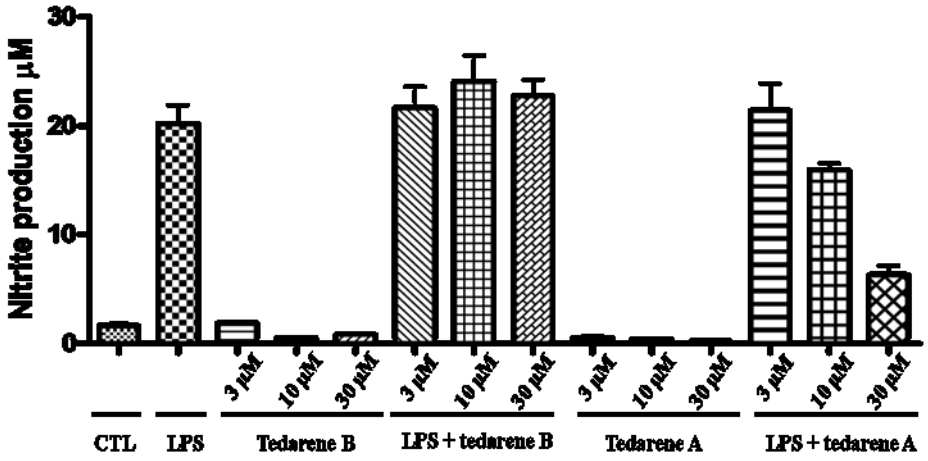

Figure 4.15: Effect of different concentrations of tedarene B (**2**) and tedarene A (**1**) on the production of NO_2^- by J774 macrophages stimulated with LPS (1 μg/mL). Each point represents the mean ± S.E.M. of three separate experiments run in triplicate.

4.6 Experimental section

General experimental procedures

High Resolution ESI-MS and ESI-MS/MS spectra were performed on a Thermo LTQ Orbitrap XL mass spectrometer. The spectra were recorded by infusion into the ESI source using MeOH as solvent. Optical rotations were measured at 589 nm on a Jasco P-2000 polarimeter using a 10-cm microcell. NMR spectra at variable temperature were determined on Varian UnityInova spectrometers at 500 and 700 MHz; chemical shifts were referenced to the residual solvent signal (CD_3OD: δ_H = 3.31, δ_C = 49.0; DMSO-d_6: δ_H = 2.54, δ_C = 40.45). For an accurate measurement of the coupling constants, the one-dimensional ^1H NMR spectra were transformed at 64K points (digital resolution: 0.09 Hz). Homonuclear ^1H connectivities were determined by a COSY experiment. Through-space ^1H connectivities were calculated using a ROESY experiment with a mixing time of 450 ms. The single-quantum heteronuclear correlation (HSQC) and multiple-bond heteronuclear correlation (HMBC) spectra were adjusted for an average $^1J_{CH}$ of 142 Hz and a $^{2,3}J_{CH}$ of 8.3 Hz, respectively. High performance liquid chromatographies (HPLC) were performed on a Varian Prostar 210 apparatus equipped with an Varian 350 refractive index and UV detectors.

Collection, extraction and isolation

Specimens of *Tedania ignis* were collected in the Mangroves of Sweeting Cay (Grand Bahama Island) during the 2007 Pawlik expedition. They were frozen immediately after collection and kept frozen until extraction. The

sponge (58 g of dry weight after extraction) was cut in small pieces and the extraction was carried out using MeOH (5 × 1 L), followed by $CHCl_3$ (2 × 1 L), as solvent. The MeOH extracts were partitioned between H_2O and *n*-BuOH, and the BuOH layer was combined with the $CHCl_3$ extract and concentrated *in vacuo*. The organic extract (12.8 g) was chromatographed on a column packed with RP-18 silica gel. A fraction eluted with MeOH/H_2O 8:2 (195 mg) was subjected to reversed-phase HPLC [MeOH/H_2O (8:2), flow=3ml/min], thus affording two fractions containing compound **1** (retention time=29 min) and compound **2** (retention time=4 min). Pure compound **1** (1.5 mg) was obtained by HPLC on SiO_2 column, using as eluent *n*-Hexane-Isopropanol 95:5. Instead, compound **2** has been purified by means of HPLC on an analytical reverse-phase column using as solvent MeOH/H_2O (1:1). Finally it was separated by choline (counter ion) on PFP column [MeOH/H_2O (1:1)], getting pure tedarene B (500 μg).

Tedarene A (1): Colorless amorphous solid, ^{1}H- and ^{13}C-NMR data at variable temperatures are shown in table 4.1. High-resolution ESI-MS (positive ion mode, MeOH) gave a peak at *m*/*z* 301.1205 ($[M+Na]^{+}$, corresponding to $C_{19}H_{18}O_2Na$).

Table 4.1: ^{1}H and ^{13}C NMR data at variable temperature of tedarene A (**1**).

			–23 °C (250 K), CD_3OD		**80 °C, DMSO-d_6**
Position			**δ_H [mult., *J* (Hz)]**	**δ_C**	**δ_H [mult., *J* (Hz)]**
1	C		-	151.5	
2	C		-	154.0	
3	CH		5.37 (m)	117.6	5.38 (d, 1.9)
4	C		-	131.4	–
5	CH		6.52 (dd, 7.8, 1.2)	121.5	6.50 (dd, 7.9, 1.9)
6	CH		6.64 (d, 7.8)	116.1	6.65 (d, 7.9)
7	CH_2		2.97 (dd, 13.7. 6.3)	36.9	2.94 (d, 7.9)
			2.93 (dd, 13.7, 9.7)		
8	CH		5.46 (m)	133.8	5.48 (15.1, 7.9, 7.9)
9	CH		5.71 (dd, 15.1, 11.0)	129.6	5.66 (dd, 15.1, 11.0)
10	CH		5.95 (t, 11.0)	131.7	5.94 (dd, 11.0 e 11.0)
11	CH		5.34 (ddd, 11.0, 8.6, 8.6)	129.4	5.31 (ddd, 11.0, 8.6, 8.6)
12	CH_2		2.41 (m)	32.9	2.35 (m)
13	CH_2	a	3.06 (br. dd, 12.0, 4.7)	35.9	2.74 (br. s)
		b	2.52 (ddd, 12.0, 12.0, 2.1)		
1'	C		-	156.3	–
2'	CH		7.06 (dd, 8.3, 1.9)	125.6	6.91 (d, 7.7)
3'	CH		7.38 (dd 8.3, 1.3)	131.5	7.20 (d, 7.7)
4'	C		-	140.9	–
5'	CH		7.08 (dd, 8.3, 1.3)	133.3	7.20 (d 7.7)
6'	CH		6.81 (dd, 8.3, 1.9)	123.8	6.91 (d, 7.7)

Tedarene B (2): Colorless amorphous solid, $[\alpha]_D^{25}$ = +33 (*c* = 0.11 in CH_3OH). High-resolution ESI-MS (negative ion mode, MeOH) gave a peak at 357.0796 *m/z* (M^- corresponding to molecular formula $C_{19}H_{17}O_5S$). ^1H- and ^{13}C-NMR data of both conformers are found in Tables 4.2 and 4.3

Table 4.2: ^1H and ^{13}C NMR data of major conformer of tedarene B (**2**) in CD_3OD.

Position				δ_H [mult., *J* (Hz)]	δ_C [mult.]
1	C			-	149.8
2	C			-	130.8
3	C			-	150.4
4	C			-	142.5
5	CH			7.20 (br. d, 8.3)	125.4
6	CH			7.46 (dd, 8.3, 1.0)	120.5
7	CH_2	a	α	2.86 (dddd, 15.2, 7.8, 1.2, 1.2)	31.8
		b	β	2.78 (ddddd, 15.2, 11.9, 6.4, 1.2, 1.2)	
8	CH_2	a	α	2.17 (dddd, 13.5, 11.9, 11.4, 7.8)	32.9
		b	β	1.98 (ddd, 11.4, 6.4, 5.8)	
9	CH		β	3.35 (dddddd, 13.5, 7.2, 5.8, 1.2, 1.0, 1.0)	48.3
10	CH			3.86 (dd, 16.6, 7.2)	140.2
11	CH			5.34 (dddd, 16.6, 9.3, 5.6, 1.0)	126
12	CH_2	a	α	2.48 (dddd, 12.1, 5.6, 4.1, 2.7)	37.0
		b	β	1.49 (ddddd, 12.5, 12.1, 9.4, 4.7, 1.0)	
13	CH_2	a	β	2.88 (ddd, 12.5, 4.7, 2.7)	38.0
		b	α	2.35 (ddd, 12.5, 12.5, 4.1)	
1'	C			-	154.1
2'	C			-	120.0
3'	CH			6.08 (d, 2.1)	145.1
4'	C			-	131.9
5'	CH			6.96 (dd, 8.1, 2.1)	129.2
6'	CH			6.80 (d, 8.1)	118.3

N.B. The coupling between H-7a (δ 2.86) and H-8b (δ 1.99) is zero, suggesting a trans geometry for these protons (dihedral angle 90°).

Table 4.3: ^{1}H and ^{13}C NMR data of minor conformer of tedarene B (**2**) in CD_3OD.

Posizione				**δ_H [mult., *J* (Hz)]**	**δ_C [mult.]**
1	C			-	150.2
2	C			-	132.3
3	C			-	147.5
4	C			-	143.3
5	CH			7.2079 (br. d, 8.3) (+ some LR)	125.3
6	CH			7.5326 (br. d, 8.3) (+ 1 LR~0.6)	121.4
7	CH_2	a	α	2.9926 (ddd, 15.9, 9.3, 5.7) (+ 2 LR,~ 0.6)	32.0
		b	β	2.8241 (ddd, 15.9, 9.2, 6.7) (+ 1LR 0.9)	
8	CH_2	a	β	2.2539 (dddd, 13.1, 9.5, 8.7, 5.8)	32.9
		b	α	1.8190 (dddd, 13.1, 9.3, 6.7, 5.9)	
9	CH		β	3.2576 (ddd, 10.0, 8.7, 5.9)	52.2
10	CH			5.1154 (dd, 15.6, 10.0) (+ 2 LR,~ 0.6)	140.8
11	CH			3.9619 (dddd, 15.6, 10.0, 6.1)	131.2
12	CH_2	a	α	2.3171 (m) (dddd, 12.7, 10.0, 9.7, 5.3) (+ 1 LR,~ 0.7)	30.9
		b	β	2.2973 (m) (dddd, 12.7, 9.4, 6.1, 5.2) (+ 1 LR,~0.9)	
13	CH_2	a	α	2.9498 (ddd, 13.2, 9.7, 5.2)	33.8
		b	β	2.8118 (ddd, 13.2, 9.4, 5.3)	
1'	C			-	153.2
2'	C			-	122.4
3'	CH			6.5657 (d, 2.1) (+ 1 LR,~ 0.6)	143.8
4'	C			-	131.3
5'	CH			6.8357 (dd, 8.1, 2.1)	130.7
6'	CH			6.6929 (d, 8.1)	116.9

Cell culture

The murine monocyte/macrophages cell line J774 was from ECACC. J774 cells were grown in Dulbecco's modified Eagle's medium (DMEM; Biowhittaker) and cultured at 37 °C in humidified 5% CO_2/95% air. The cells were plated in 24 well culture plates (Falcon) at a density of 2.5×10^6 cells/mL/well and allowed to adhere for 2 h. Thereafter, the medium was replaced with fresh medium and cells were activated by lipopolysaccharide (LPS 1 μg/mL) from *E. coli* (Fluka) for 24 h in the presence or absence of different concentrations of test compounds. The culture medium was then removed and centrifuged, and the supernatant was used for the determination of nitrite (NO_2^-) production. Cell viability (>95%) was determined with the MTT assay.

NO_2^- assay

NO_2^- levels in culture media from J774 macrophages were measured 24 h after LPS with the Griess reaction as previously described (Ianaro et al., 2000). Results are expressed as nmol/mL of NO_2^- and represent the mean ± S.E.M. of *n* experiments run in triplicates.

4.7 NMR data

4.7.1 NMR spectra of tedarene A

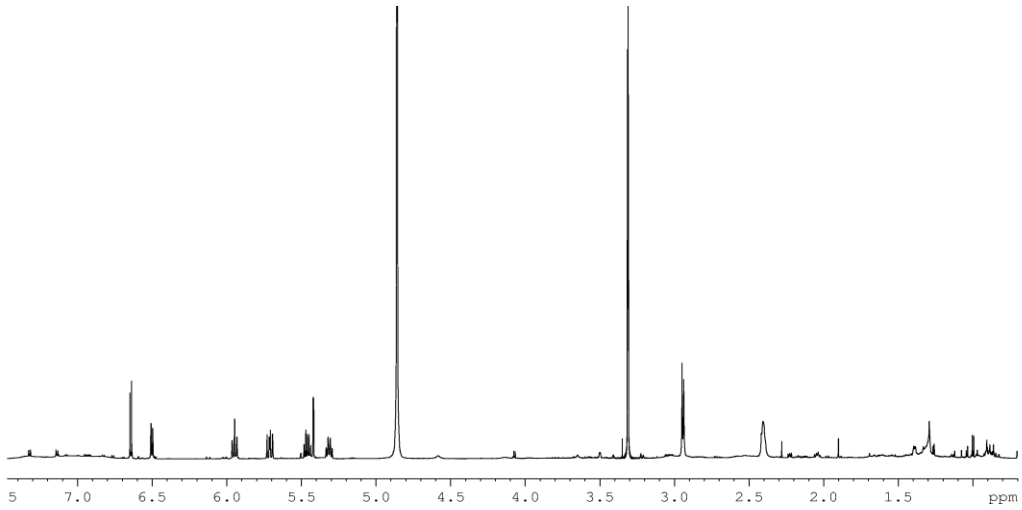

^{1}H NMR spectrum (500 MHz, 25 °C, CD_3OD) of tedarene A (**1**)

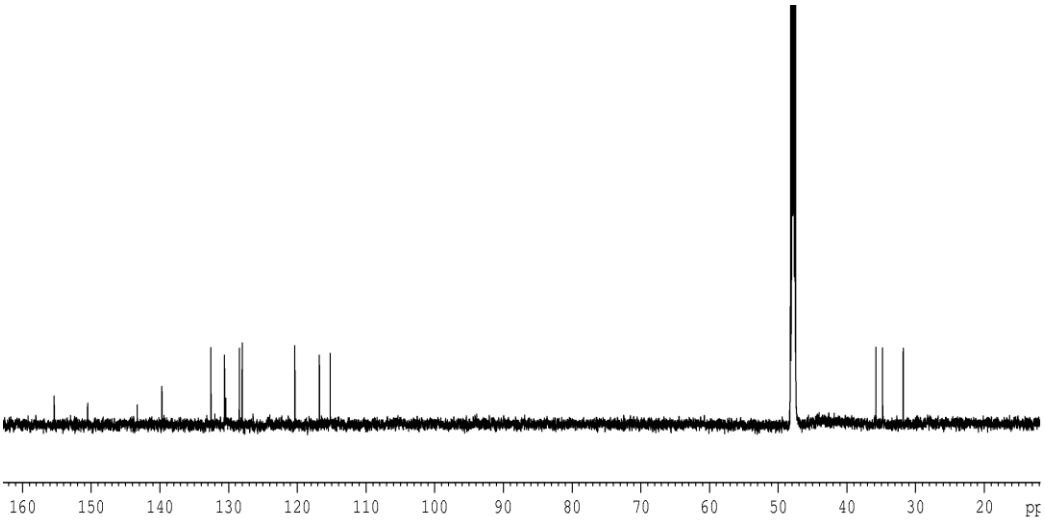

^{13}C NMR spectrum (175 MHz, 25 °C, CD_3OD) of tedarene A (**1**)

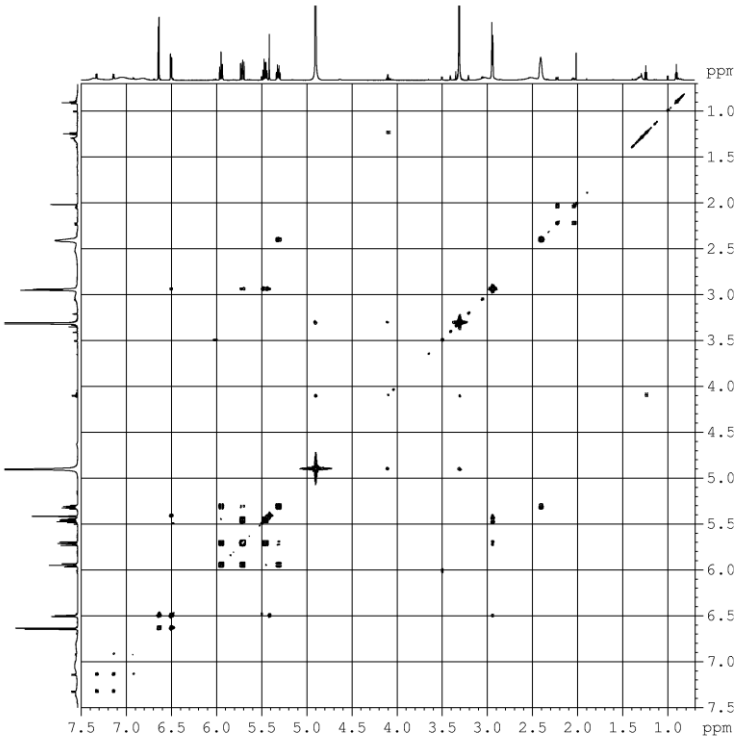

COSY spectrum (700 MHz, 25 °C, CD_3OD) of tedarene A (**1**)

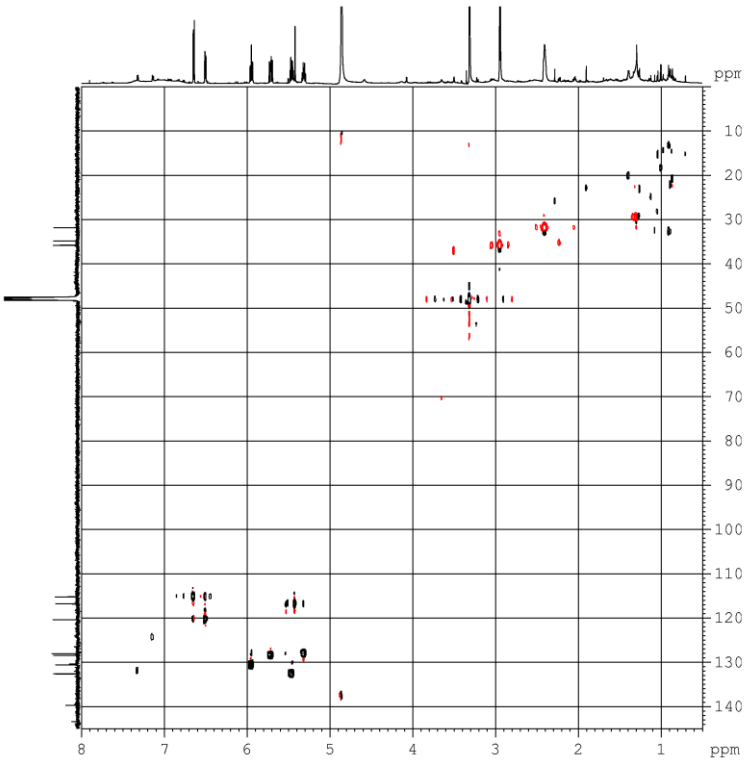

HSQC spectrum (500 MHz, 25 °C, CD_3OD) of tedarene A (**1**)

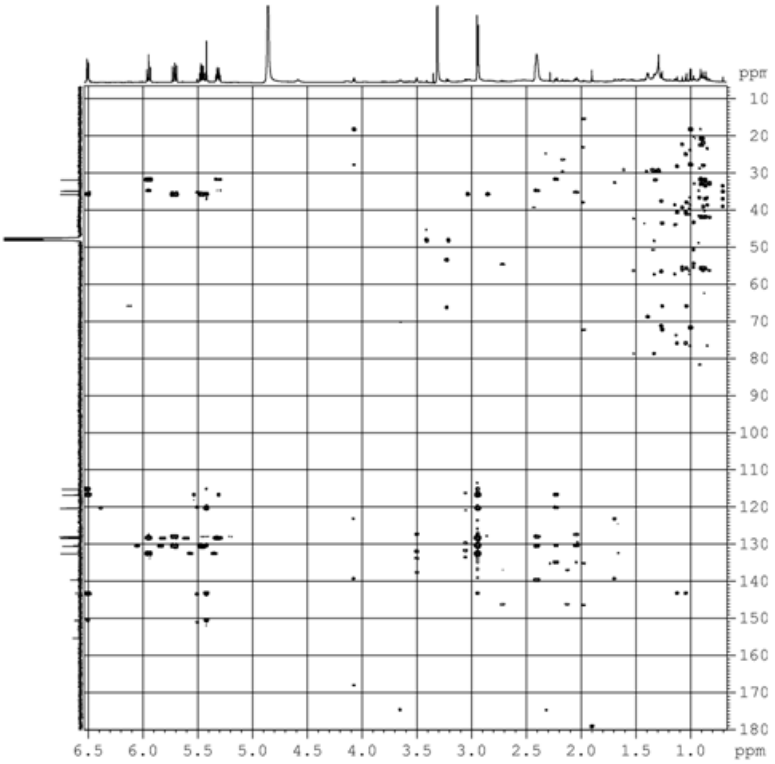

HMBC spectrum (500 MHz, 25 °C, CD_3OD) of tedarene A (**1**)

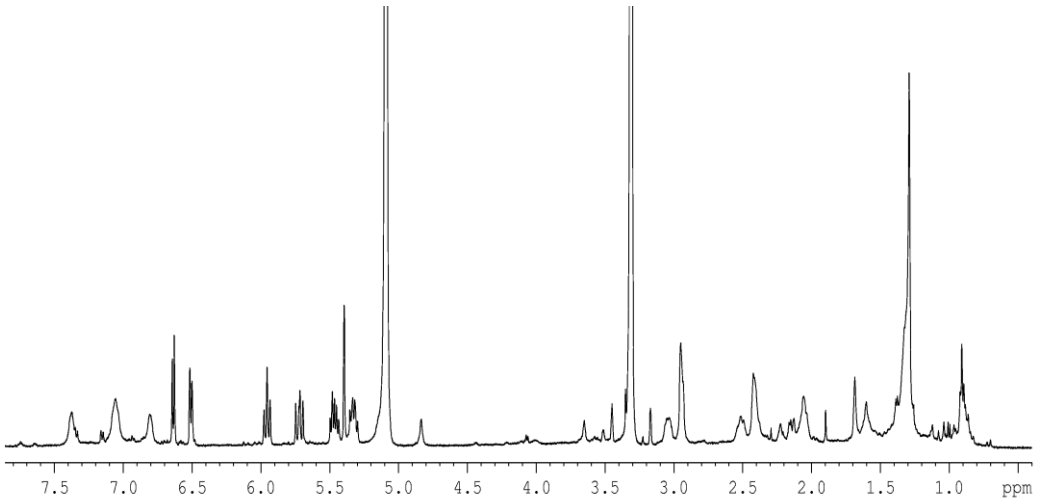

^{1}H NMR spectrum (500 MHz, 0 °C, CD_3OD) of tedarene A (**1**)

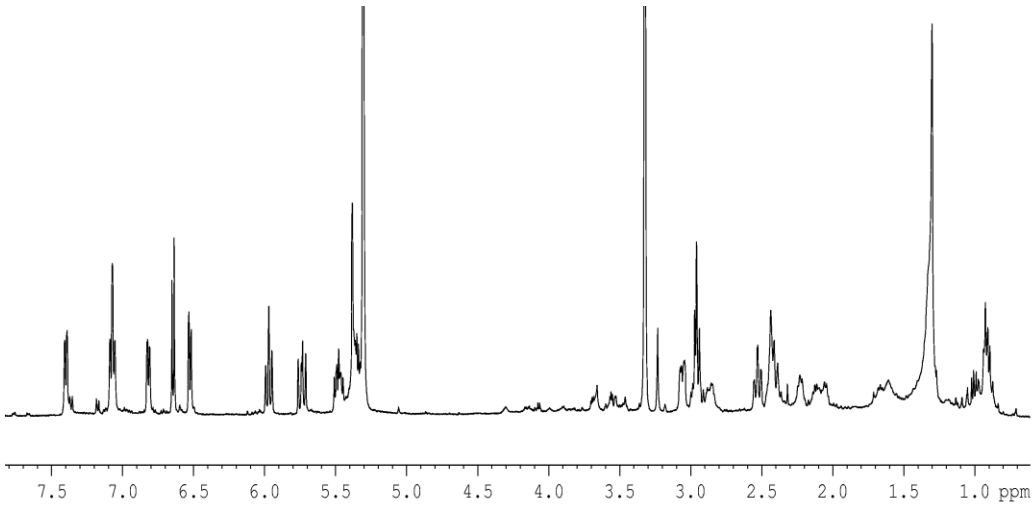

^{1}H NMR spectrum (500 MHz, -23 °C, CD_3OD) of tedarene A (**1**)

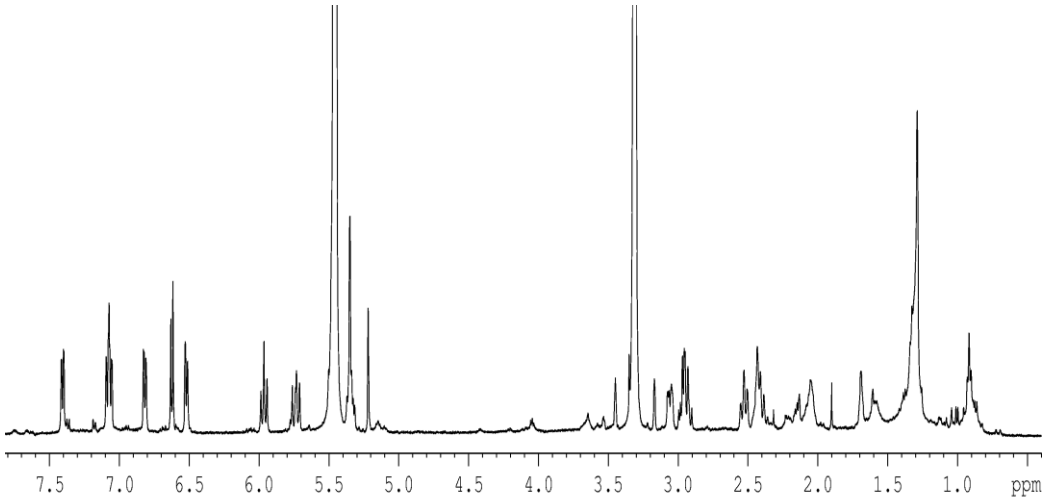

^{1}H NMR spectrum (500 MHz, -40 °C, CD_3OD) of tedarene A (**1**)

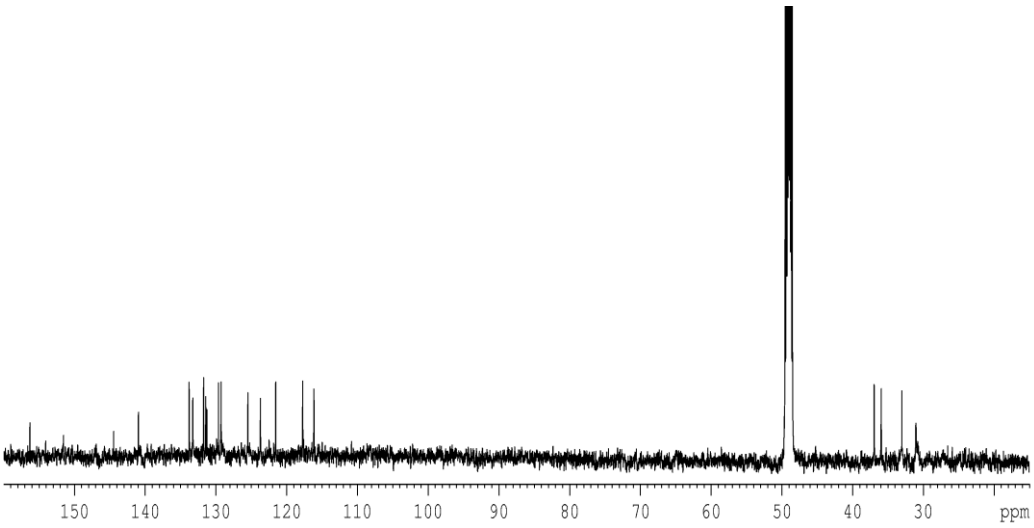

^{13}C NMR spectrum (175 MHz, -23 °C, CD_3OD) of tedarene A (**1**)

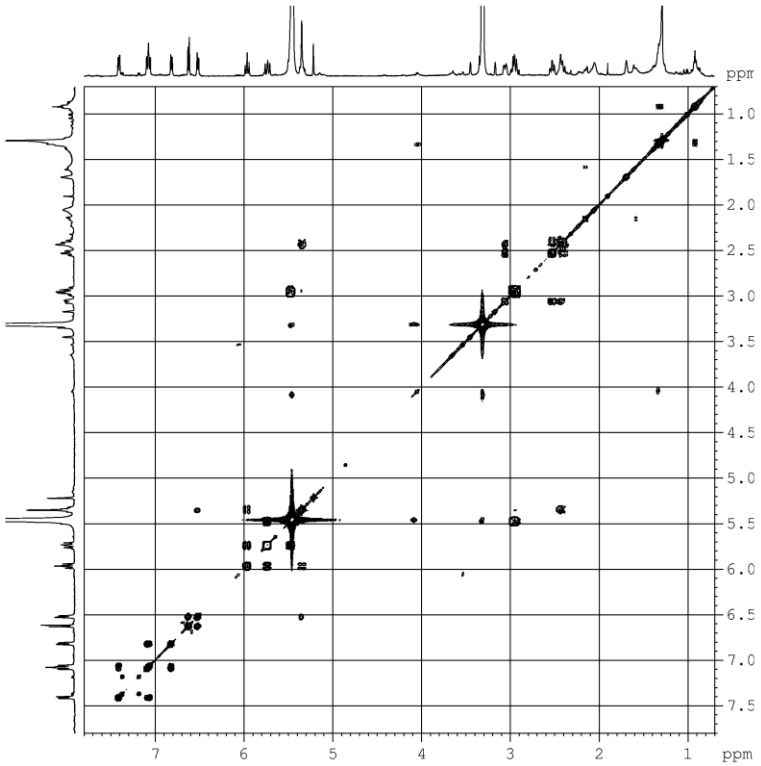

COSY spectrum (500 MHz, -40 °C, CD_3OD) of tedarene A (**1**)

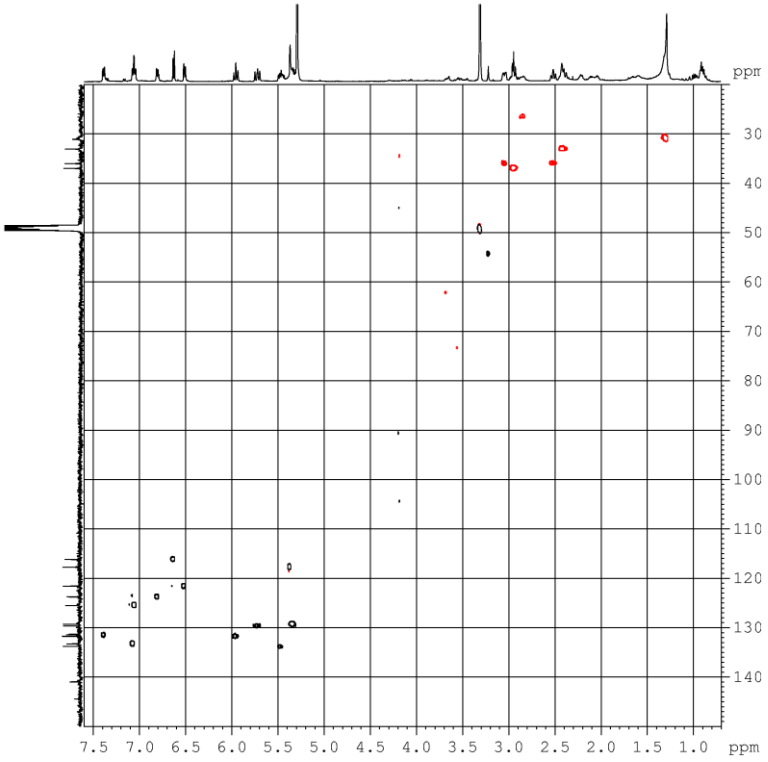

HSQC spectrum (500 MHz, -23 °C, CD_3OD) of tedarene A (**1**)

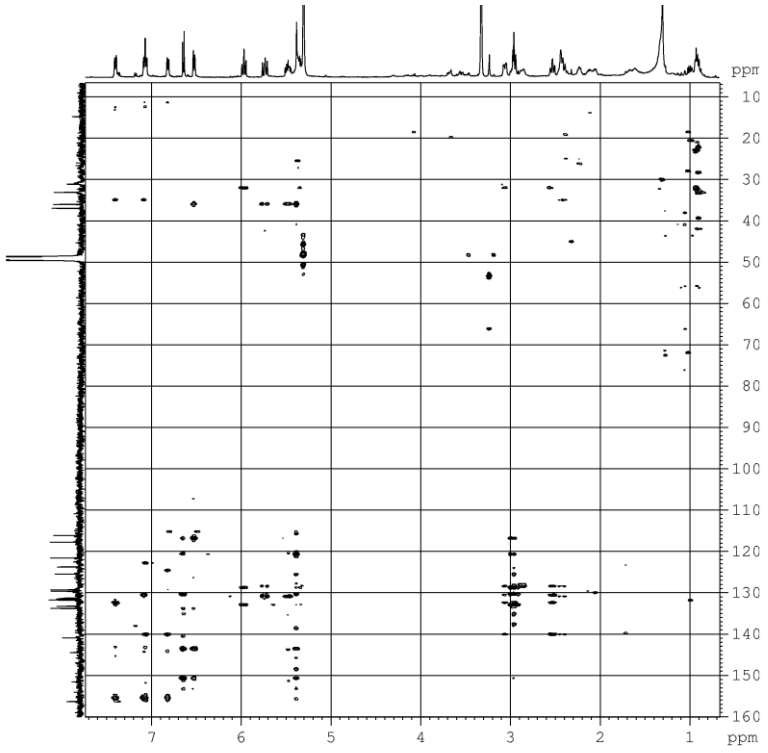

HMBC spectrum (500 MHz, -23 °C, CD_3OD) of tedarene A (**1**)

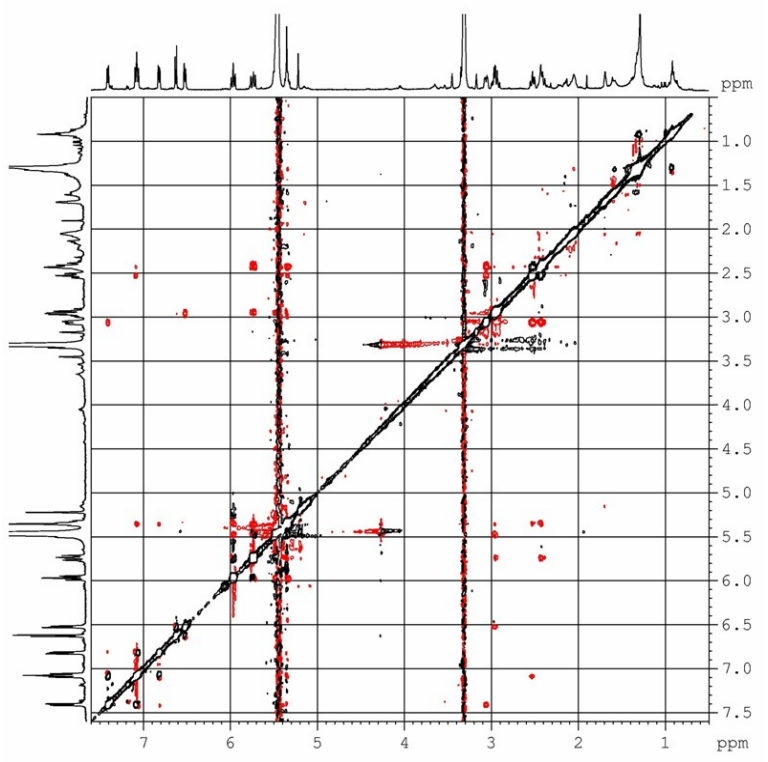

ROESY spectrum (500 MHz, -40 °C, CD_3OD) of tedarene A (**1**)

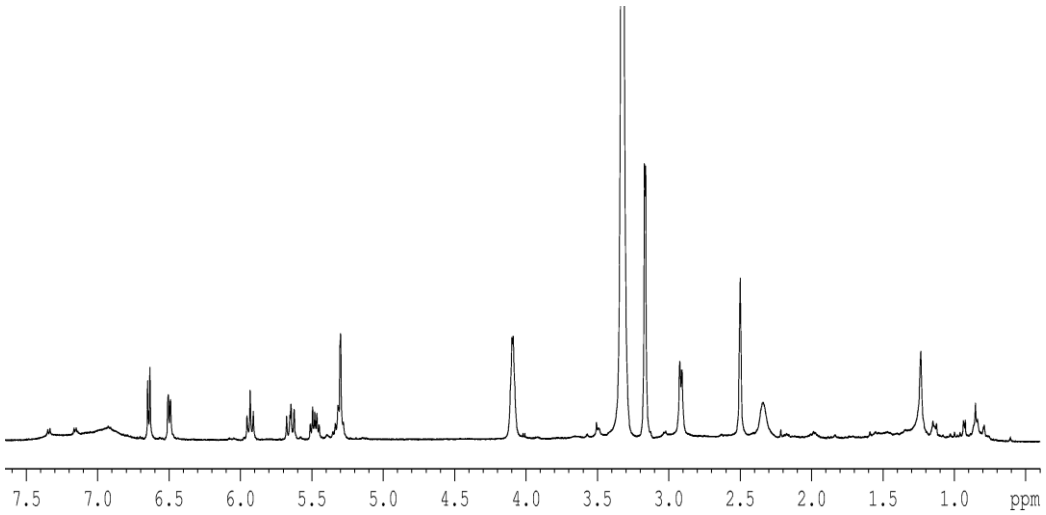

^{1}H NMR spectrum (500 MHz, 25 °C, DMSO-d_6) of tedarene A (**1**)

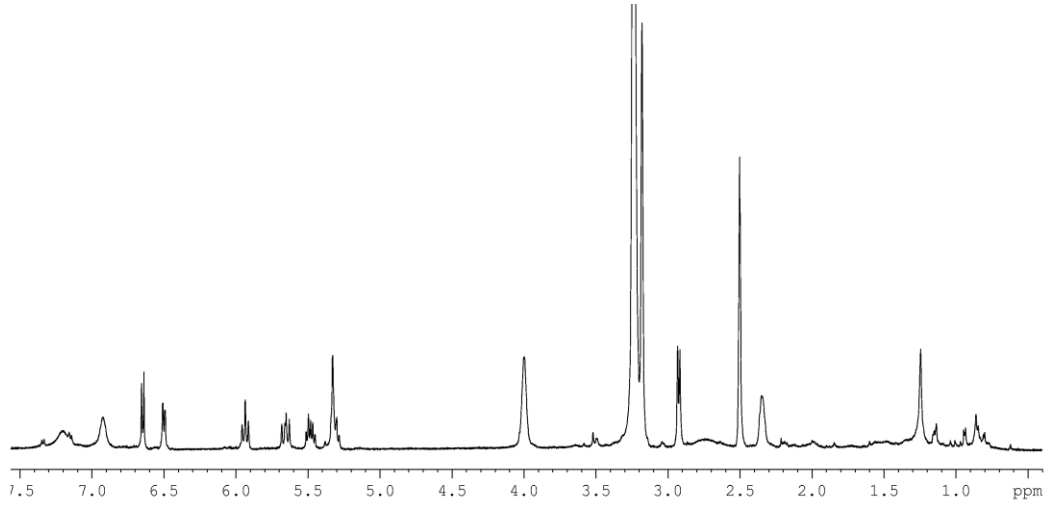

^{1}H NMR spectrum (500 MHz, 45 °C, DMSO-d_6) of tedarene A (**1**)

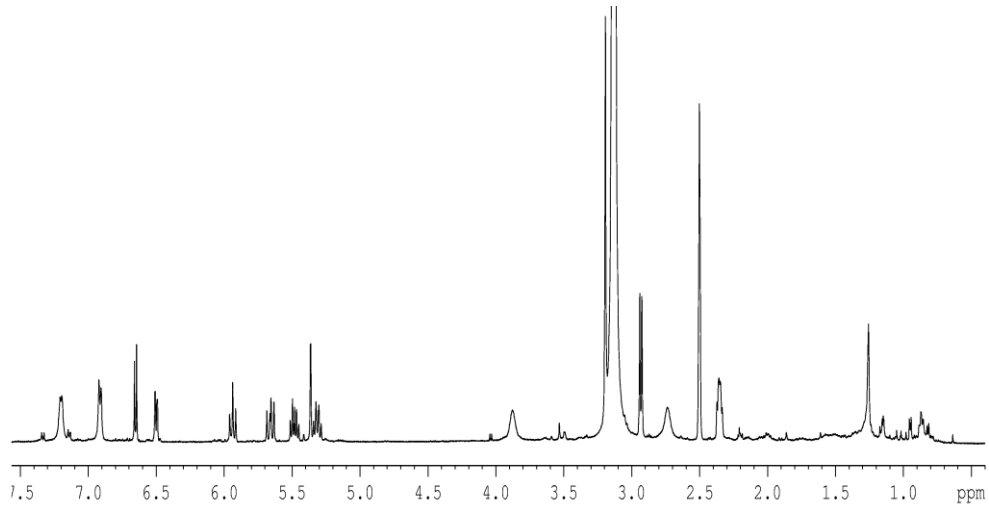

^{1}H NMR spectrum (500 MHz, 70 °C, DMSO-d_6) of tedarene A (**1**)

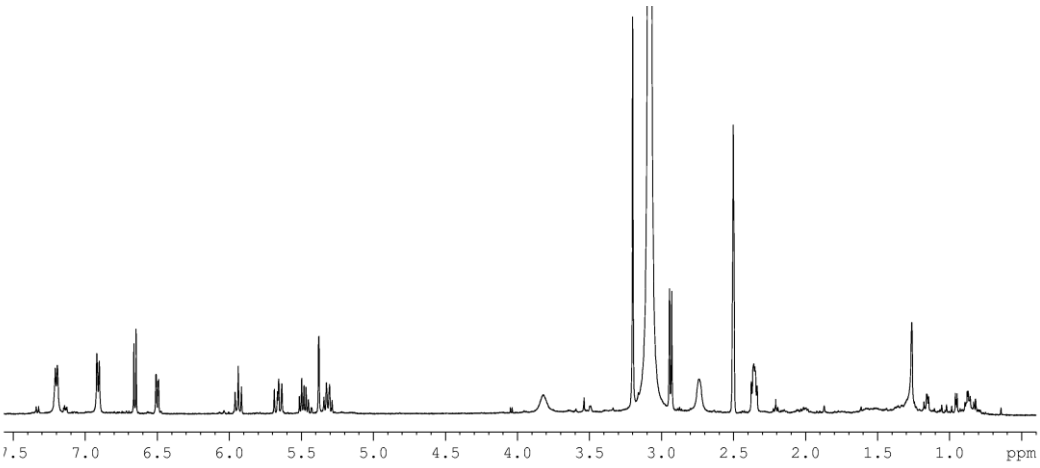

^{1}H NMR spectrum (500 MHz, 80 °C, DMSO-d_6) of tedarene A (**1**)

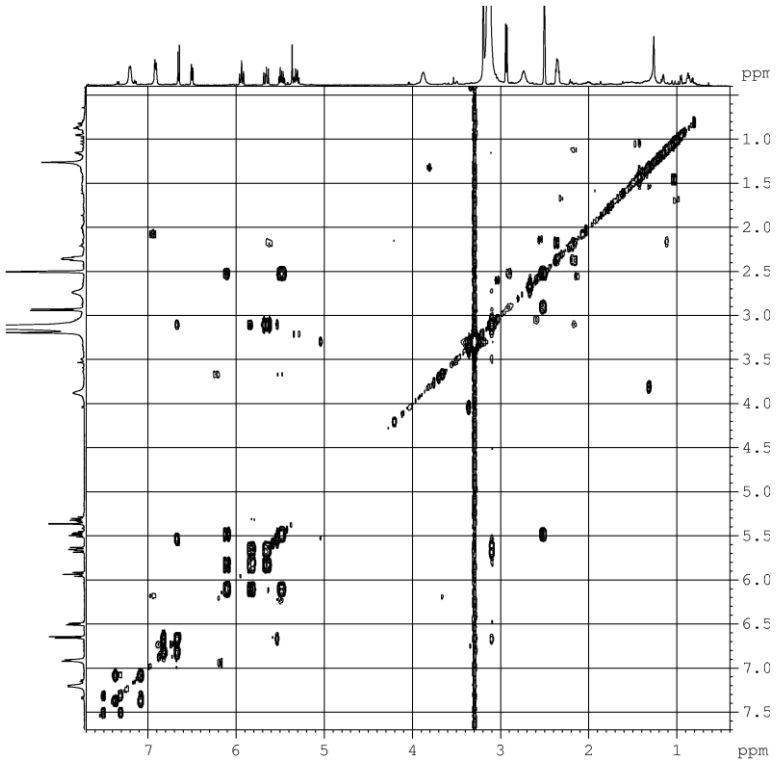

COSY spectrum (500 MHz, 70 °C, DMSO-d_6) of tedarene A (**1**)

4.7.2 NMR spectra of tedarene B

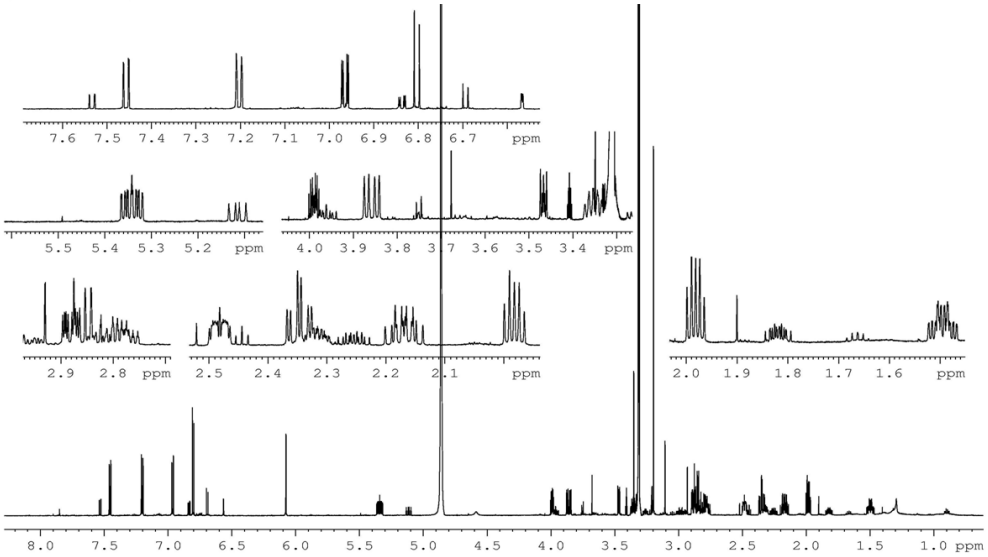

^{1}H NMR spectrum (700 MHz, CD_3OD) of tedarene B (**2**)

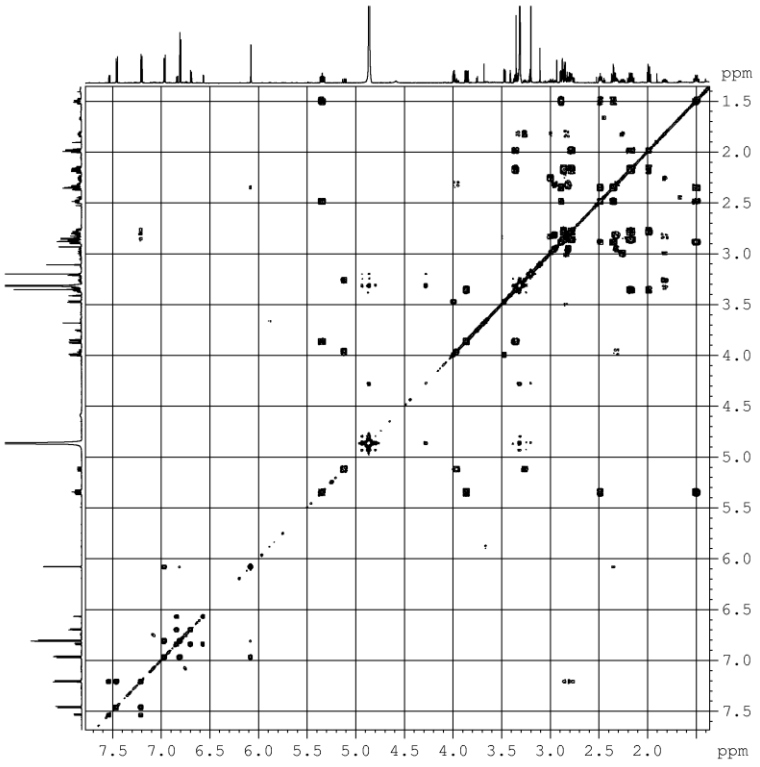

COSY spectrum (700 MHz, CD_3OD) of tedarene B (**2**)

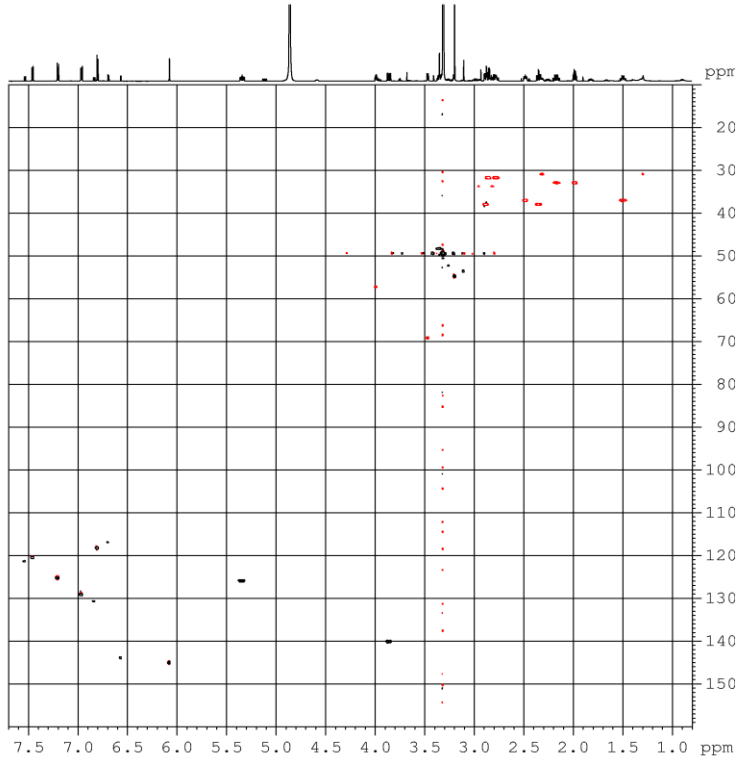

HSQC spectrum (700 MHz, CD_3OD) of tedarene B (**2**)

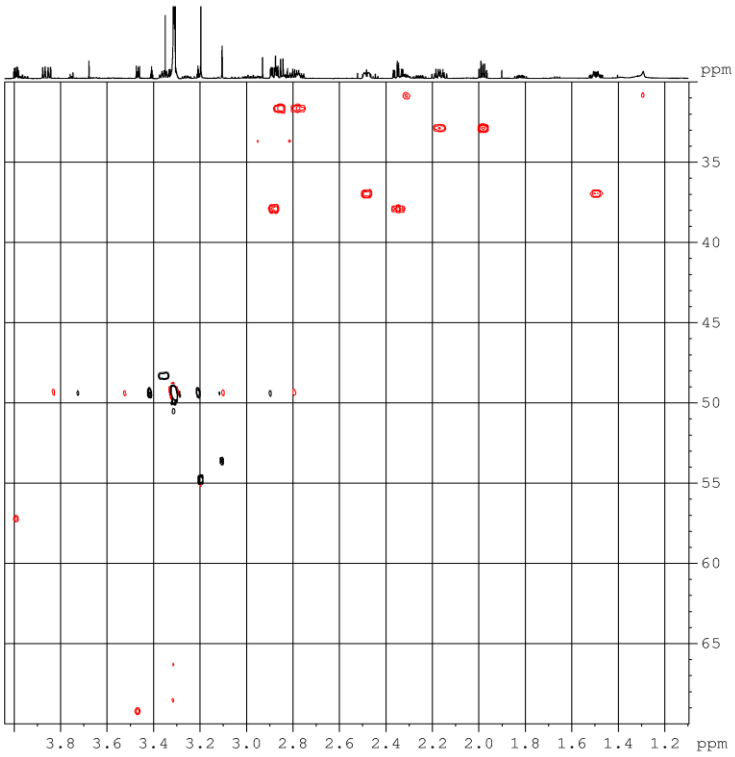

HSQC spectrum (700 MHz, CD_3OD, high-field region) of tedarene B (**2**)

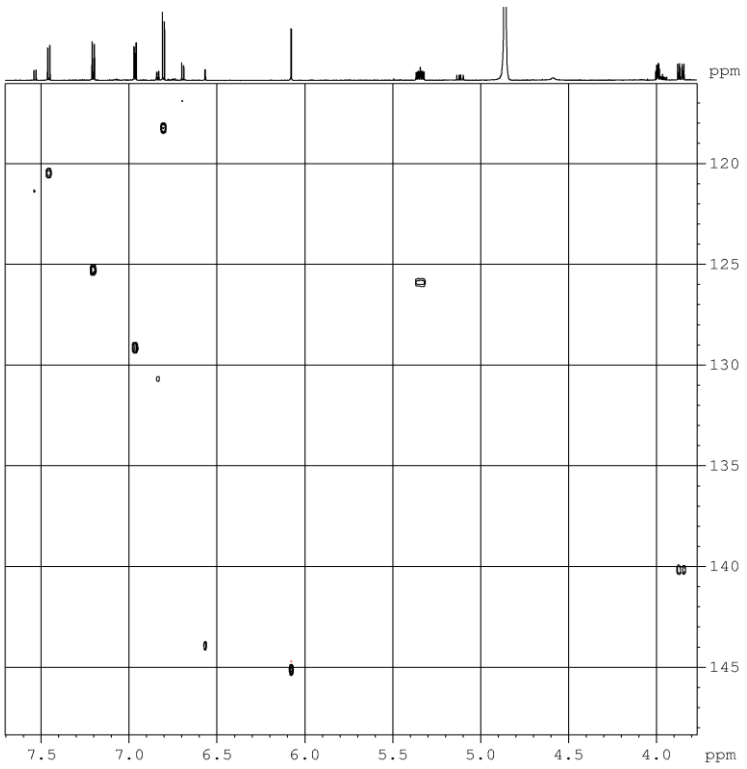

HSQC spectrum (700 MHz, CD_3OD, low-field region) of tedarene B (**2**)

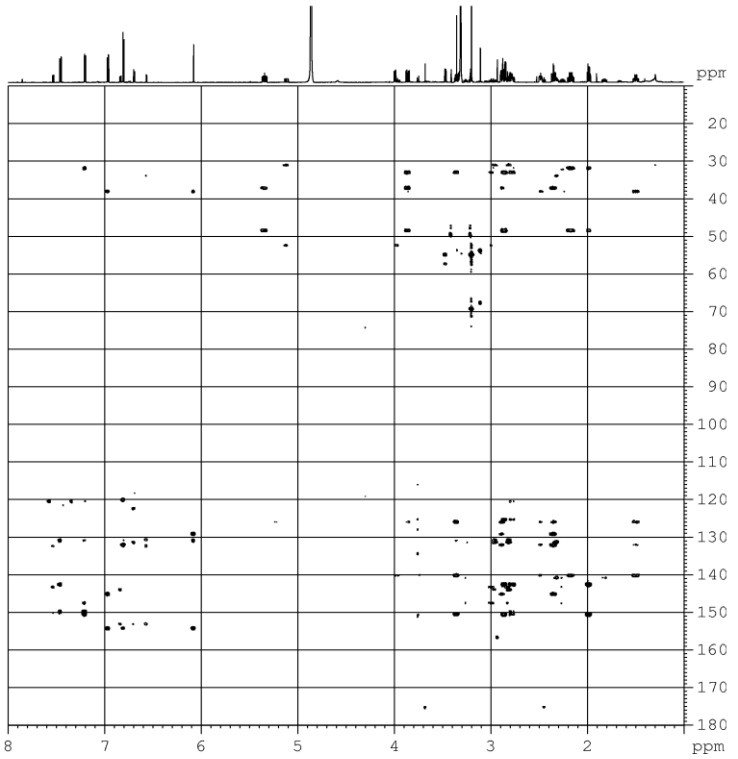

HMBC spectrum (700 MHz, CD_3OD) of tedarene B (**2**)

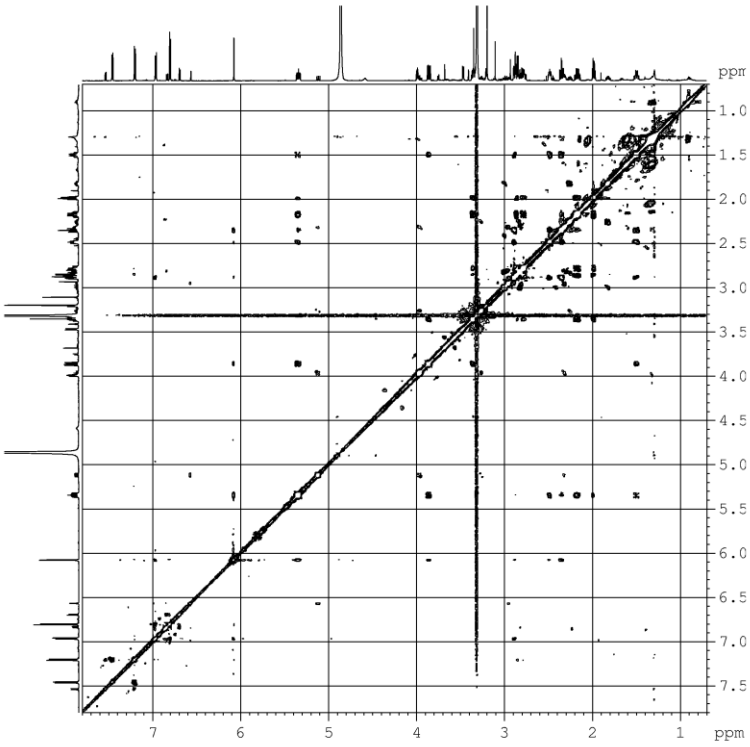

ROESY spectrum (500 MHz, CD_3OD) of tedarene B (**2**)

Chapter 5

Analysis of the sponge *Pseudaxinella flava*

In the frame of our research program, which identifies novel compounds that can be used as leads and scaffolds necessary for the elaboration of efficacious drugs or disease indications, the chemistry of the Caribbean sponge *Pseudoaxinella flava* was studied. This study led to the isolation of one new diterpene isonitrile compound (**1**) and three known analogues (**2-4**), all of which are closely related to each other but differ in the number and position of the isonitrile functional groups and double bonds (Figure 5.1).

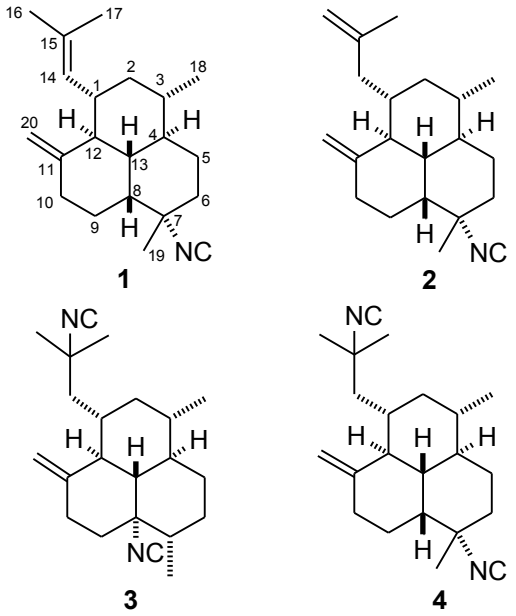

Figure 5.1: Structure of isonitrile diperpenes (**1-4**) isolated from the Caribbean sponge *Pseudaxinella Flava*.

Terpenes that contain isocyano and isothiocyano groups are secondary metabolites often found in marine invertebrates, such as sponges.[31]

During the last fifteen years, this unusually functionalized class of marine natural products have attracted broad interest in the scientific community because of their bioactivity. In fact, one of the most potent marine anti-malarial compounds is a diterpene isonitrile that was originally isolated from a tropical sponge and is characterized by an amphilectane skeleton.[32,33]

5.1 An *in vitro* evaluation of the anticancer activity of diterpene isonitriles in apoptosis-sensitive and apoptosis-resistant cancer cell lines

According to a new project in collaboration with Universitè libre de Bruxelles aimed at the identification of new compounds from marine invertebrates with potential anti-tumor activity, the *in-vitro* anti-proliferative effects of four isonitrile diterpenes (**1-4**), isolated from the sponge *Pseudaxinella f.*, were evaluated. The four diterpenes were tested at different concentrations in various human cancer cell lines using the MTTcolorimetric assay to determine IC_{50} growth inhibitory concentrations[34, 35] and quantitative videomicroscopy to decipher the mechanisms of action.[36, 37]

[31] Garson, M. J.; Simpson J. S. *Nat Prod. Rep*. **2004**, *21*, 164-179.
[32] Konig, G. M.; Wright, A. D. *J. Org. Chem*. **1996**, *61*, 3259-3267.
[33] Wright, A. D.; Wang, H.; Gurrath, M.; Konig, G. M.; Kocak, G.; Neumann, G.; Loria, P.; Foley, M.; and Tilley, L. *J. Med. Chem*. **2001**, *44*, 873-885.
[34] Van Quaquebeke, E.; Simon, G.; Andre, A.; Dewelle, J.; Yazidi, M.E.; Bruyneel, F.; Tuti, J.; Nacoulma, O.; Guissou, P.; Decaestecker, C.; Braekman, J.C.; Kiss, R.; Darro, F. *J. Med. Chem*. **2005**, *48*, 849-856.

Compounds **1**–**4** displayed similar activity in human PC3 prostate cancer cells, which are sensitive to pro-apoptotic stimuli. Compounds **3** and **4** demonstrated similar growth inhibitory effects in three apoptosis-sensitive cancer cell lines and in three cancer cell lines that possess various levels of resistance against pro-apoptotic stimuli. Quantitative videomicroscopy analyses revealed that compounds **1** and **2** exerted their anticancer activity through non-apoptotic cytotoxic effects *in vitro*. Compounds **3** and **4**, on the other hand, seemed to mediate anticancer activity through cytostatic effects. These results identify diterpene isonitriles as potential hits in anti-cancer drug discovery.

5.2 Isolation, purification, and structure elucidation

Samples of the sponge *Pseudoaxinella flava*, collected by SCUBA along the coast of the Grand Bahamas (Sweeting Cay) during the 2007 Pawlik expedition, were immediately cut into small pieces and frozen. The samples were then shipped to our laboratory and were sequentially extracted with MeOH and $CHCl_3$. The MeOH extract was dried and partitioned between water and BuOH, and the combined BuOH and $CHCl_3$ extracts were subjected to reversed-phase column chromatography. The fraction that eluted with MeOH/H_2O (9:1) contained the diterpene isonitrile compounds,

[35] Lamoral-Theys, D.; Andolfi, A.; Van Goietsenoven, G.; Cimmino, A.; Le Calvé, B.; Wauthoz, N.; Mégalizzi, V.; Gras, T.; Bruyère, C.; Dubois, J.; Mathieu, V.; Kornienko, A.; Kiss, R.; Evidente, A. *J. Med. Chem*. **2009**, *52*, 6244-6256.

[36] DeHauwer, C.; Camby, I.; Darro, F.; Migeotte, I.; Decaestecker, C.; Verbeek, C.; Danguy, A.; Brotchi, J.; Salmon, I.; Van Ham, Ph.; Kiss, R**.** *J. Neurobiol*. **1998**, *37*, 373-382.

[37] Delbrouck, C.; Doyen, I.; Belot, N.; Decaestecker, C.; Ghanooni, R.; de Lavareille, A.; Kaltner, H.; Choufani, G.; Danguy, A.; Vandenhoven, G.; Gabius, H.J.; Hassid, S.; Kiss, R. *Lab. Invest*. **2002**, *82*, 147-158.

which were first purified on a SiO_2 column and then on an HPLC using *n*-hexane/AcOEt (95:5) as the eluent. Compounds **3** and **4** (Figure 5.1) were obtained with high purity, whereas compounds **1** and **2** eluted as a mixture. This mixture was subjected to an additional HPLC separation (SiO_2, 0.05% *i*-PrOH in *n*-hexane) to yield the pure compounds **1** and **2** (Figure 5.1).

The structures of known compounds **2-4** were confirmed by comparing their MS, ^{1}H NMR, ^{13}C NMR, and optical rotation data with those reported in the literature (spectroscopic data are reported in ref.[38], whereas subsequently revised structures are reported in ref.[39]).

A high-resolution ESI-MS measurement of compound **1** showed an $[M+Na]^+$ pseudomolecular ion peak at *m/z* 320.2351 ($C_{21}H_{31}NNa$), corresponding to the molecular formula $C_{21}H_{31}N$. Compound **1** is therefore isomeric with compound **2**. The fragment peak at *m*/*z* 293.2234 ($C_{20}H_{30}Na$) present in the MS/MS spectrum was due to the loss of HCN. These peaks, together with the signal at δ 154.5 in the ^{13}C NMR spectrum, indicated the presence of an isonitrile group in compound **1**.

The analyses of the ^{1}H and ^{13}C NMR spectra of compound **1** showed that most signals were very similar to compound **2**. In particular, the ^{13}C resonances of all the carbons of the tricyclic system, except for C-1, were within 1 ppm of the corresponding resonances of compound **2**. These similarities suggested that the structure (including stereochemistry) of the tricyclic skeleton of compound **1** was the same as that in compound **2**.

[38] Ciavatta, M.L.; Fontana, A.; Puliti, R.; Scognmaglio, G.; Cimino, G. *Tetrahedron* 1999, 55, 12629-12636.

[39] Ciavatta, M.L.; Gavagnin, M.; Manzo, E.; Puliti, R.; Mattia, C. A.; Mazzarella, L.; Cimino, G.; Simpson, J.S.; Garson, M.J. *Tetrahedron* **2005**, *61*, 8049-8053.

However, the signals of the 2-methylallyl side chain (C-14/C-17) of compound **2** were not present in the spectrum of compound **1**. Instead, two methyl singlets at δ 1.63 (H_3-17) and 1.65 (H_3-16) were present in the proton spectrum and both were allylically coupled with the olefinic proton at δ 4.78 (H-14) as shown by the COSY spectrum. The latter proton was in turn coupled with H-1 (δ 2.35), thus identifying an isobutenyl group at C-1. The presence of an isobutenyl group was confirmed by the ^{13}C spectrum, which contained an olefinic CH (δ 129.6, C-14) and C (δ 129.2, C-15) in addition to the signals for the exocyclic double bond at C-11. Analysis of the 2D COSY, HSQC, HMBC, and ROESY experiments fully confirmed the proposed structures and allowed assignment of all the ^{1}H and ^{13}C signals (Table 5.1).

5.3 Anticancer activity

We obtained small amounts of compounds **1** and **2** and therefore analyzed the *in vitro* anticancer activity of these compounds on one cancer cell line (Figure 5.2A), i.e., the human apoptosis-sensitive PC3 prostate cancer cell line, using the MTT colorimetric assay and quantitative videomicroscopy.[40] Compounds **3** (Figure 5.2B) and **4** (Figure 5.2C) were assayed in parallel with compounds **1** and **2** in this PC3 prostate cancer model and also in five additional human cancer cell lines.

[40] Dumont, P.; Ingrassia, L.; Rouzeau, S.; Ribaucour, F.; Thomas, S.; Roland, I.; Darro, F.; Lefranc, F.; Kiss R. *Neoplasia* **2007**, *9*, 766-776.

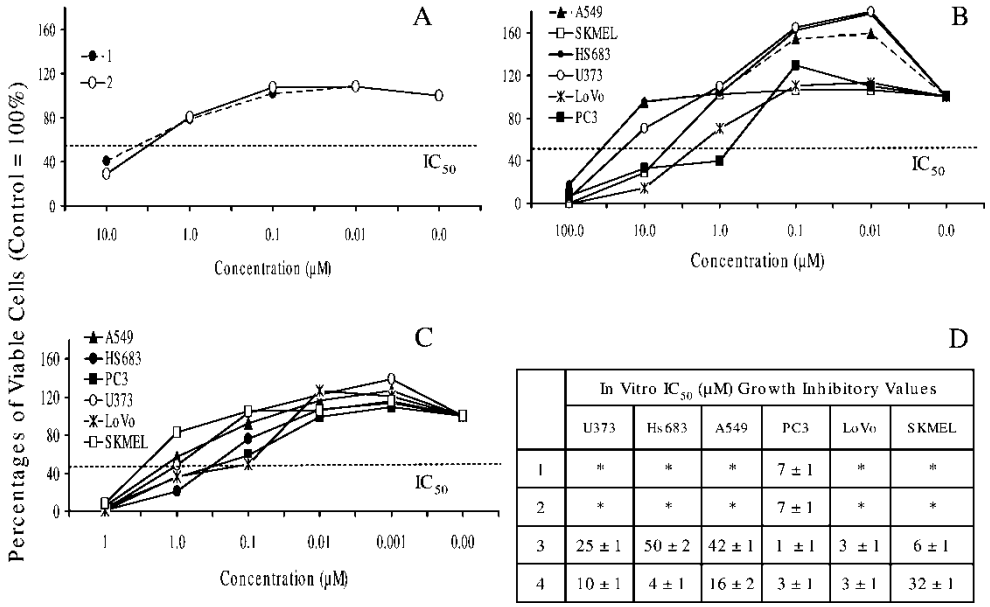

	In Vitro IC_{50} (μM) Growth Inhibitory Values					
	U373	Hs683	A549	PC3	LoVo	SKMEL
1	*	*	*	7 ± 1	*	*
2	*	*	*	7 ± 1	*	*
3	25 ± 1	50 ± 2	42 ± 1	1 ± 1	3 ± 1	6 ± 1
4	10 ± 1	4 ± 1	16 ± 2	3 ± 1	3 ± 1	32 ± 1

Figure 5.2: MTT colorimetric assay determination of *in vitro* IC_{50} growth inhibitory concentration. Compounds **1** and **2** were assayed in the human PC3 prostate cancer cell line (A), while compounds **3** (B) and **4** (C) were assayed in six human cancer cell lines. The mean IC_{50} values ($\pm$ SEM) were calculated for 6 independent samples in each experimental condition (D).

As shown in Figure 5.2D, the four compounds displayed similar *in vitro* anticancer activity in the human PC3 prostate cancer cell line, with IC_{50} growth inhibitory values of 1 $\pm$ 1 μM for **3**, 3 $\pm$ 1 μM for **4**, and 7 $\pm$ 1 μM for **1** and **2**.

However, while displaying similar IC_{50} growth inhibitory values (Figure 5.2D), compounds **1-4** did not seem to exert their *in vitro* anticancer activity through the same mechanism. Indeed, low-magnification morphological analyses suggested that compounds **1** and **2** exerted their anticancer activity through direct cytotoxic effects, whereas compound **3** and **4** exerted their anticancer activity through cytostatic effects, both of which led to cell death (Figure 5.3).

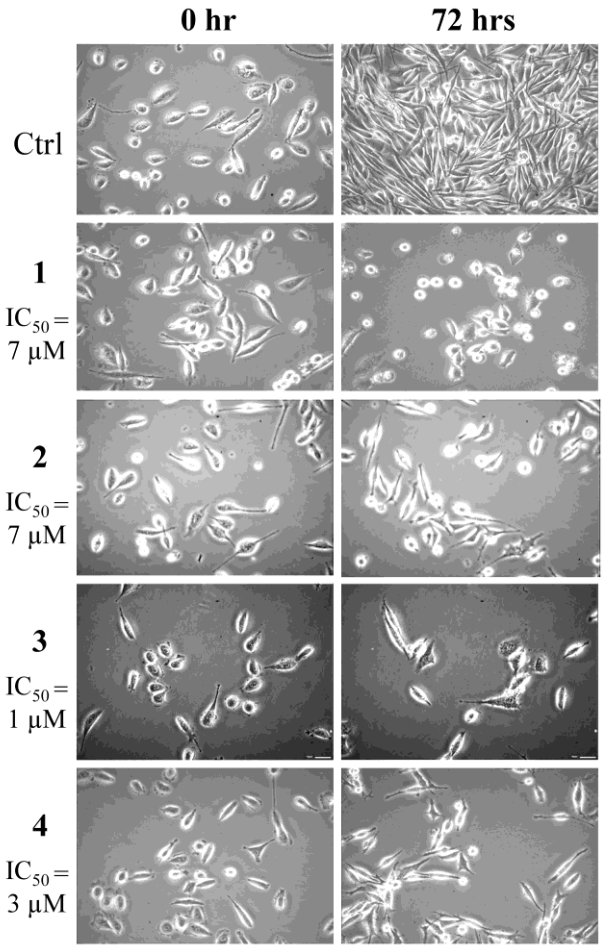

Figure 5.3: Quantitative videomicroscopy analyses of compounds **1-4** in the human PC3 prostate cancer cell line. The IC_{50} values were calculated using the MTT colorimetric assay (see Figure 5.2) and the current morphological analyses were carried out at low magnification, i.e., Gx100.

Cells that died appeared as white, rounded refringent cells under quantitative videomicroscopy analyses. The proportion of this cell type in PC3 prostate cancer cells was higher following treatment with compounds **1** and **2** at their IC_{50} growth inhibitory concentrations for 72 hrs than with compounds **3** and **4**. High-magnification morphological analyses confirmed these features (Figure 5.4). Indeed, compound **1** induced marked vacuolization processes, which in turn, led to cell death (Figure 5.4). These

marked compound **1**-induced vacuolization processes could be due to either lysosomal membrane permeabilization[41] and/or sustained autophagy[42] cell death. In contrast, compound **3** seemed to exert its anticancer activity through cytostatic effects, i.e., the inhibition of cell proliferation rather than the induction of cell death (Figure 5.4).

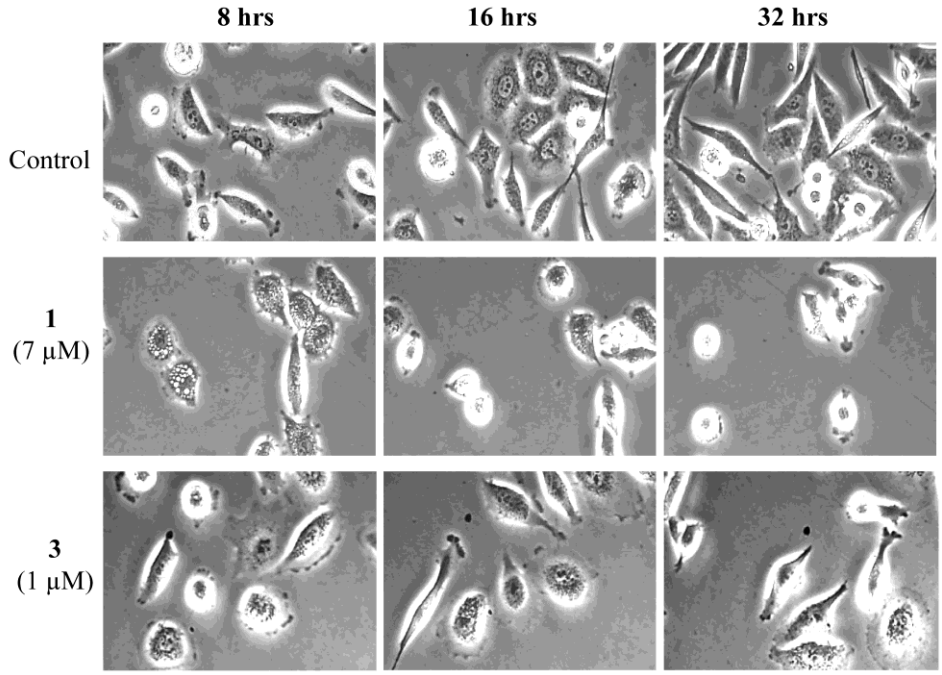

Figure 5.4: Quantitative videomicroscopy analyses of compounds **1** and **3** in the human PC3 prostate cancer cell line. The IC_{50} values were calculated using the MTT colorimetric assay (see Figure 35) and the current morphological analyses were carried out at high magnification, i.e., Gx500.

Altogether, these data suggest that when the compounds under study exert their anticancer effects through cytotoxic-related mechanisms, cell death processes occur independently of apoptosis induction based on the absence of pathognomonic morphological features. In order to validate this

[41] Mijatovic, T.; Mathieu, V.; Gaussin, J.F.; De Neve, N.; Ribaucour, F.; Van Quaquebeke, E.; Dumont, P.; Darro, F.; Kiss, R. *Neoplasia* **2006**, *8*, 402-412.
[42] Lefranc, F.; Mijatovic, T.; Kondo, Y.; Sauvage, S.; Roland, I.; Krstic, D.; Vasic, V.; Gailly, P.; Kondo, S.; Blanco, G.; Kiss, R. *Neurosurgery* **2008**, *62*, 211-222

hypothesis at the experiment level, we assayed compounds **3** and **4** (for which sufficient amounts were available) in apoptosis-sensitive cancer cell lines and in cancer cell lines resistant to pro-apoptotic stimuli. We used three human apoptosis-sensitive cancer cell lines: the PC3 prostate cancer,[33] the Hs683 oligodendroglioma,[43] and the LoVo colon cancer[44] cell lines. In the same manner, we used three human cancer cell lines that are resistant to proapoptotic stimuli: the U373 glioblastoma cell line (which is resistant to apoptosis[45] but sensitive to autophagy-related cell death),[35] the A549 non-small-cell lung cancer (NSCLC) cell line (which is resistant to apoptosis[14] and to autophagy-related cell death,[34] but is sensitive to lysosomal membrane permeabilization-related cell death),[34] and the SKMEL-28 melanoma model.[46] The data illustrated in Figures 5.2B (compound **3**) and 5.2C (compound **4**) indicate that compounds **3** and **4** displayed similar *in vitro* anticancer activity in the three apoptosis-sensitive cancer cell lines (PC3, Hs683 and LoVo) when compared to the three cancer cell lines that display various levels of resistance to pro-apoptotic stimuli (U373, A549, SKMEL-28). Figure 5.2D provides mean + SEM IC_{50} values for each compound and each cancer cell line that was assayed in the current study.

The current data, while preliminary, must be evaluated with respect to the most recent pharmacological therapeutics developed against cancers

[43] Branle, F.; Lefranc, F.; Camby, I.; Jeuken, J.; Geurts-Moespot, A.; Sprenger, S.; Sweep, F.; Kiss, R.; Salmon, I. *Cancer* **2002**, *95*, 641-655.

[44] Yao, Y.; Jia, X.Y.; Tian, H.Y.; Jiang, Y.X.; Xu, G.J.; Qian, Q.J.; Zhao, F.K. *Biochim. Biophys. Acta* **2009**, *1794*, 1433-1440.

[45] Ingrassia, L.; Lefranc, F.; Dewelle, J.; Pottier, L.; Mathieu, V.; Spiegl-Kreinecker, S.; Sauvage, S.; El Yazidi, M.; Dehoux, M.; Berger, W.; Van Quaquebeke, E.; Kiss, R. *J. Med. Chem*. **2009**, *52*, 1100-1114.

[46] Mathieu, V.; Pirker, C.; Martin de Lassalle, E.; Vernier, M.; Mijatovic, T.; DeNeve, N.; Gaussin, J.F.; Dehoux, M.; Lefranc, F.; Berger, W.; Kiss, R. *J. Cell Mol. Med*. **2009**, *9B*, 3960-3972

associated with dismal prognoses. Indeed, before the cancer has metastasized, surgery remains the best treatment for cancer patients because total tumor removal can be curative. In contrast, if the cancer has already metastasized by the time of diagnosis, adjuvant therapies with surgery are essential for combating the disease. These adjuvant therapies include radiotherapy and chemotherapy. More than 80% of the chemotherapeutics used today to treat cancers are pro-apoptotic agents, though numerous cancer types are naturally resistant to apoptosis, such as gliomas,[47] melanomas,[48] pancreatic cancers,[49] NSCLCs,[50] esophageal cancers,[51] and above all, metastatic cancers.[52,53] It is therefore highly important to identify novel therapeutics that can eliminate apoptotic-resistant cancer cells.

5.4 Conclusion

The chemistry of the Caribbean sponge *Pseudoaxinella flava* was studied in search of new model compounds for anti-cancer drug discovery. The preliminary data reported in the current study suggest that diterpene isonitriles represent interesting chemical scaffolds that could be pharmacologically optimized to combat cancer cells that are resistant to proapoptotic stimuli.

[47] Lefranc, F.; Brotchi, J.; Kiss, R. *J. Clin. Oncol*., **2005**, *23*, 2411-2422.
[48] Soengas, M.S.; Lowe, S.W. *Oncogene*, **2003**, *22*, 3138-3151.
[49] El Maalouf, G.; Le Tourneau, C.; Batty, G.N. ; Faivre, S. ; Raymond, E. *Cancer Treat. Rev*., **2009**, *35*, 167-174.
[50] Denlinger, C.E. ; Rundall, B.K. ; Jones, D.R. *Semin. Thorac. Cardiovasc. Surg*., **2004**, *16*, 28-39.
[51] D'Amico, T.A. ; Harpole, D.H.Jr. *Chest Surg. Clin. N. Am.*, **2000**, *10*, 451-469.
[52] Savage, P. ; Stebbing, J. ; Bower, M. ; Crook, T. *Nat. Clin. Pract. Oncol.*, **2009**, *6*, 43-52.
[53] Wilson, T.R. ; Johnston, P.G. ; Longley, D.B. *Curr. Cancer Drug Targets*, **2009**, *9*, 307-319.

5.5 Experimental section

General experimental procedures

High Resolution ESI-MS and ESI-MS/MS spectra were performed on a Thermo LTQ Orbitrap XL mass spectrometer. The spectra were recorded by infusion into the ESI source using MeOH as the solvent. Optical rotations were measured at 589 nm on a Jasco P-2000 polarimeter using a 10-cm microcell. NMR spectra were determined on Varian UnityInova spectrometers at 500 and 700 MHz; chemical shifts were referenced to the residual solvent signal ($CDCl_3$: δ_H = 7.26, δ_C = 77.0). For an accurate measurement of the coupling constants, the one-dimensional ^1H NMR spectra were transformed at 64K points (digital resolution: 0.09 Hz). Homonuclear ^1H connectivities were determined by a COSY experiment. Through-space ^1H connectivities were calculated using a ROESY experiment with a mixing time of 450 ms. The single-quantum heteronuclear correlation (HSQC) and multiple-bond heteronuclear correlation (HMBC) spectra were adjusted, respectively, for an average $^1J_{CH}$ of 142 Hz and a $^{2,3}J_{CH}$ of 8.3 Hz. High performance liquid chromatographies (HPLC) were performed on a Varian Prostar 210 apparatus equipped with an Varian 350 refractive index detector.

Collection, extraction and isolation

Specimens of *Pseudoaxinella flava* were collected along the coast of Grand Bahamas (Sweeting Cay) during the 2007 Pawlik expedition and identified by Prof. S. Zea (University of Colombia) aboard of the vessel. They were

frozen immediately after collection and kept frozen until extraction. The sponge (220 g of dry weight after extraction) was homogenized and extracted with methanol (3 × 1 L) and then with chloroform (3 × 1 L); the combined extracts were partitioned between H_2O and *n*-BuOH. The organic layer was concentrated *in vacuo* and afforded 16.3 g of a dark green oil, which was chromatographed on a column packed with RP-18 silica gel. A fraction (825 mg) eluted with CH_3OH/H_2O (9:1) was further chromatographed on SiO_2 column, giving a fraction, mainly composed of isonitrile terpenes [250 mg, eluent *n*-hexane/EtOAc (9:1)]. This fraction was subjected to HPLC separation on an SiO_2 column [eluent: *n*-hexane/EtOAc (95:5)], giving pure compounds **3** (145 mg) and **4** (38 mg), and a mixture (21 mg) of compounds **1** and **2**. The mixture was subject to a further HPLC separation (SiO_2 column, 0.05% *i*-PrOH in *n*-hexane) giving pure **1** (10.3 mg) and **2** (2.9 mg).

Compound 1: colorless oil; $[\alpha]_D^{25}$ +103 (*c* 0.11, $CHCl_3$); ^{1}H- and ^{13}C-NMR data are found in Table 5.1; HRESIMS (positive ion mode, MeOH) *m/z* of 320.2351 ($[M+Na]^+$, calcd. for $C_{21}H_{31}NNa$, 320.2349).

Table 5.1: NMR Spectroscopic Data (700 MHz, $CDCl_3$) for Compound **1**.

Position		δ_H (*J* in Hz)	δ_C,mult.
1		2.35 (dddd, 11.5, 10.4, 9.0, 4.0)	38.2, CH
2	α	0.93 (ddd, 13.5, 11.5, 11.5)	42.7, CH_2
	β	1.64 (ddd, 13.5, 4.0. 4.0)	
3		1.21[a]	39.8, CH
4		1.28 (m)	40.5, CH
5	α	1.97 (dddd, 14.2, 6.8, 6.8, 6.8)	24.7, CH_2
	β	1.08 (dddd. 14.2, 10.2, 6.6, 6.6)	
6	α	1.81 (ddd, 13.4, 6.6, 6.6)	34.0, CH_2
	β	1.60 (m)	
7		-	59.8, C
8		1.50 (m)	42.4, CH
9	α,β	1.77 (m)	21.3, CH_2
10	α	2.46 (br.d, 15.4)	33.0, CH_2
	β	2.23(ddd, 15.4, 9.5, 9.5)	
11		-	148.2, C
12		1.74 (t, 10.4)	49.5, CH
13		1.22[a]	44.6, CH
14		4.78 (br. d, 9.0)	129.6, CH
15		-	129.2, C
16		1.65 (br. s)	25.7, CH_3
17		1.63 (br. s)	17.9, CH_3
18		0.89 (d, 6.3)	19.3, CH_3
19		1.41 (br. s)	28.9, CH_3
20	pro-*E*	4.76 (br. s)	107.4, CH_2
	pro-*Z*	4.48 (br. s)	
21		-	154.5, C

[a] Overlapping signals

Anti-cancer activity evaluation

We evaluated the IC_{50} *in vitro* growth inhibitory values of the four compounds under study using the MTT colorimetric assay as detailed in previous studies.[27, 28, 38] Briefly, the cell lines were incubated for 24 h in 96-microwell plates (at a concentration of 10,000 to 40,000 cells/mL culture medium depending on the cell type) to ensure adequate plating prior to cell growth determination. The MTT colorimetric assay measures cell population growth based on the capability of living cells to reduce the yellow reactant MTT (3-(4,5)-dimethylthiazol-2-yl)-2,5-diphenyltetrazolium bromide) to the blue product formazan via a reduction reaction in the mitochondria. The number of living cells after 72 h of culture in the presence (or absence: control) of the various compounds was directly proportional to the intensity of the blue, which was quantitatively measured by spectrophotometry. The experiments in this study were carried out using a Biorad Model 680XR (Biorad, Nazareth, Belgium) at a 570 nM wavelength (with a reference of 630 nM). Each experiment was carried out in sextuplicate. The origin of the cell lines used in the current study and the culture media are also fully detailed in references. [27, 28, 38]

5.6 Mass and NMR data

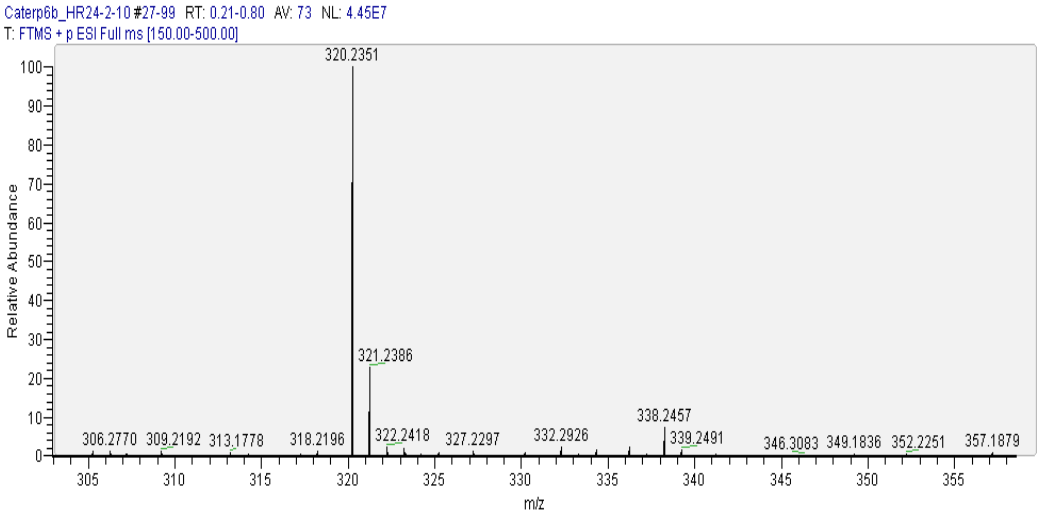

High-resolution ESI MS spectrum of compound **1**

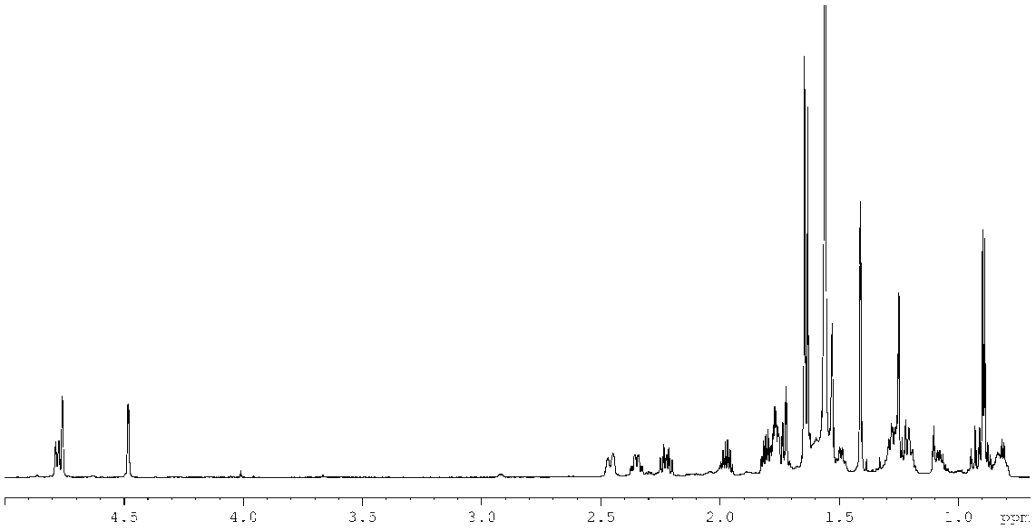

^{1}H-NMR spectrum (700 MHz, $CDCl_3$) of compound **1**

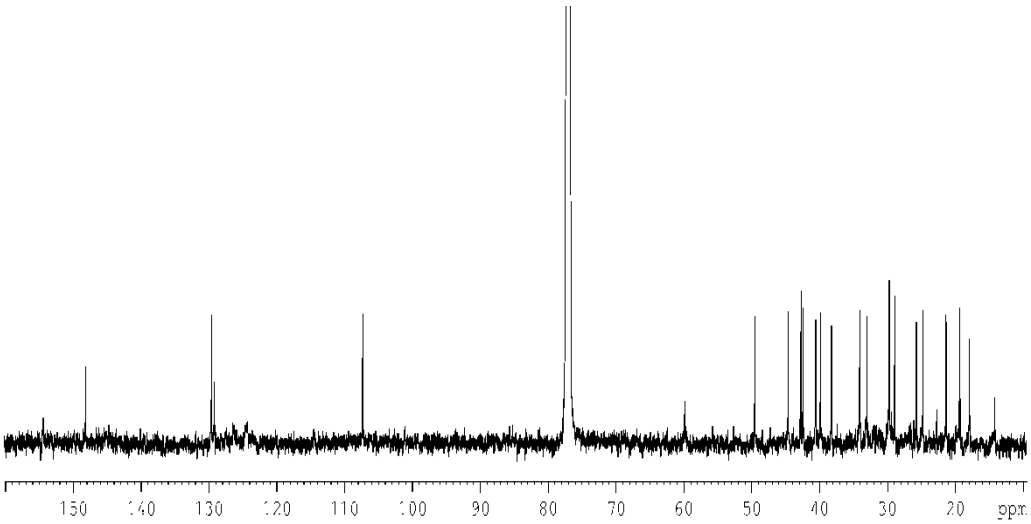

^{13}C-NMR spectrum (175 MHz, $CDCl_3$) of compound **1**

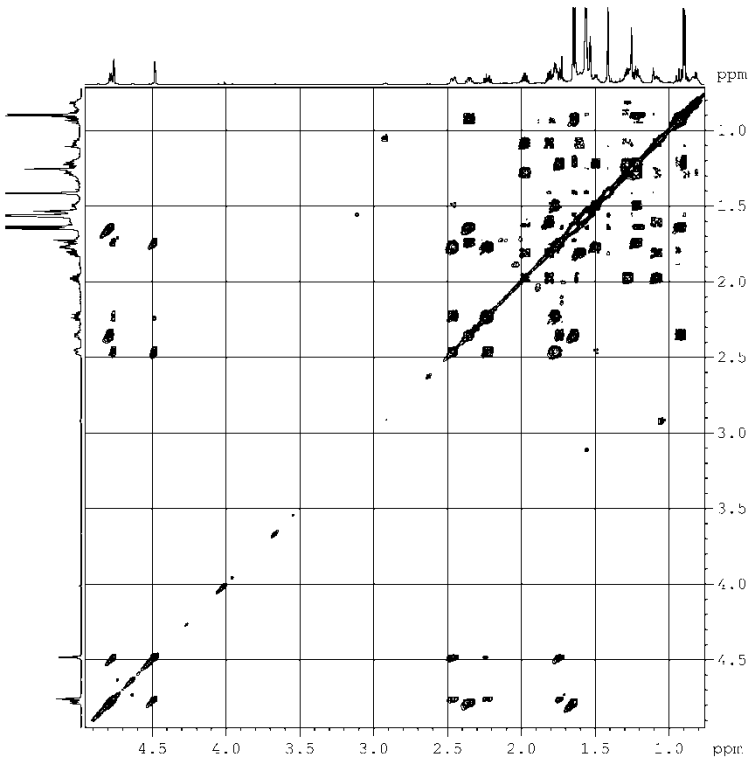

COSY spectrum (700 MHz, $CDCl_3$) of compound **1**

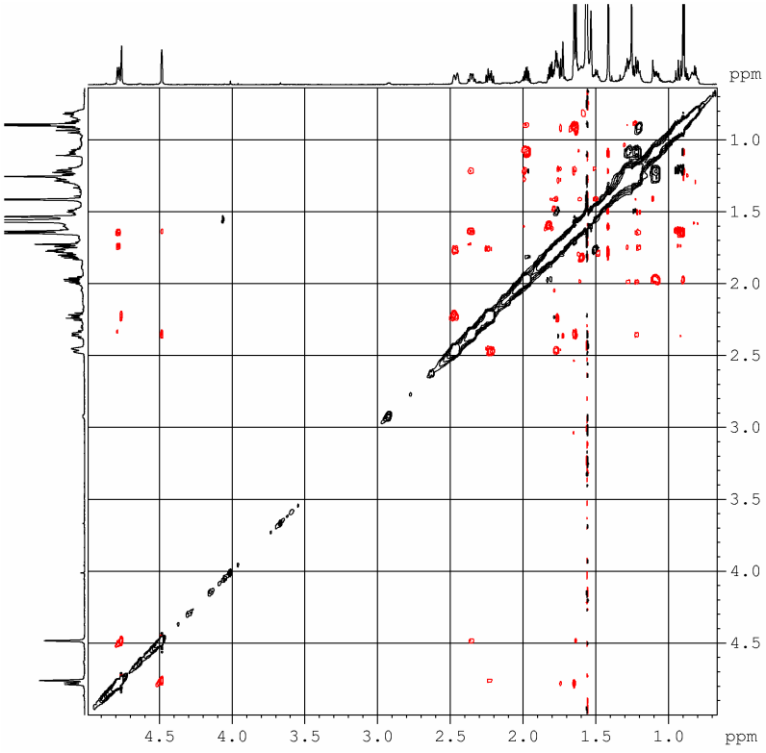

ROESY spectrum (700 MHz, $CDCl_3$) of compound **1**

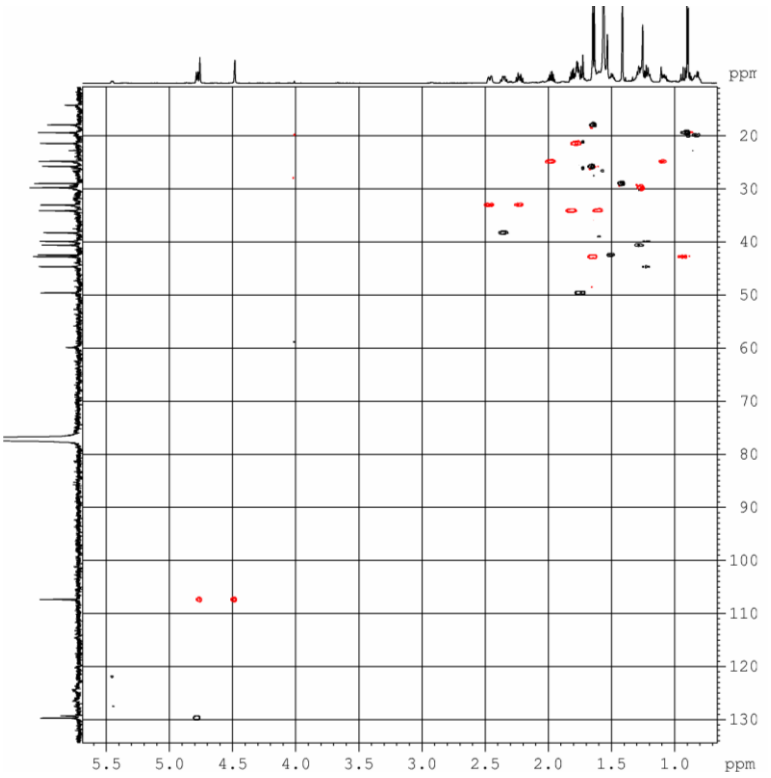

HSQC spectrum (500 MHz, $CDCl_3$) of compound **1**

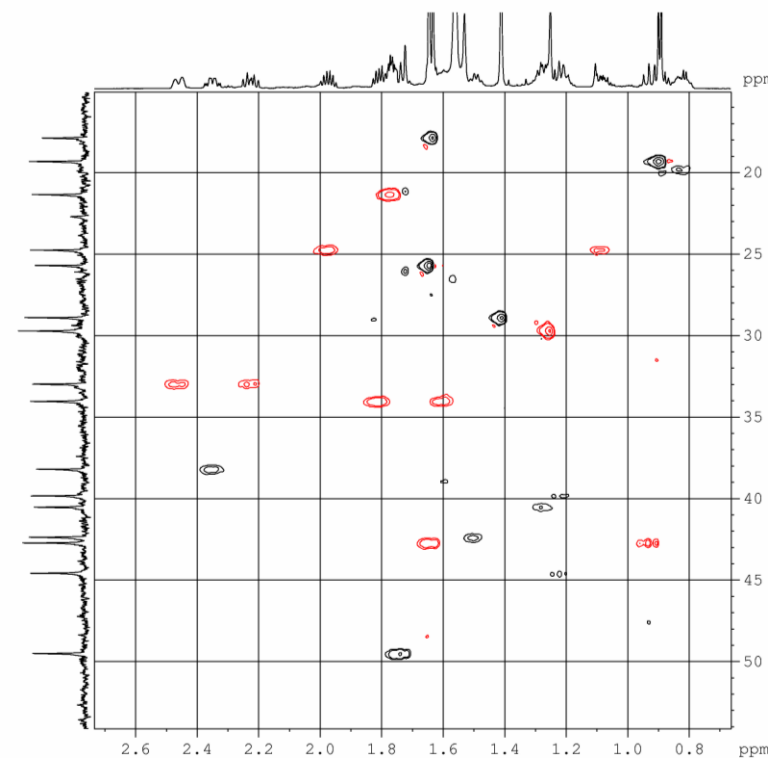

HSQC spectrum (500 MHz, $CDCl_3$, high-field region) of compound **1**

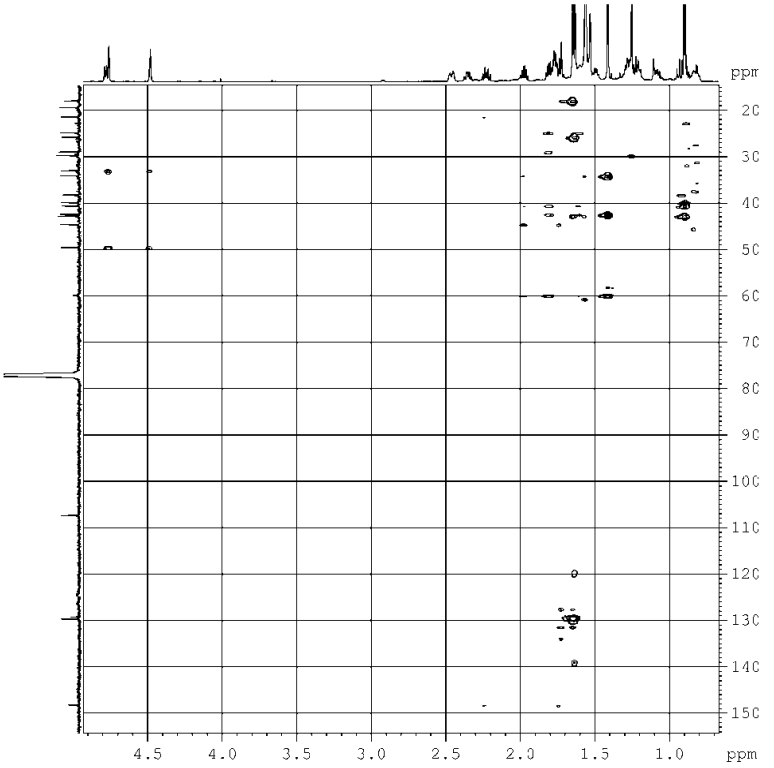

HMBC spectrum (500 MHz, $CDCl_3$) of compound **1**

Chapter 6

Analysis of the sponge *Plakortis simplex*

The Caribbean sponge *Plakortis simplex* is known to contain a large array of secondary metabolites, and therefore is the subject of ongoing investigations because of its rich chemistry (Figure 6.1).

Plakortin (**a**),[54] a peroxide polyketide with antimalarial activity, is by far the most abundant secondary metabolite produced by the sponge, and alone accounts for over 25% of the total lipophilic extract.

During the past years, chemical analyses of the Caribbean sponge *Plakortis simplex* have been extensively carried out by our research group. An incredible variety and abundance of secondary metabolites, including unusual glycolipids and other amphiphilic compounds, was isolated. Many of these molecules are novel compounds endowed with interesting and promising bioactivitities.

However, in addition to a number of new glycolipids (Figure 6.1), such as plakosides A (**b**) and B (**c**),[55] simplexides (**d**, see chapter 7),[56] crasseride (**e**)[57] and discoside (**f**, isolated for the first time from the Caribbean sponge *Discodermia dissoluta*, but also found in specimens of *Plakortis s.*),[58] this sponge was shown to produce also several polyketide, alkaloid metabolites

[54] Higgs M.D., Faulkner D.J., *J. Org. Chem,.* **1978**, 43, 3454 3457
[55] Costantino V., Fattorusso E., Mangoni A., Di Rosa M., Ianaro A., *J. Am. Chem. Soc .*,**1997**, 119, 12465–12470
[56] Costantino V., Fattorusso E., Mangoni A., Di Rosa M., Ianaro A., *Bioorg .Med. Chem. Let.t* **1999**, 9, 271–276
[57] Costantino V., Fattorusso E., Mangoni A., *J. Org. Chem,,.* **1993**, 58, 186–191
[58] Barbieri L., Costantino V., Fattorusso E., Mangoni A., *J. Nat. Prod.,* **2005**, 68, 1527-1530

and bacteriohopanoids. In this regard, bacteriohopanetetrol (**g**),[59] the 12-methyl bacteriohopanetetrol (**h**)[60] and 32,35-anhydro bacteriohopanetetrol (**i**)[61] are very common in *P. simplex* (Figure 6.1).

They are triterpenoids based on the hopan skeleton, typical of bacteria, and can amount to 50% of the total sterol fraction in weight.

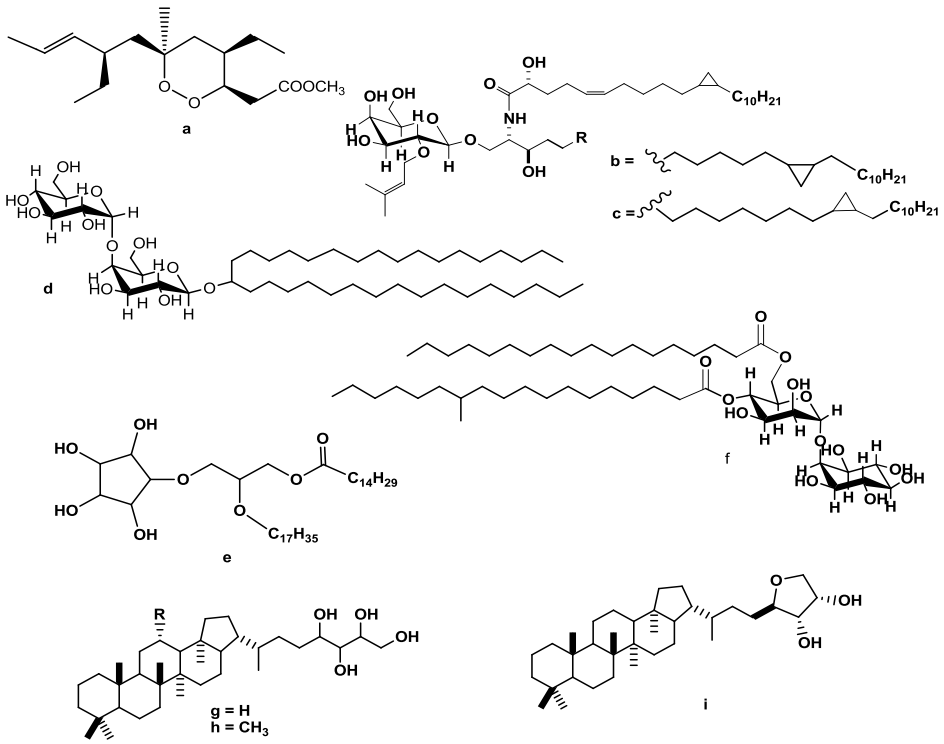

Figure 6.1: Chemical structures of some metabolites from *P. simplex*: plakortin (**a**), plakoside A (**b**) and plakoside B (**c**), simplexide (**d**), crasseride (**e**), discoside (**f**), bacteriohopanetetrol (**g**), 12-methyl-bacteriohopanetetrol (**h**) and 32,35-anhydro-bacteriohopanetetrol (**i**).

The high bacterial content in *P. simplex* was demonstrated by Laroche et al.[62] who asserted that not only bacteriohopanoids, but also other secondary

[59] Rohmer M., Ourisson G., *Tetrahedon Lett*., **1976**, 3633-3636
[60] Costantino V., Fattorusso E., Imperatore C., Mangoni A. *Tetrahedron,* **2000**, 56, 3781–3784
[61] Costantino V., Fattorusso E., Imperatore C., Mangoni A. *Tetrahedron,* **2001**, 57, 045–4048

metabolites, such as glycosphingolipids and plakortin, are very likely of microbial origin.

Recently, due to the high interest in *Plakortis simplex*, the chemical analysis of an Indonesian specimen has been undertaken.

6.1 Plakohopanoid, a new inositol-hopanoid from an Indonesian specimen of *Plakortis simplex*

The glycolipidic composition of an Indonesian specimen of *Plakortis simplex* was compared with that of Caribbean specimens, already extensively studied.

In spite of the geographical distance, the glycolipidic content of the Indonesian and Caribbean specimens was very similar.

However, the Indonesian *P. simplex* also contained a new glycolipid, plakohopanoid (compound **1a**, Figure 6.2), which is a hopanoyl inositol combining structural features of bacteriohopanetetrol (BHT) and discoside, compounds **g** and **f** respectively (Figure 6.1).

Like discoside (**f**), it is composed of a mannosil inositol unit, in which the acylic part is replaced by a C-32 hopanoic acid.

To the best of our knowledge, it is the first time that a C_{32} hopanoic acid is isolated from a marine organism.

Actually, C_{32} hopanoic acids are identified as geohopanoids because mostly present in sediments and are considered diagenetic products, formed from

[62] M. Laroche, C. Imperatore, L. Grozdanov, V. Costantino, A. Mangoni, U. Hentschel, E. Fattorusso, *Ma.r Biol*., **2007**, 151, 1365–1373

an abiotic degradation of biohopanoids (BHT) in bacteria. Diagenetic transformation from biohopanoids to geohopanoids can take place quickly after the death of bacteria.

This finding in a marine organism is worthy of note because shows that also a biogenetic pathway can lead to a C-32 hopanoic acid.

Since the content of symbiotic bacteria in *Plakortis simplex* constitutes more than 50% of the sponge mass, it is very likely that it could be synthesized by bacteria and not from sponge cells.

It is possible to assume that this structure comes from the bacteriohopanetetrol via natural oxidative cleavage and subsequent degradation of the side chain C32/C35 by bacteria which live in symbiosis with the sponge.

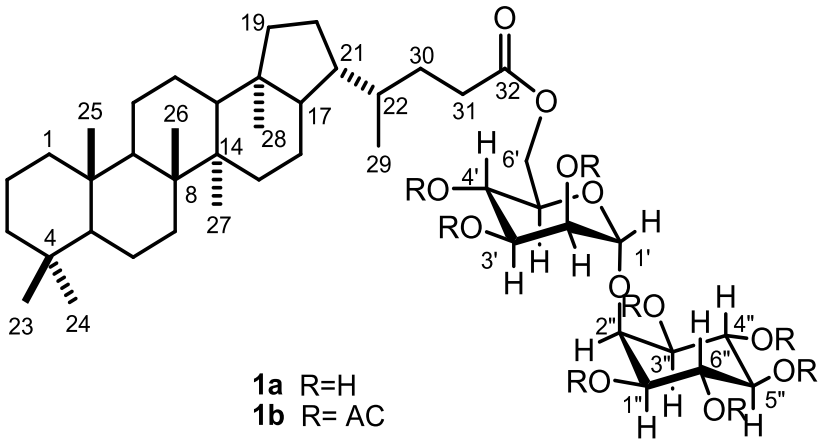

Figure 6.2: Structure of compounds **1a** and **1b**

6.2 Isolation of plakohopanoid

The MeOH extract of the marine sponge *Plakortis simplex* (collected in the Bunaken Marine Park of Manado, Indonesia) was partitioned between BuOH and H_2O. The organic layer was added to $CHCl_3$ extract and purified

by reversed-phase chromatography followed by normal-phase chromatography, yielding a crude fraction mainly composed of glycolipids. This fraction was subjected to acetylation with Ac_2O in pyridine. The peracetilated glycolipid fraction was chromatographed by HPLC (*n*-hexane-EtOAc 6:4), getting the pure plakohopanoid as its peracetyl derivative (**1b**). This derivatization procedure, generally useful in the study of glycolipids, was particularly important in this case. Natural hopanoids are often very insoluble compounds and therefore very hard to purify, while their peracetylated derivatives are well soluble in non polar organic solvent and easy to separate by normal-phase chromatography. In addition, NMR-based structure elucidation is made easier by the better signal dispersion. Unfortunately, compound **1b** could not be deacetylated to give natural inositol-hopanoid **1a** because of the ester-linked hopanoid. We tried to isolate plakohopanoid **1a** from nonacetylated crude glycolipid fraction, but we did not success because of the difficulty of solubilizing it in common organic solvent and of separating nonacetylated glycolipids.

6.3 Structure determination of plakohopanoid

High resolution mass spectrometry showed the presence of an intense pseudomolecular ion peak $[M+Na]^+$ at *m/z* 1153.5886 supporting the molecular formula $C_{60}H_{90}NaO_{20}^+$.

Indeed high resolution-mass spectrum of the no-acetylated glycolipid fraction showed a peak $[M+Na]^+$ at *m/z* 817.5143, corresponding to the

molecular formula $C_{44}H_{74}NaO_{12}^{+}$ of compound **1a**. This result allowed to assume that the natural compound has no acetyl groups in its structure.

Structure elucidation of compound **1b** was mainly based on a comparison of the ^{1}H and ^{13}C NMR spectra of plakohopanoid with those of compound **f** for the polar moiety and compounds **g** and **i** for the triterpene moiety (see figure 6.1).

The structure of the two moieties was confirmed by 2D NMR experiments. The HMBC correlation peak between C-32 (δ 173.4, C_6D_6) of the triterpene moiety and H-6′a (δ 4.57, C_6D_6) and H-6′b (δ 4.44, C_6D_6) of the polar moiety proved the ester connection between the two moieties: 2-*O*-[*α*-mannopyranosyl]-*myo*-inositol and the C_{32} hopanoic acid.

As usual for molecules with these structure features, many resonances overlapped, preventing their analysis. To narrow this problem, NMR spectra were recorded in two different solvents ($CDCl_3$ and C_6D_6).

Concerning the polar moiety of plakohopanoid, mono and bidimensional NMR data showed chemical shifts and coupling constants just alike to saccharidic moiety of discoside peracetate.[57]

In HSQC NMR experiment (C_6D_6), the signal at δ 100.4 (C-1′), correlating to a proton at δ 4.99 (H-1′), was indicative of an anomeric carbon atom and confirmed the presence of only one sugar. Using the H-1′ resonance as the starting point, analysis of COSY correlation peaks permitted the identification in sequence of four methine protons at δ 5.65 (H-2′), δ 5.77 (H-3′), δ 5.85 (H-4′), δ 4.52 (H-5′), and δ 4.57 (H-6′a) and δ 4.44 (H-6′b).

These data proved that the sugar has a hexose structure, which is in the pyranose form because of the relatively shielded chemical shift of H-5′.

At this point, the analysis of coupling constant was necessary to disclose the nature of the hexopyranose. The large coupling constant (*J*= 10 Hz) between H-4′ and H-5′ was indicative of the *trans*-diaxal nature of these protons, while the large (*J*=10 Hz) and small (*J*=3.3 Hz) coupling constants of H-3′ showed that this is an axial proton flanked by the axial H-4′ and the equatorial H-2′. Thus, the configuration of the hexopyranose unit was defined as *manno*.

The α anomeric configuration of the sugar unit was proved by the calculation of the coupling constant between H-1′ and C-1′ in the HSQC ($^1J_{CH}$=~170 Hz). Indeed, it is known that $^1J_{CH}$ coupling constant of an axial anomeric proton is approximately 158-162 Hz, while that of an equatorial anomeric proton is 169-171 Hz.

The other six oxymethine resonances in the mild-field region were assigned to an inositol unit, as reported in Costantino et al. 2005. In ^{1}H NMR spectrum, recorded in C_6D_6, the proton H-2″ (δ 4.2) was coupled with two protons at δ 4.88 (H-1″) and δ 5.01 (H-3″), which were coupled with signals at δ 5.89 (H-6″) and δ 5.9 (H-4″) respectively. The signal at δ 5.32 was indeed assigned to H-5″ which was coupled with H-4″ and H-6″. The coupling constants displayed the relative configuration of this spin system. It is a *myo*-inositol glycosilated at C-2″ because of the upfield chemical shift of H-2″ (δ 4.2), confirmed by an HMBC correlation between H-1′ and C-2″ and between H-2″ and C-1′.

Thus, the mannose links in position 1′ the 2″-hydroxyl group of the *myo*-inositol unit but, unlike discoside (**f**), signals attributable to the two linear alkyl chains were not present. Rather, the HMBC experiment in C_6D_6 revealed an intense correlation peak between the protons H-6′a (δ 4.57) and H-6′b (δ 4.44) and the carbon at δ 173.4, which were assigned to the carbonyl of the triterpene moiety.

Regarding the structure elucidation of this moiety, the high-field region of ^{1}H NMR spectrum of compound **1b** (between δ 0.69 and 0.94 in $CDCl_3$) showed six methyl singlets and a methyl doublet, as bacteriohopanetetrol (**g,** figure 6.1), thus suggesting that **1b** has the same methyl groups. In contrast, the mild-field region was not comparable to that of compound **g**, indicating that the sugar-derived side chain was not present. In ^{13}C NMR spectrum ($CDCl_3$) in the low field region, apart from the signals between 169.34 and 169.86 ppm corresponding to acetyl carbonyls, a further signal at δ 173.9 (δ 173.4 in C_6D_6) was observed.

This carbon has a chemical shift value typical of a carbonyl and in the HMBC spectrum ($CDCl_3$) showed intense correlation peaks not only with the protons of the polar moiety H-6′a (δ 4.25) and H-6′b (δ 4.08), but also with proton resonating at δ 2.24 and δ 2.37, which were assigned to H-31a and H-31b respectively.

Further HMBC and COSY correlations allowed to define the hopanoic side chain. Specifically, in the COSY spectrum the correlations of H-31a (δ 2.24) and H-31b (δ 2.37) with two protons resonating at δ 1.8 and 1.29 were

observed. By means of HSQC the two groups of protons were assigned to C-31 (δ 30.8) and C-30 (δ 30.5) respectively.

The polycyclic skeleton was devoid of functional groups and most proton signals were severely overlapping. As usual, part structures of compound **1b** were elucidated from long-range proton-carbon coupling constants of angular methyl protons and, afterward, linked by means of COSY correlations (Figure 6.3 and table 6.1).

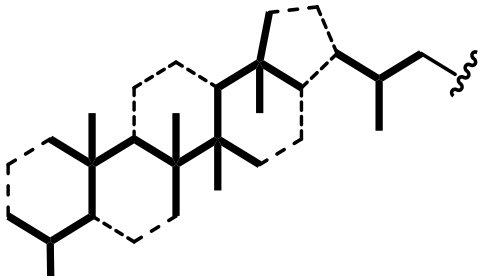

Figure 6.3: Structure determinated from HMBC correlations (bold lines) and COSY correlations (dotted lines).

These data displayed that the triterpene moiety is a C_{32} hopanoic acid and it is worth to suppose that this structure comes from the bacteriohopanetetrol (**g** in figure 6.1) via natural oxidative cleavage and subsequent degradation of side chain C32/C35.

Once defined the planar structure of compound **1b**, an attempt of deacetylation in mild condition was performed in order to get the compound **1a**. The compound **1b** was reacted with sodium carbonate in MeOH, but this reaction led to compound **2** (Figure 6.4), the methyl ester of C_{32} hopanoic acid, already known in literature. [63]

[63] Peiseler B. and Rohmer M., *J. Chem. Soc. Perkin trans.* (1991), 1, 2449-2453

The ^{1}H chemical shifts of methyl groups [δ 0.69 (s, H_3-28), δ 0.78 (s, H_3-24), δ 0.80 (s, H_3-25), δ 0.84 (s, H_3-23), δ 0.92 (d, H_3-29), 0.93 (s, H_3-26) and 0.94 (s, H_3-27)] were very similar to those reported in the paper and also the specific optical rotation ($[\alpha]_D^{25}$ +84) was the same in absolute value. These results allowed to define both relative and absolute configuration of the triterpene moiety (Figure 6.4).

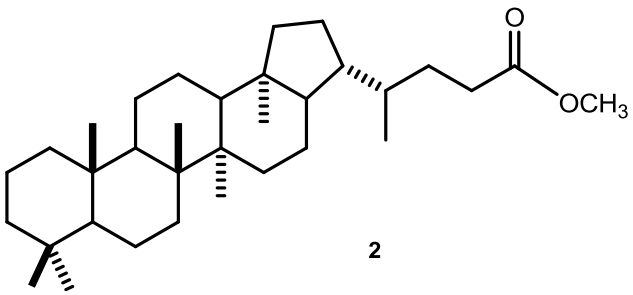

2

Figure 6.4: Absolute stereochemistry of compound **2**.

Finally, the absolute configuration of the mannose has to be determinated. Therefore, the benzoylation of the polar moiety will be performed and its ^{1}H NMR and CD spectra will be recorded and compared with those of an authentic sample of known stereochemistry.

6.4 Experimental section

General methods

High Resolution ESI-MS and ESI-MS/MS spectra were performed on a Thermo LTQ Orbitrap XL mass spectrometer. The spectra were recorded by infusion into the ESI source using MeOH as the solvent. Optical rotations were measured at 589 nm on a Jasco P-2000 polarimeter using a 10-cm microcell. NMR spectra were determined on Varian UnityInova spectrometers at 500 MHz; chemical shifts were referenced to the residual solvent signals ($CDCl_3$: δ_H = 7.26, δ_C = 77.0, C_6D_6: δ_H= 7.15, δ_C =128.15). For an accurate measurement of the coupling constants, the one-dimensional ^1H NMR spectra were transformed at 64K points (digital resolution: 0.09 Hz). Homonuclear ^1H connectivities were determined by a COSY experiment. Through-space ^1H connectivities were calculated using a ROESY experiment with a mixing time of 450 ms. The single-quantum heteronuclear correlation (HSQC) and multiple-bond heteronuclear correlation (HMBC) spectra were adjusted, respectively, for an average $^1J_{CH}$ of 142 Hz and a $^{2,3}J_{CH}$ of 8.3 Hz. High performance liquid chromatographies (HPLC) were performed on a Varian Prostar 210 apparatus equipped with an Varian 350 refractive index detector.

Collection, extraction and isolation

A specimen of *Plakortis simplex* was collected in January 2010 along the coasts of the Bunaken island in the Bunaken Marine Park of Manado. The sponge (380 ml of volume before extraction and 50 g of dry weight after

extraction) was cut into pieces and extracted with MeOH (3 x 1.5 L), MeOH/$CHCl_3$ (4 x 1.5 L) and $CHCl_3$(2 x 1.5 L). The MeOH extracts were partioned with H_2O and BuOH; the organic layer was added to $CHCl_3$ extracts, affording 8.5 g of a dark brown oil, which was chromatographed on a column packed with RP-18 silica-gel. The fraction eluted with $CHCl_3$ 100% (1.8 g) was subjected to a further chromatography on a SiO_2 column with solvent of increasing polarity. The fraction eluted with AcOEt/MeOH 7:3 was mainly composed of glycolipds. This fraction was acetylated with Ac_2O in pyridine overnight and subjected to HPLC separation on a SiO_2 column [eluent: *n*-hexane/EtOAc (6:4)], thus affording the pure plakohopanoid as its peracetyl derivative (1.2 mg).

Plakohopanoid Peracetate (1b): white powder; HRESIMS (positive ion mode, MeOH), $[M+Na]^+$ at *m/z* 1153.5885, molecular formula $C_{60}H_{90}NaO_{20}^+$, ^{1}H-NMR (500 MHz, C_6D_6): δ 1.44 (H-30b), 2.05 (H-30a), 2.40 (1-H, ddd, J=15.9, 9.1 and 6.9 Hz, H-31b), 2.46 (1 H, ddd, J=15.9, 10.0 and 5.4 Hz, H-31a), 4.2 (1 H, t, J= 2.4 Hz, H-2″), 4.44 (1 H, dd, J=12.2 and 1.5 Hz, H-6′b), 4.52 (1 H, ddd, J=9.83, 5.34 and 1.5 Hz, H-5′), 4.57 (1 H, dd, J=12.2 and 3.8 Hz, H-6′a), 4.88 (1 H, dd, J=10.5 and 2.4 Hz, H-1″), 4.99 (1 H, d, J=2.3 Hz, H-1′), 5.01 (1 H, dd, J=10.5 and 2.4Hz, H-3″), 5.32 (1H, t, J=9.61 Hz, H-5″), 5.65 (1 H, dd, J=3.4 and 2.3 Hz, H-2′), 5.77 (1-H, dd, J=10 and 3.3 Hz, H-3′), 5.85 (1-H, t, J=10 Hz, H-4′), 5.89 (1H, t, J=10.04 Hz, H-6″), 5.9 (1H, t, J=10.04, H-4″); ^{13}C-NMR (500 MHz, C_6D_6): δ 31.4 (CH_2, C-30), 31.6 (CH_2, C-31), 62.4 (CH_2, C-6′), 66.4 (CH, C-4′),

69.7 (CH, C-3′), 70.4 (CH, C-6″), 70.7 (CH, C-1″), 70.8 (CH, C-2′), 70.9 (CH, C-5′), 71.0 (CH, C-4″), 71.1 (CH, C-3″), 71.7 (CH, C-5″), 77.7 (CH, C-2″), 100.4 (CH, C-1′), 173.4 (C, C-32).

^{1}H and ^{13}C NMR (500 MHz, $CDCl_3$): table 6.1.

Methyl (22*R*)-33,34,35-trinorbacteriohopan-32-oate: $[\alpha]_D^{25}$= +84 (*c* = 0.11 in $CHCl_3$), 400 μg of compound **1b** was dissolved in 100 μL of $CHCl_3$ and 100 μL of a solution (10 mM) of Na_2CO_3 in MeOH were added. After 48 h, the reaction mixture was dried under N_2 flow and chromatographed by HPLC on an analytical column in *n*-hexane/AcOEt 95:5, giving the pure compound **2** (100 μg).

^{1}H (500 MHz, $CDCl_3$): 0.69 (3 H, s, H_3-28), 0.78 (3 H, s, H_3-24), 0.80 (3 H, s, H_3-25), 0.84 (3 H, s, H_3-23), 0.92 (3 H, d, 7.6 Hz, H_3-29), 0.93 (3 H, s, H_3-26), 0.94 (3 H, s, H_3-27), δ 3.66 (3 H, s, $-OCH_3$).

Table 6.1: ^{1}H and ^{13}C NMR data of plakohopanoid peracetate **1b** ($CDCl_3$)

Position		δ_H [mult., *J* (Hz)]	δ_C [mult.]
1″		4.99 (dd, 10.6, 2.4)	69.4
2″		4.29 (t, 2.4)	76.3
3″		5.08 (dd, 10.6, 2.4)	70.1
4″		5.53 (t, 10.16)	69.3
5″		5.19 (t, 9.8)	70.4
6″		5.49 (dd, 10.6, 9.9)	69.1
1′		4.95 (d, 1.45)	99.2
2′		5.36 (dd, 2.05, 0.26)	69.36
3′		5.40 [a]	65.3
4′		5.41[a]	68.43
5′		4.17 (dt, 8.54, 3.4)	69.2
6′	a b	4.25 (dd, 12.4, 4.27) 4.08 (dd, 12.4, 12.13)	61.5
1	a b	1.64[b] 0.76[b]	40.1
2	a b	1.52[b] 1.32[b]	18.6
3	a b	1.11 (ddd, 13.5, 13.5, 4.0) 1.33[b]	42.1
4		-	33.4
5		0.70 (br. s.)	56.1
6	a b	1.32[b]	18.6
7		1.33[b]	33.2
8		-	41.7
9		1.23 [a]	50.4
10		-	37.3
11	a b	1.52[b] 1.7[b]	22.8
12		1.4[b]	23.9
13		1.3[b]	49.2
14		-	41.6
15	a b	1.22[b] 1.34 [b]	33.6
16	a b	1.28 [b] 1.51[b]	20.9

Position		δ_H [mult., *J* (Hz)]	δ_C [mult.]
17		1.28[b]	54.4
18		-	44.3
19	a b	1.5[b] 0.89[b]	41.5
20	a b	1.52[b] 1.8[b]	27.5
21		1.7[b]	45.8
22		1.50[b]	36.3
23		0.84 (s)	33.3
24		0.78 (s)	21.5
25		0.80 (s)	15.9
26		0.93 (s)	16.4
27		0.94 (s)	16.5
28		0.69 (s)	15.6
29		0.92 (d, 7.6)	19.7
30	a b	1.8[b] 1.29[b]	30.5
31	a b	2.24 (ddd, 15.6, 10.5, 6.3) 2.37 (ddd, 15.6, 10.5, 5.2)	30.8
32		-	173.9
Ac's		2.14 (s), 2.09 (s), 2.07 (s), 2.06 (s), 2.04 (s), 2.03 (s), 2.01 (s), 2.0 (s).	20.9-20.5 (CH_3) 169.86-169.34 C=O)

a. Notfirst-order multiplet
b. overlapped

6.5 Mass and NMR data

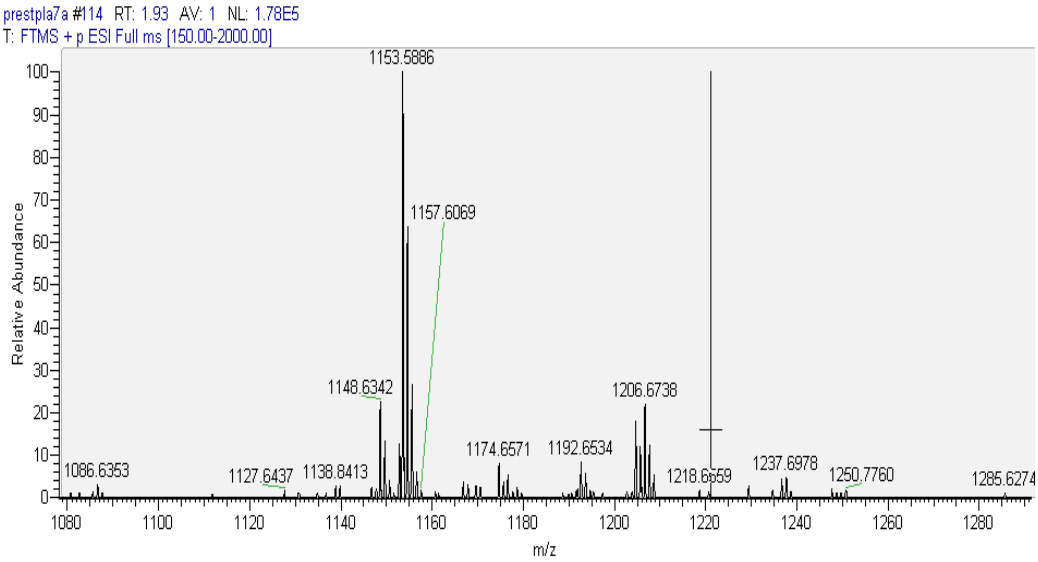

High-resolution ESI MS spectrum of compound **1b**

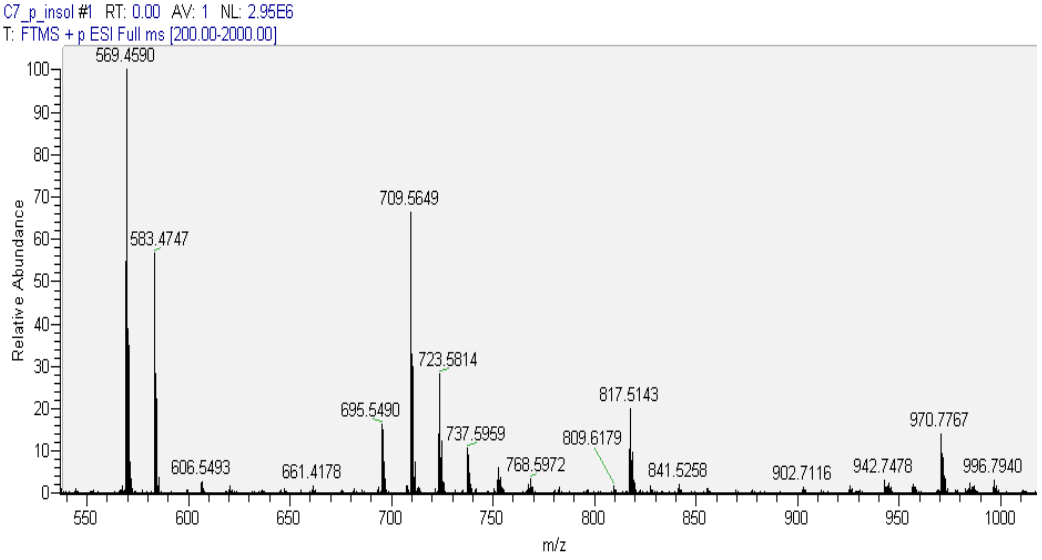

High-resolution ESI-MS spectrum of compounds not soluble in CH_3OH of no-acetylated glycolipid fraction: *m/z* 569.4590 (bacteriohopanetetrol, **g**), 583.4747 (12-Methyl-bacteriohopanetetrol, **f**), 709.5649 and 723.5814 (crasserides, **e**), 817.5143 (plakohopanoide, **1a**), 970.7767 (Plakoside A, **b**)

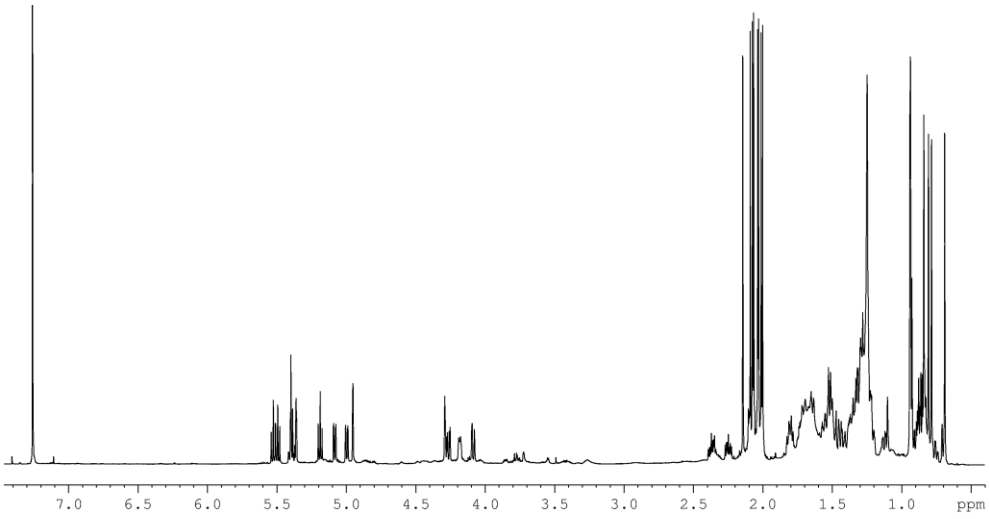

^{1}H NMR spectrum (500 MHz, $CDCl_3$) of plakohopanoid peracetate (**1b**)

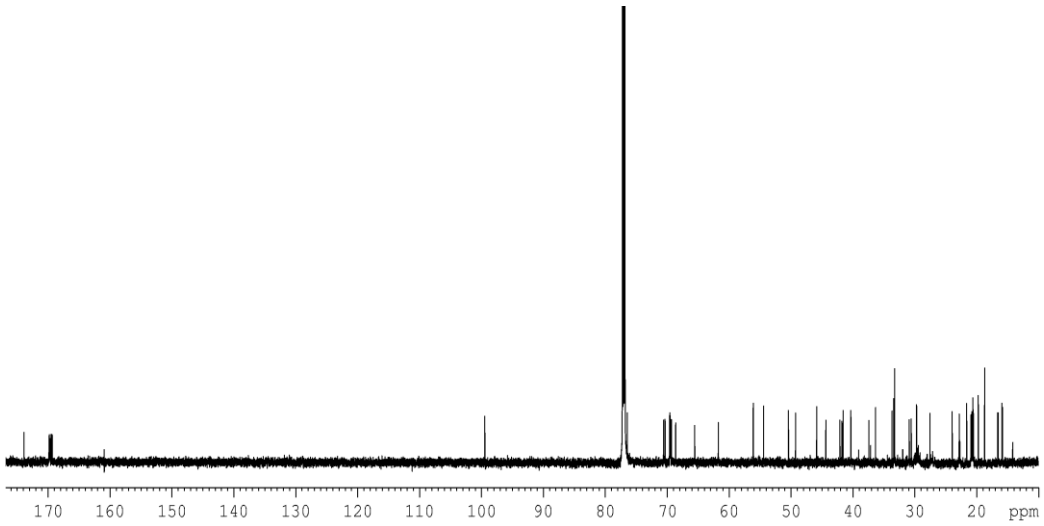

^{13}C NMR spectrum (500 MHz, $CDCl_3$) of plakohopanoid peracetate (**1b**)

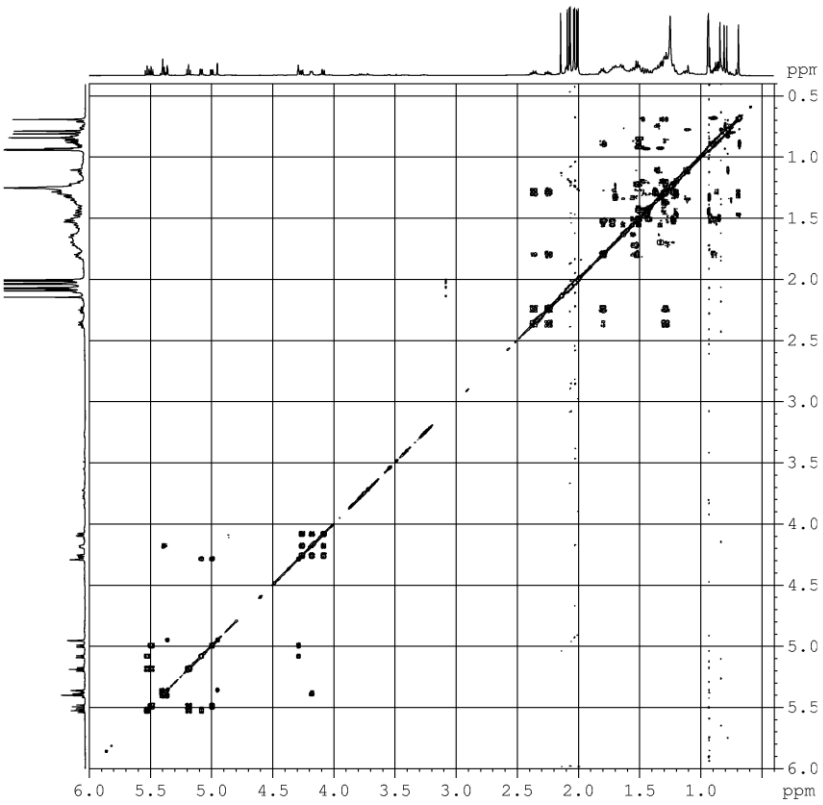

COSY spectrum (500 MHz, $CDCl_3$) of plakohopanoid peracetate (**1b**)

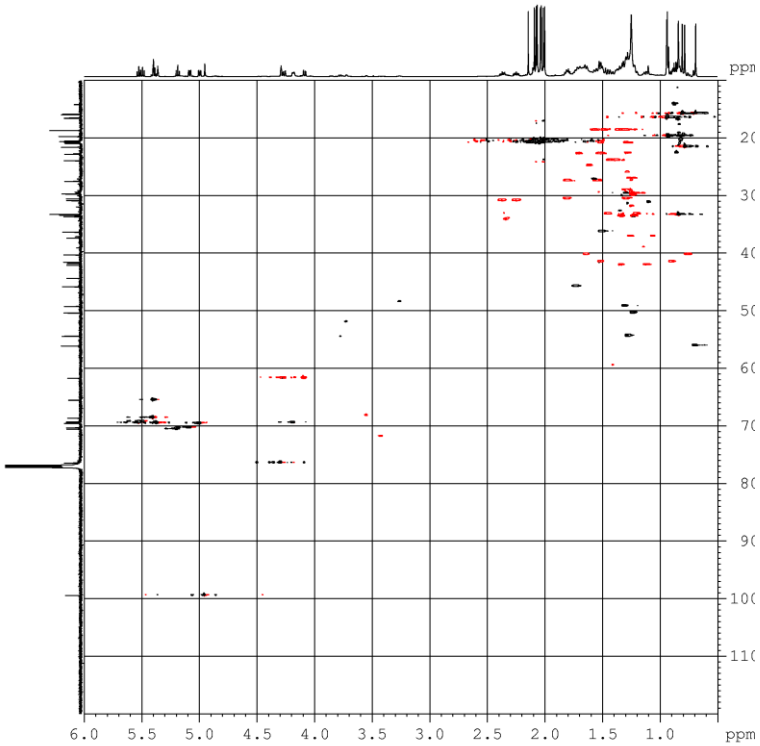

HSQC spectrum (500 MHz, $CDCl_3$) of plakohopanoid peracetate (**1b**)

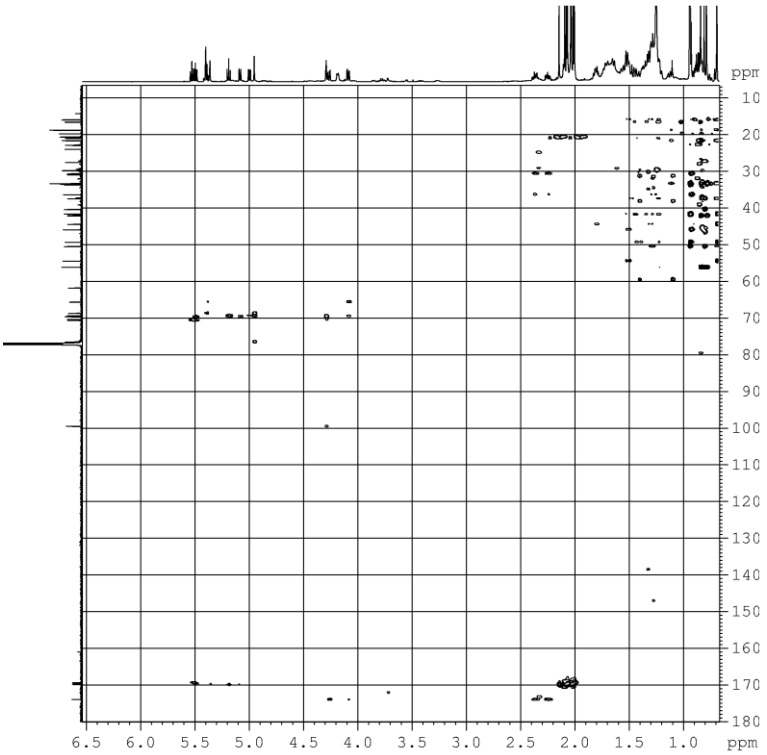

HMBC spectrum (500 MHz, $CDCl_3$) of plakohopanoid peracetate (**1b**)

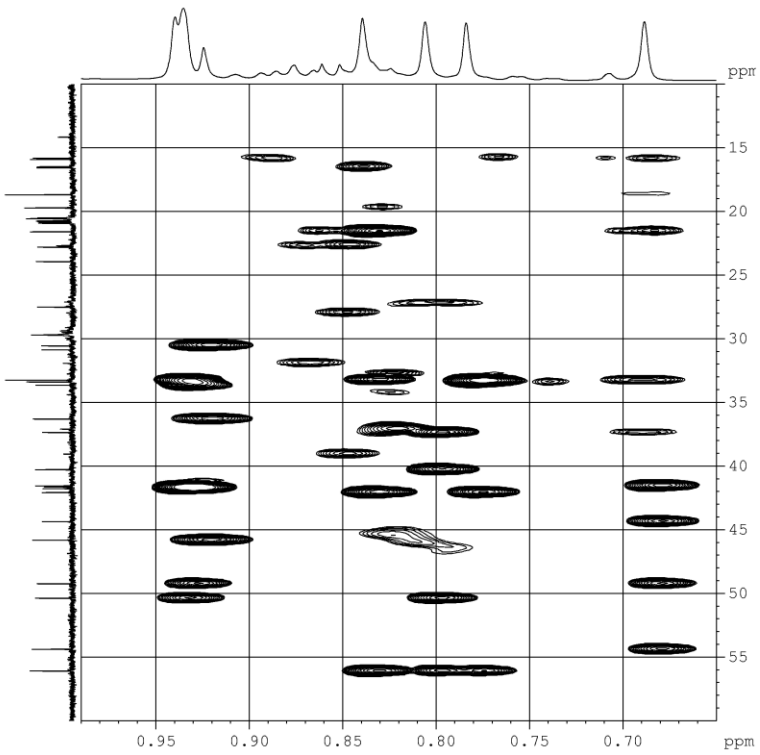

HMBC spectrum (500 MHz, $CDCl_3$, methyl region) of plakohopanoid peracetate (**1b**)

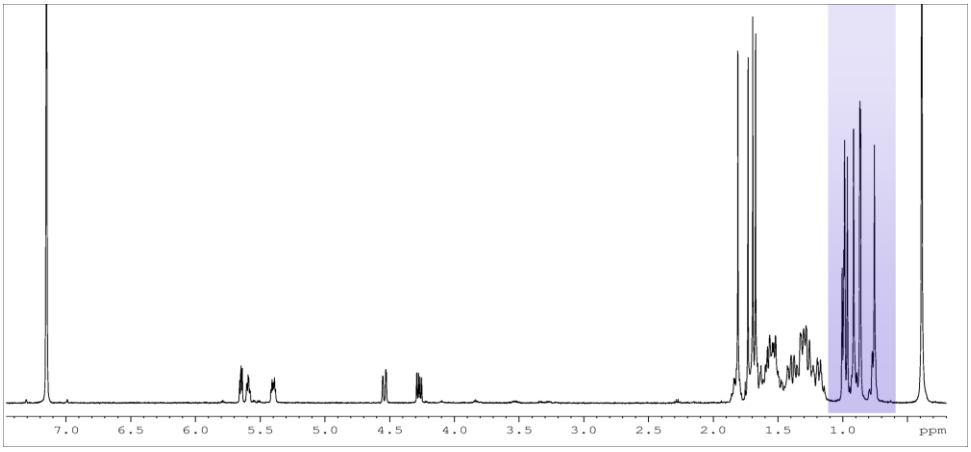

^{1}H NMR spectrum (500 MHz, C_6D_6) of BHT peracetate

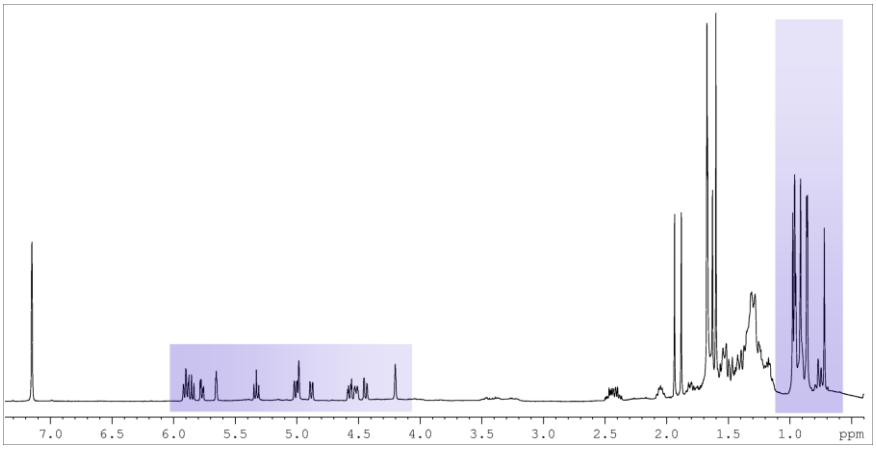

^{1}H NMR spectrum (500 MHz, C_6D_6) of plakohopanoid peracetate (**1b**)

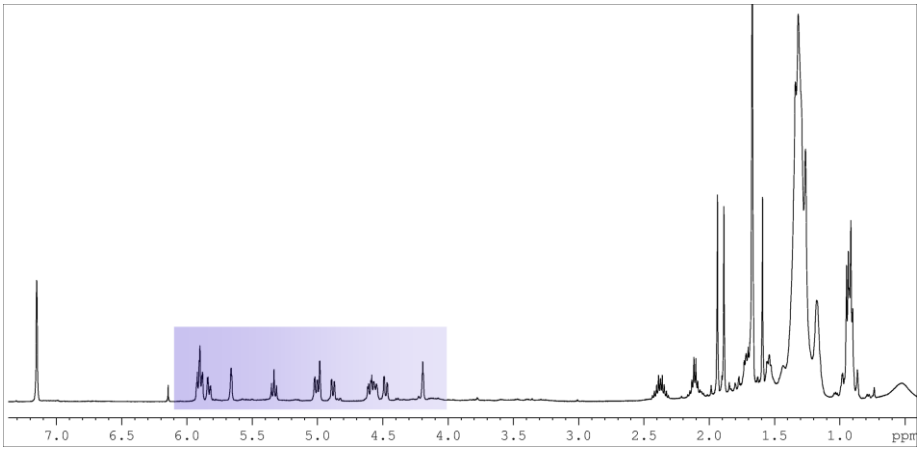

^{1}H NMR spectrum (500 MHz, C_6D_6) of discoside peracetate

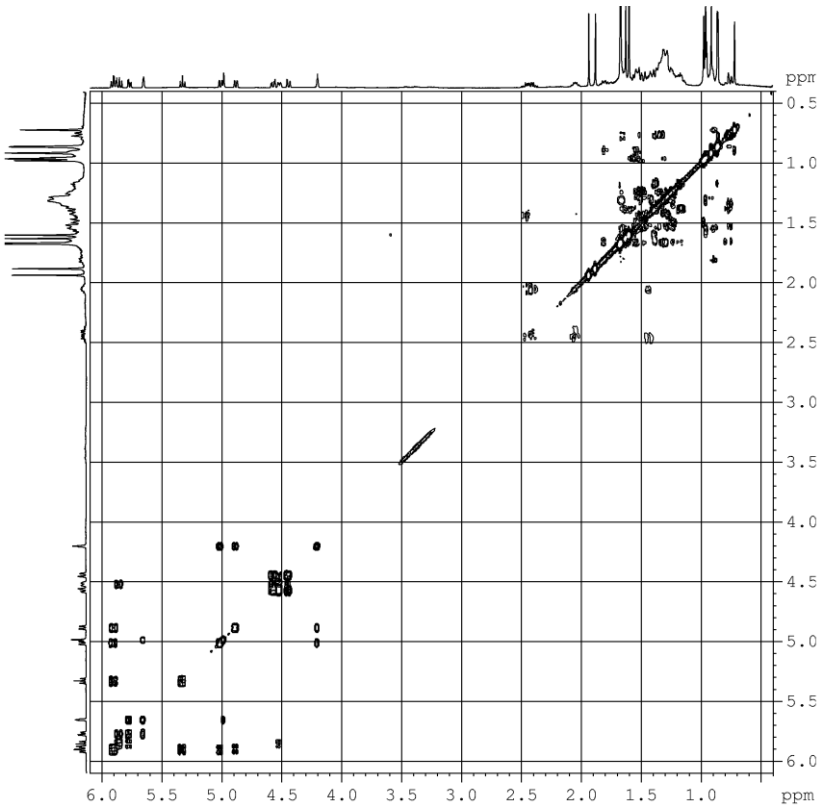

COSY spectrum (500 MHz, C_6D_6) of plakohopanoid peracetate (**1b**)

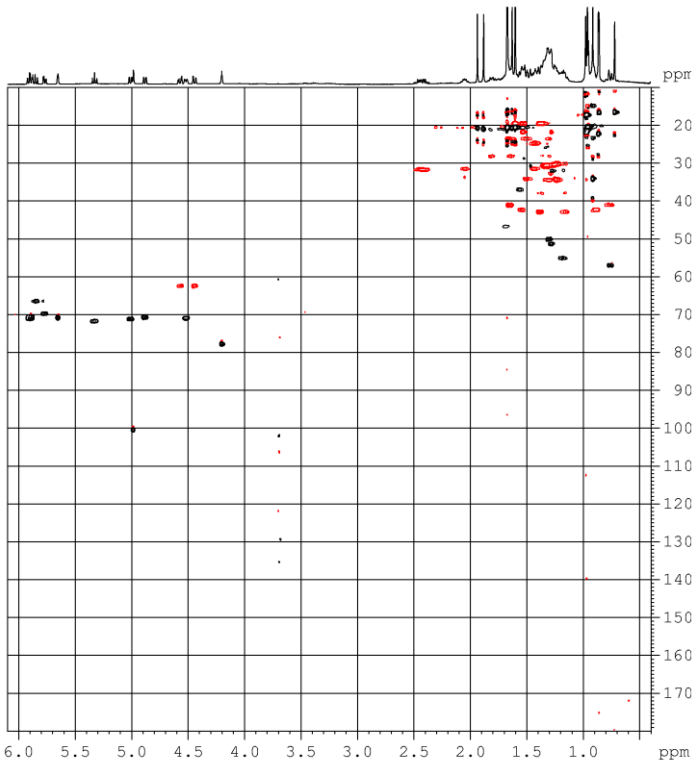

HSQC spectrum (500 MHz, C_6D_6) of plakohopanoid peracetate (**1b**)

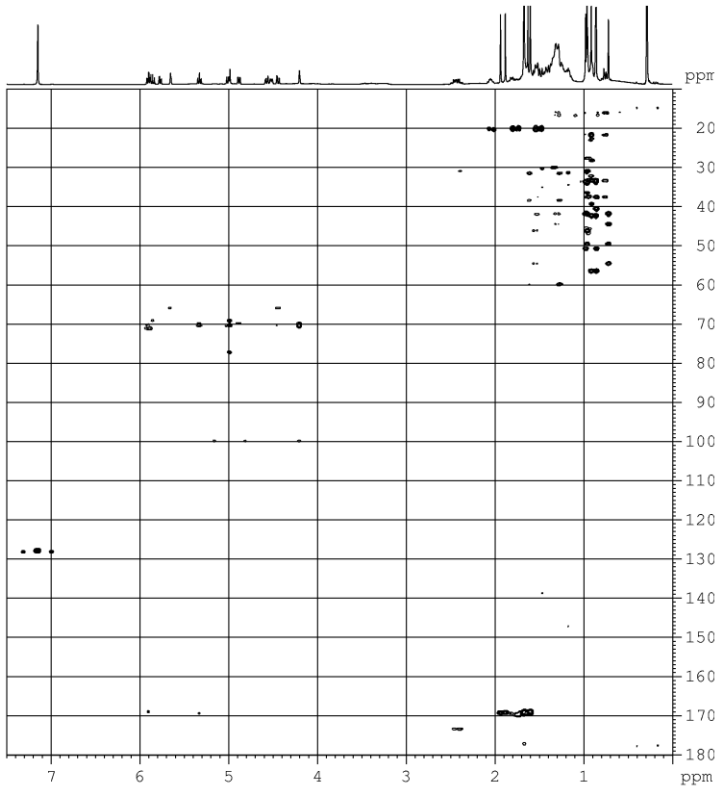

HMBC spectrum (500 MHz, C_6D_6) of plakohopanoid peracetate (**1b**)

Chapter 7

The marine glycolipid simplexide: synthesis of an analogue

In the last years, the knowledge and experience about secondary metabolites have been growing. The reason of this increase could be ascribed to new chromatographic and spectroscopic methods which led to the discovery of new bioactive molecules with interesting pharmacological activities.

Because of the high interest of these compounds and because of the natural sources shortage and difficulty for their supply, innovative approaches are to be used to get them, such as synthesis.

If a molecule shows an interesting pharmacological characteristic, further studies are carried out in order to understand the Structure-Activity-Relations and to identify the pharmacophore, which is responsible of the activity. Total synthesis of natural compounds or analogues allows to emulate and/or improve activities of the lead-compounds.

In recent years our research team focused on the analysis of glycolipids from marine organisms and addressed to the isolation of several new structures and evaluation of their pharmacological activity. In particular, simplexide is a new glycolipid isolated from the Caribbean sponge *Plakortis*

simplex[64] and attracted great attention for the interesting perspective to be used as an immunoregulatory agent in cancer and autoimmune diseases.

Simplexide is a glycolipid with atypical structure, being a glycosylated long-chain secondary alcohol, but it share with glycosphingolipids the presence of two lipophilic long alkyl chains and a polar sugar head.

It is composed of a disaccharide [Glc(1α→4)Gal] residue β-linked to a mixture of secondary long chain alcohols (C_{34}–C_{37}). (see figure 7.1).

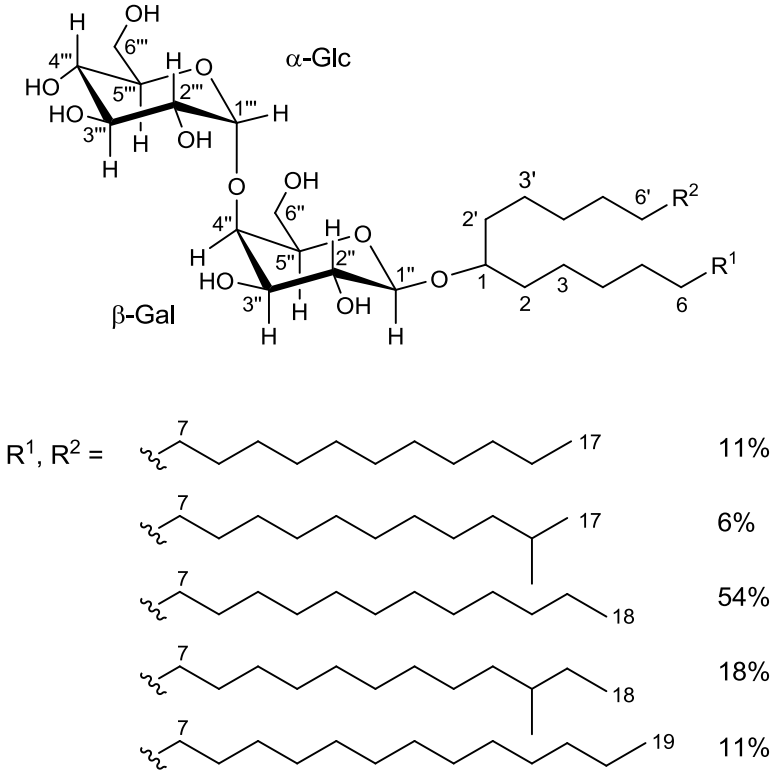

Figure 7.1: Structure of simplexide

Due to the remarkable bioactivity and the therapeutic perspectives of simplexide, the synthesis of an analogue of this glycolipid has been undertaken in order to elaborate on the mechanism of action.

[64] Costantino, V.; Fattorusso, E.; Mangoni, A.; Di Rosa, M; Ianaro, A. J. *Am. Chem. Soc.* , **1997,** 119, 12465-12470

7.1 Immunoregolatory role of simplexide[65]

Innate immunity plays a key role in defense against bacterial and viral infections, in tumor surveillance and for regulating adaptive immune responses by modulating T and B cell functions. Peptides, carbohydrates and lipid molecule are responsible of the innate response and are also known as danger signals because are recognized by pathogen-associate molecular pattern (PAMP) receptors (Toll-like, mannose receptors). Binding of these receptors activates intracellular signaling pathways that mediate a variety of cell responses such as production of inflammatory cytokines, chemokines and growth factors, upregulation of adhesion molecule, stimulation of humoral and cell-mediated immune responses, and activation of vascular endothelial cells. Blood monocytes are major effector cells of innate immunity: they contribute directly to the defense against infections and serve as precursors for macrophages and dendritic cells.

Many naturally glycolipids have long been recognized as modulators of innate and adaptive immunity and are increasingly being recognized as potent activators of immune cell functions.

Preliminary studies on simplexide have shown to inhibit concanavalin A-induced proliferation of murine T cells but the mechanism of this immunosuppressive effect was not investigated. Recently, studies conducted on human blood monocytes have demonstrated that simplexide is a potent stimulus for the production of cytokines and chemokines.

[65] Triggiani et al., *The marine glycolipid simplexide induces CD1d-dependent cytokine production from blood monocytes*, manuscript in preparation.

Simplexide induces expression and release of IL-6, IL-8 and, in a smaller quantities, TNF- α and IL-10.

Simplexide is as potent to induce IL-6 and IL-8 as LPS, but induces smaller quantities of TNF-α and IL-10 as compared to LPS and activates transcription of IL-6 and IL-8, but not TNF-α, a gene whose transcription is strongly induced by LPS. These data clearly indicate that simplexide activates monocytes through signaling pathways that are different from those activated by LPS (Figure 7.2).

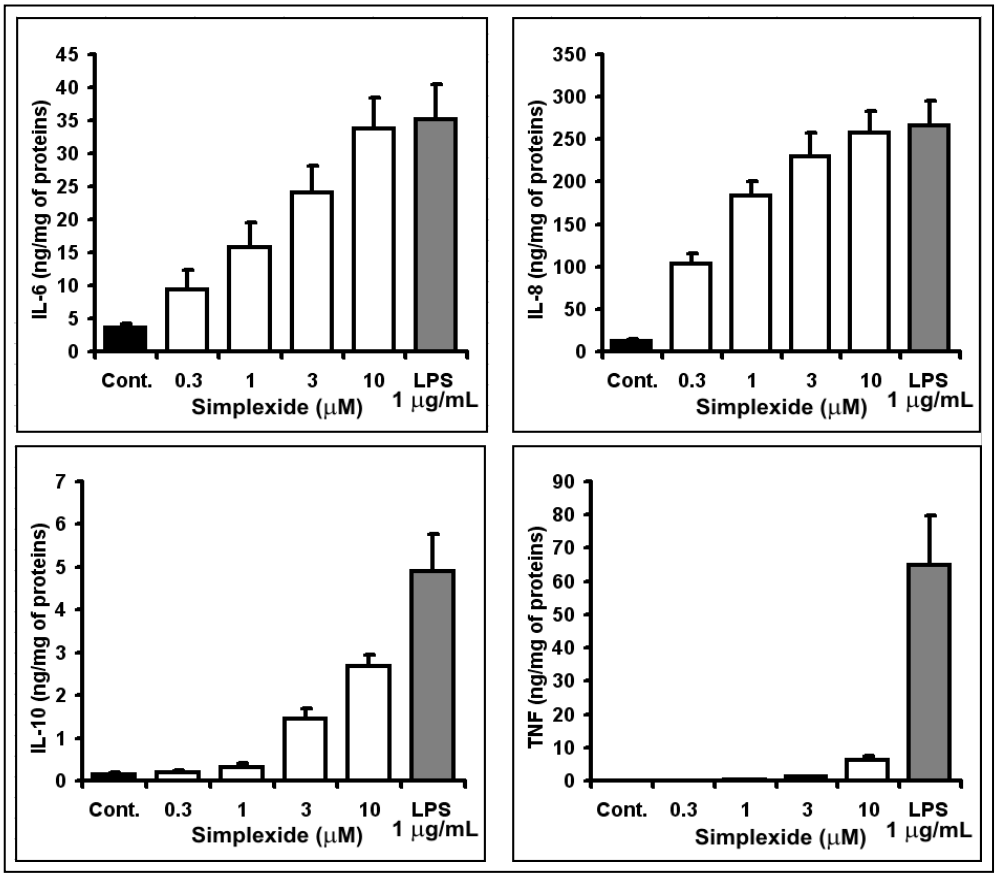

Figure 7.2: Effects of simplexide on the production of IL-6, IL-8, IL-10 and TNF-α

Since glycolipid can function as antigen primarly by interacting with CD1d expressed on APC, the interaction of simplexide with CD1d was tested by comparison of the effect of this glycolipid with that of α-galcer, the best

known ligand for CD1d. The experiments have demonstrated that both glycolipid induce the same profile of cytokines/chemokines from monocytes, but simplexide is more effective and is 30- to 100-fold more potent than α-galcer inducing IL-6 and IL-8 (Figure 7.3).

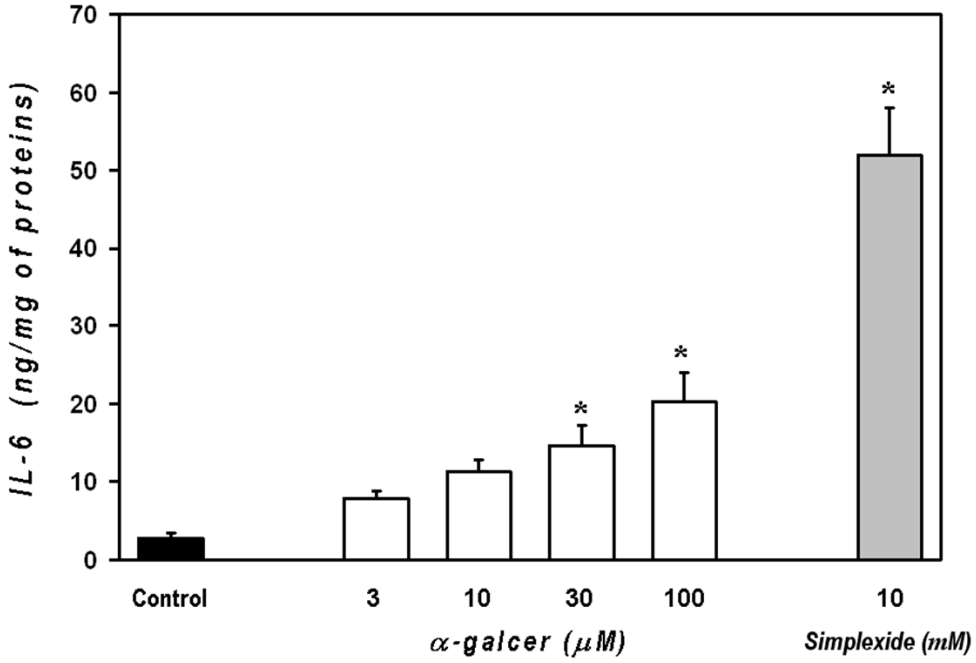

Figure 7.3: Comparison of the effect of simplexide with that of α-galcer.

In spite of simplexide and α-galcer display some structural differences (Figure 7.4), i.e. the aglycon of simplexide is a simple secondary alcohol, while that of α-galcer is a ceramide, both molecules contain two long saturated alkyl chains that can fit the CD1d lipid-binding groove. Thus, it is reasonable to hypothesize the simplexide binds CD1d in a similar way as α-galcer. In the case of simplexide, the inner sugar could substitute for functionalized part of the ceramide of α-galcer, while the outer sugar, an α -glucose, possesses the α anomeric configuration which is characteristic of α-

galcer and is considered essential for the immunoregulatory activity of monoglucosylceramides.

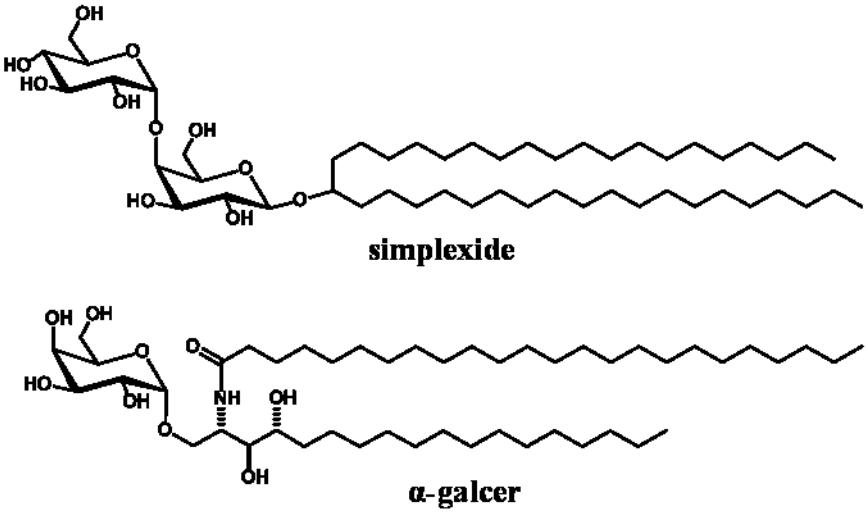

Figure 7.4: Structure of simplexide and α-galcer.

A number of indirect evidence strongly provided that simplexide activates monocyte via CD1d and further experiments are required to demonstrate conclusively that its action takes place by binding CD1d. However, it has been recently reported that certain glycolipids, structurally similar to α-galcer, containing $C_{20:2}$, can directly load onto CD1d at the cell surface. Since the simplexide is more potent than α-galcer, it is possible to assume that it may directly bind to CD1d on the surface and not by internalization within monocytes, but this hypothesis is to be verified.

These data suggest that this glycolipid may behave as a danger signal and may be involved in the activation of innate immunity responses. Thus, the studies accomplished so far opens interesting perspectives on the therapeutics use of simplexide as an immunoregulatory agent in cancer and autoimmune diseases.

7.2 Aim and synthesis design

The aim of this work is the synthesis of 18-*O*-(β-D-galactopyranosyl)-pentatriacontanol (**1**), in which a secondary alcohol with 35 carbon atoms is linked to a galactose through a β-glycosidic bond (Figure 7.5).

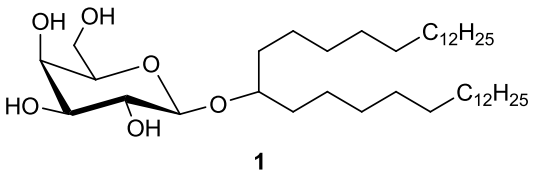

1

Figure 7.5: Synthetic analogue of simplexide.

In the long-chain secondary alcohol, the two alkyl chains linked to the carbinol have the same length with no branches, avoiding the problem of controlling the stereochemistry of carbinol carbon; while, the disaccharide [Glc(1α→4)Gal] residue of simplexide is reduced to one sugar.

It is possible to distinguish two *building blocks* for the synthesis of compound **1**: a monosaccharide unit, D-Galactose, and a long-chain secondary alcohol, pentatriacontan-18-ol (Figure 7.6).

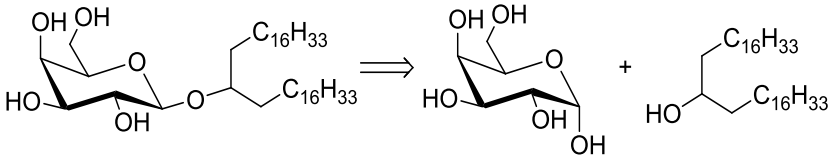

Figure 7.6: Synthetic retro-scheme of compound **1**

The reaction of β-glycosylation (between the alcohol and the sugar) represents the crucial step for the synthesis of compound **1**.

The glycosilation reaction is widely known in literature.[66] This reaction involves the coupling of a glycosyl donor and an acceptor via initiation using an activator under proper reaction conditions.

As in conventional reactions, donor glycosides have good leaving groups that must be activated by heavy metal salts or Lewis acid (i.e. trichloroacetimidate glycosil donors are commonly used in glycosilation reaction).[67]

Recently, an efficient microwave-assisted glycosylation method was proposed by Shimizu et al..[68] This new glycosylation system, using methyl glycosides as donors with microwave irradiation, led to new glycosylated compounds with high yields. Methyl glycosides are widely available and relatively easy to prepare if compared with other monosaccharide donors.

Two alternative glycosilation methods were investigated for the synthesis of compound **1**:

- The trichloroacetimidate glycosylation in which a glycoside has a good leaving group;
- A new glycosylation system using methyl glycosides as donors.

The reactions were carried out under conventional heating and microwave irradiation.

[66] Koenigs, W.; Knorr, E. Ber. Dtsch. Chem. Ges., **1901,** 34, 957; Deslongchamp, P.*; "Stereoelectronic Effects in organic chemistry",* Pergamon Press, Oxford, **1983,** p.29; Lemieux, R.U. and Koto, S. *Tetrahedron* , **1974,** 30, 1933

[67] Schmidt, R. "*Synthesis of Glicosides*" in Trost, B.M.(ed.). Comprehensive Organic Synthesis, Pergamon Press, Londra, **1990.**

[68] Shimizu H.; Yoshimura Y.; Hinou H.; Nishimura S.I. *Tetrahedron Lett*. **2005**, 46, 4701–4705.

7.3 Materials and methods

7.3.1 Glycosyl trichloroacetimidate donor

2,3,4,6-tetra-*O*-acetyl-α-Galactose trichloroacetimidate (**5**) was prepared using D-(+)-galactose (**2**) as starting product (Scheme 1). The protection of hydroxyl groups is required to avoid the formation of by-products. It was realized by an acetylation with acetic anhydride in pyridine, getting an anomeric mixture of pentacetyl-D-galactose (3).

Hydrolysis of compound **3** with hydrazine acetate in DMF at 50°C allowed the deacetylation of the anomeric hydroxyl function selectively.

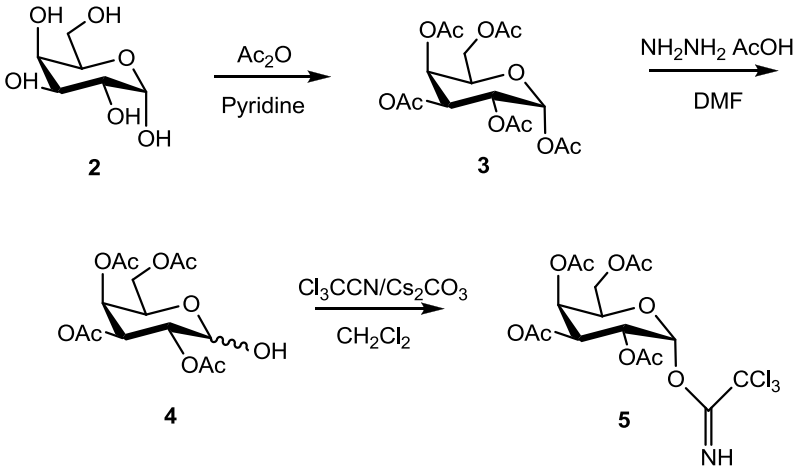

Scheme 1: Preparation of trichloroacetimidate glycoside.

Afterward, in order to activate the anomeric carbon, a good leaving group on it was inserted.

Schmidt's trichloroacetimidate glycosilation reaction

The trichloroacetimidate glycosides are synthetized from the reaction of the corresponding emyacetals with trichloroacetonitrile using a base as catalyst. With different bases both O-activated anomers may be isolated in

pure form and high yields, via kinetic and thermodynamic reaction-control. In presence of weak bases, the reaction is kinetically controlled so that the β-product is favored. While, strong bases, such as NaH or Cs_2CO_3, promote the formation of α-product, which is thermodynamically controlled because of anomeric effect[69] *(Scheme 2).*

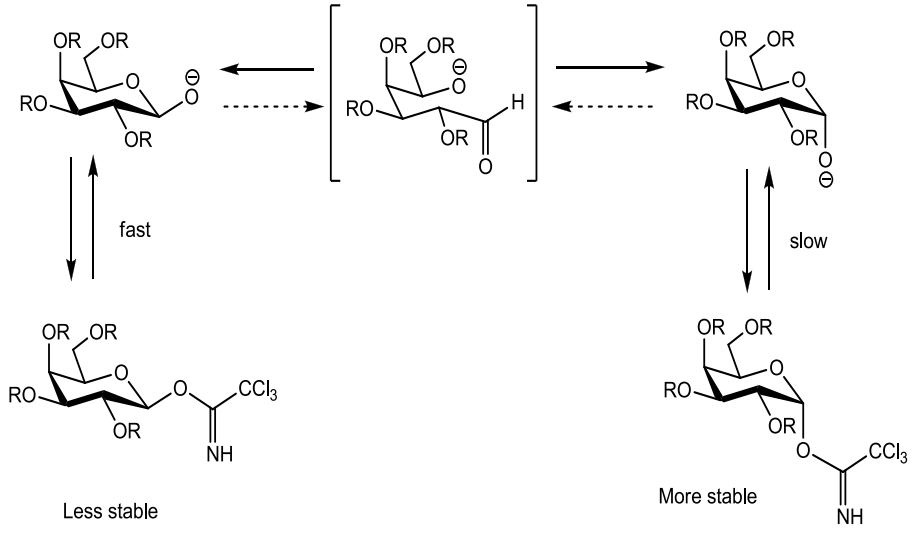

Scheme 2: Influence of the base on the stereochemistry of anomeric carbon.

For our purpose, in order to get the β-anomer of compound **1**, the reaction was carried out using trichloroacetonitrile and cesium carbonate in dichloromethane obtaining the 2,3,4,6-tetraacetyl-α-galactosetrichloroacetimidate (**5**).

7.3.2 Methyl glycoside as donor

Methyl 2,3,4,6-tetra-*O*-benzyl-β-D-galactopyranoside (**7**) was prepared from the benzylation of β-methyl-D-galactopyranoside (**6**), a commercially

[69] Grundler&Schmidt, **1985**; Sadozai et al. , **1986**.

available product. Benzylation of hydroxyl group was carried out with benzyl bromide and sodium hydride in dimethylformamide at room temperature for 12 hours (Scheme 3).

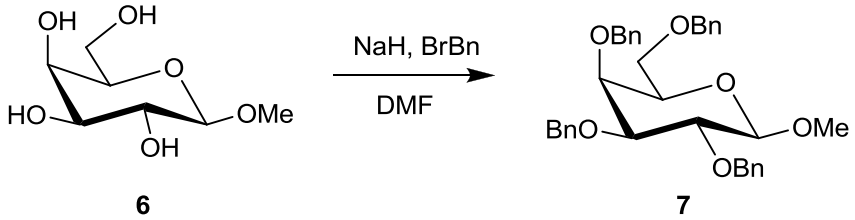

6 **7**

Scheme 3: Preparation of methyl 2,3,4,6-tetra-*O*-benzyl glycoside donor.

The compound **7** will be used as donor in the glycosilation reactions carried out with the method proposed by Shimizu et al.(2005).

Shimitzu method: methyl glycosides as donors in microwave-assisted glycosilation reaction.

Although methyl glycosides are often used for protecting anomeric center, recently a new glycosilation system with microwave irradiation led to glycosilated compounds, using methyl glycosides as donors.

In the paper,[68] it has been reported that methyl 2,3,4,6-tetra-O-benzyl-β-D-glucopyranoside is converted to octyl 2,3,4,6-tetra-O-benzyl-α,β-D-glucopyranoside with 1-octanol and a Lewis acid promoter.

There are two possibilities for the mechanism that cleaves acetal C–O bonds under acidic conditions, either for sugar rings to intermediate A or for glycosyl bond to intermediate B in scheme 4. The intramolecular reformation of sugar rings producing the intermediates B from A could be

thought as a favorable pathway when compared to intermolecular reactions that might lead to complicated compounds.

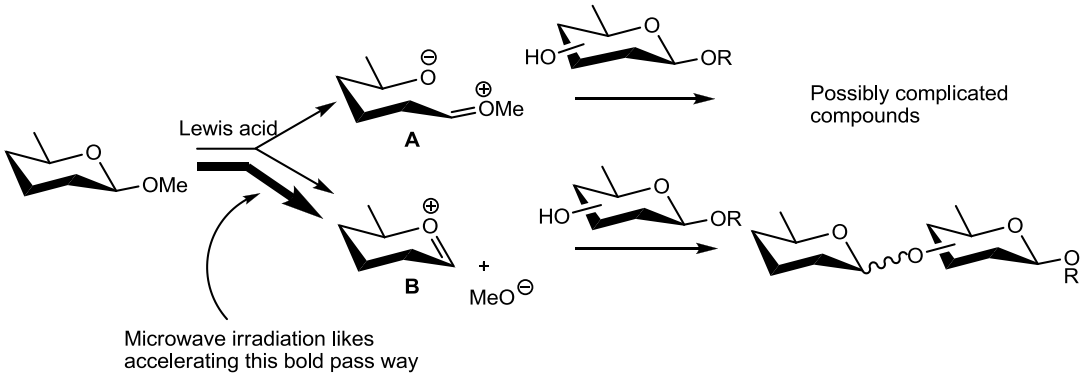

Scheme 4: Pathway of activated methyl glucoside as a glycosyl donor

7.3.3 Alcohols as acceptors

A. 1-nonanol

1-nonanol (**8**) is a primary short chain alcohol used as acceptor in the synthesis of compound **15** (see figure 7.7 in section 7.3.5).

1-nonanal was subjected to a reduction with sodium borohydride in CH_2Cl_2/CH_3OH for 2 hours at room temperature, getting the primary alcohol.

B. Pentatriacontan-18-ol

Pentatriacontan-18-ol (**13**) is a secondary alcohol used as glycosidic acceptor in the synthesis of compounds **14** (scheme 6) and **16** (scheme 8). It was synthetized from a Grignard reagent (Scheme 5).

The first step consisted in the oxidation of 1-octadecanol (**9**) in aldheide (**10**), using pyridinium chloride (PCC) as oxidant agent.

Afterwards, 1-octadecanal (**10**) was reacted with Grignard reagent (**12**), leading to the secondary-long chain alcohol (**13**).

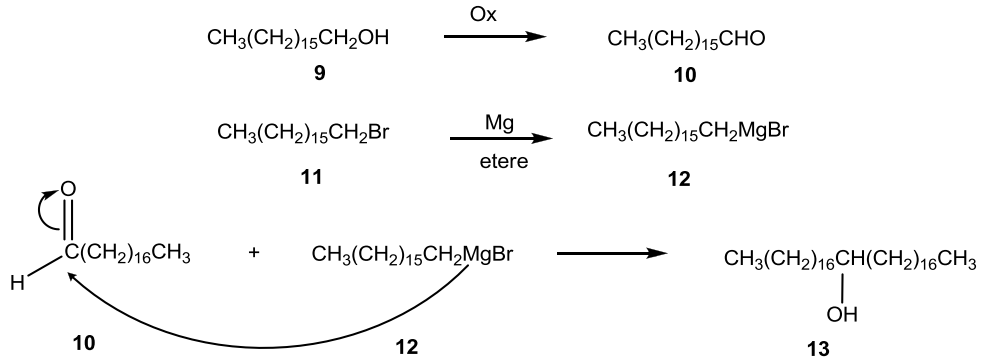

Scheme 5: Preparation of the acceptor, pentatriacontan-18-ol.

Grignard reagent

In a "Grignard reaction," a Grignard reagent RMgX is formed in an appropriate solvent SH from magnesium metal Mg and an organic halide RX. By-products may include RR, RH, R(–H), RS, SS, S(–H), and MgX_2.[70] *Moreover, traces of water or protic solvent can convert organomagnesium compound in alkane. Thus, Grignard reagents can be prepared in a variety of anhydrous aprotic solvents, including tertiary amines. Even so, one of two ethers, DEE and THF, is almost always used in practice.*

Solvent coordination has an important role in stabilizing Grignard reagents and magnesium halides. The coordination allows the solubilization of Mg in the solvent and its availability in the reaction. In Grignard reagent formation, Mg passes from a metallic state, where it is essentially unsolvated, into an ionic state (Mg^{2+}) where it is strongly coordinated by ether solvent molecules as well as ligands R and X.

[70] J.F. Garst, M.P. Soriaga *Coordination Chemistry Reviews* 248 (2004) 623–652.

Although this is an exothermic reaction, magnesium chopping and use of a catalityc amount of iodine are required to remove oxide layer from Mg and improve its availability in the reaction.

To prepare the Grignard reagent, 1-bromoheptadecan (**11**) was dissolved in anhydrous diethyl ether, and was added to magnesium metal, precedently treated with a catalytic amount of iodine. The reaction was conducted under reflux for 3 hours at 40°C and successively 1-octadecanal (**10**) was added in situ.

The nucleophilic attack of the Grignard reagent on the aldehyde forms an alkoxide ion, which is complexed by magnesium ion. In the end, the use of hydrochloric acid allowed to break this complex and to get the secondary alcohol.

Initially, using the same equivalents of Grignard reagent and 1-octadecanal, the yields of reaction (25%) were very low because of the formation of 'unwanted' products, such as alkanes, alkenes and primary alcohol, although the anhydrous conditions used to perform the reactions.

In order to improve the yield, it was decided to carry out the reaction with an excess of Grignard reagent compared to the aldehyde. The ratio 2:1 of Grignard reagent/aldehyde was the best compromise to reach a better yield (60%).

The purification of the reaction mixture was achieved by means of a sort of crystallization. The crude reaction mixture was solubilized in *n*-hexane:AcOEt (95:5) and a precipitation was observed. NMR analyses of precipitate and supernatant proved that the precipitate contained only the

pure pentatriacontan-18-ol (**13**). Since purification by means of HPLC was not necessary, it is worthy of note the obvious savings of time and solvents.

7.3.4 Glycosylation using trichloroacetimidate glycosides as donors

At first, in order to make a stereoselective glycosylation, the 'trichloroacetimidate method' was applied. This method provides the use of a glycoside donor having a good leaving group and an alcohol as nucleophilic agent, in presence of a suitable catalyst (Scheme 6).

Using 2,3,4,6-tetracetyl-α-Galactosetrichloroacetimidate (**5**) as donor and pentatriacontan-18-ol (**13**) as acceptor, several attempts of β-glycosylation were performed in order to optimize the yields.

The reactions were carried out both under conventional and microwave heating.

Under conventional heating the reactions were performed in chloroform at 60°C for 2 h in an argon saturated system, using 3 eq. of acceptor, 1 eq. of donor and 1 eq. of promoter.

The set of reactions, conducted by microwave heating, are reported in table 1S. An automated single mode microwave reactor (400 W), Biotage Initiator EXP 8, was used for the experiments, which were done in closed vessels (2-5 ml).

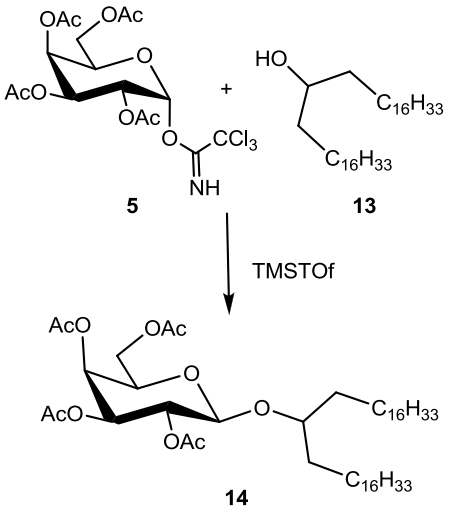

Scheme 6: Synthesis of 18-*O*-(β-D-2,3,4,6-tetra-*O*-acetylgalactopyranosyl)-pentatriacontanol.

Table 1S: Different reaction conditions performed under microwave irradiation using 'Trichloroacetimidate Method' (*2,3,4,6-tetraacetyl-α-Galactosetrichloroacetimidate).

N° of reaction	**Promoter** (eq)	**Donor** (eq)	**Acceptor** (eq)	**Reaction conditions**
A	TMSOTf (1)	Ac-Gal-OR* (1)	Pentatriacontan-18-ol (3)	DCE, 20 min, 100°C MW
B	TMSOTf (1)	Ac-Gal-OR* (1)	Pentatriacontan-18-ol (3)	$CHCl_3$, 20 min, 100°C MW
C	TMSOTf (1)	Ac-Gal-OR* (1)	Pentatriacontan-18-ol (3)	$CHCl_3$, 20 min, 130°C MW
D	TMSOTf (1)	Ac-Gal-OR* (1)	Pentatriacontan-18-ol (3)	$CHCl_3$, 30 min, 130°C MW
E	TMSOTf (1)	Ac-Gal-OR* (1)	Pentatriacontan-18-ol (3)	$CHCl_3$, 40 min, 130°C MW
F	TMSOTf (1)	Ac-Gal-OR* (1)	Pentatriacontan-18-ol (3)	$CHCl_3$,170°C, 20 min MW

7.3.5 Glycosylation using methyl glycosides as donors (Shimizu method)

The new glycosylation method proposed by Shimizu et al 2005 (see section 7.3.2), was also applied to get the compound **1**.

Initially the synthesis of the 'model A' compound (**15**, Figure 7.7) was carried out, using the same reagents and conditions reported in the paper (3 eq. of acceptor, 1 eq. of donor and 1 eq. of promoter). The glycosylation of a short chain alcohol was performed in order to verify the reproducibility of the method.

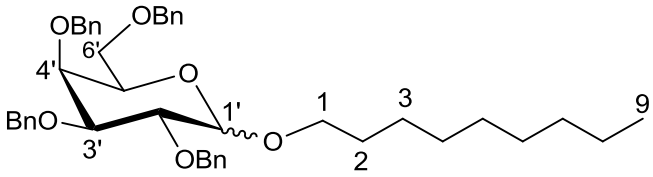

15

Figure 7.7: Structure of 1-*O*-(D-2,3,4,6-tetra-*O*-benzylgalactopyranosyl)-nonanol.

The donor, methyl 2,3,4,6-tetra-*O*-benzyl-β-D-galactopyranoside (**7**), was reacted under microwave irradiation with the acceptor, 1-nonanol (**8**), using TMSOTf as promoter and dichlomethane as solvent (see Scheme 7).

The microwave-assisted reactions were performed in a CEM Discover LabMate reactor, and the results were compared with those obtained by conducting the reactions under conventional heating, by means of traditional heat transfer equipment (oil bath).

The reactions performed to get 'model A compound'(**15**) are reported in the table 2S:

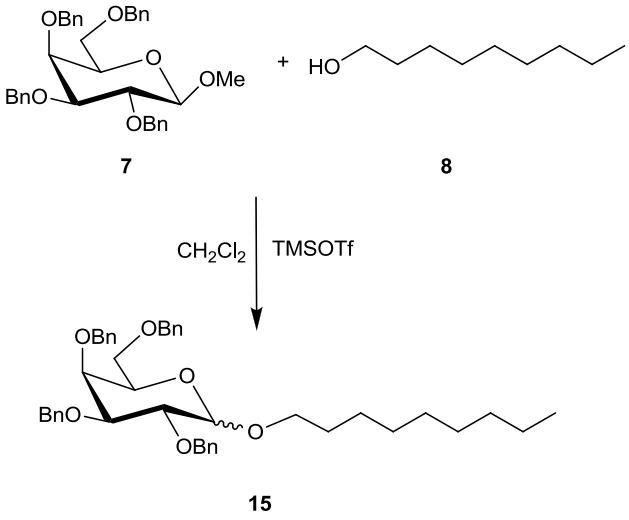

Scheme 7: Glycosylation using a short chain alcohol as acceptor.

Table 2S: Set of reactions carried out to get compound **15** (***** methyl 2,3,4,6-tetra-*O*-benzyl-β-D-galactopyranoside).

N° of reaction	**Promoter** (eq)	**Donor** (eq)	**Acceptor** (eq)	**Reaction conditions**
A	TMSOTf (1)	β-Me-GalBn * (1)	1-nonanol (3)	DCM, 35°C, 1h
B	TMSOTf (1)	β-Me-GalBn * (1)	1-nonanol (3)	DCM, 35°C, 4h
C	TMSOTf (1)	β-Me-GalBn * (1)	1-nonanol (3)	DCM, 100°C 8 min 30W (MW)
D	TMSOTf (1)	β-Me-GalBn * (1)	1-nonanol (3)	DCM, 100°C 8 min 30W (MW) Under reflux

Since the good yields (see section 7.4.2), the synthesis of compound **1** (Figure 7.5) was investigated. The reactions were performed with both conventional and microwave heating. Donor (methyl 2,3,4,6-tetra-*O*-benzyl-β-D-galactopyranoside, compound **7**) and promoter (TMSOTf) were the same of the previous reactions (scheme 7), while in this case the acceptor was the pentatriacontan-18-ol (**13**) (Scheme 8). The same equivalents of reagents used for the reaction reported in the scheme 7 were used.

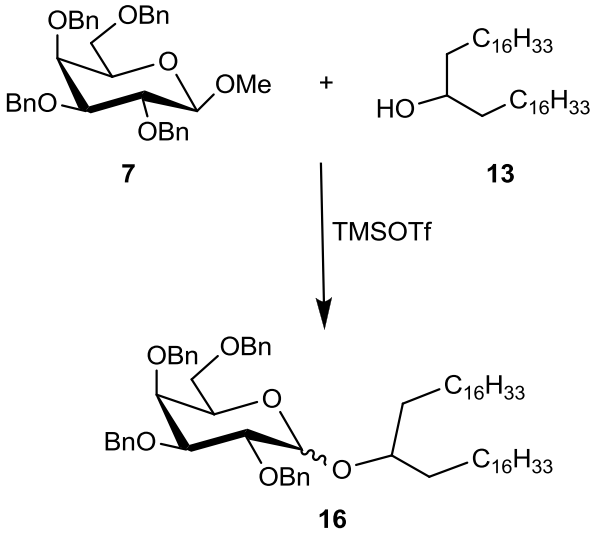

Scheme 8: Synthesis of 18-*O*-(D-2,3,4,6-tetra-*O*-benzylgalactopyranosyl)-pentatriacontanol.

The reactions performed by means of traditional heat transfer equipment (oil bath) were refluxed in an argon saturated system, using different solvents, such as toluene or $CHCl_3$ (reactions A-C in the table 3S). Concerning the reactions carried out with microwave heating, they were performed using a single mode microwave reactor (400 W), Biotage Initiator EXP 8 (reactions D-I in table 3S).

Table 3S: Set of reactions carried out using 'Shimizu method' to get compound **16**: A-C are the reactions performed under conventional heating; D-I are the reactions performed under MW. (*methyl 2,3,4,6-tetra-*O*-benzyl-β-D-galactopyranoside)

N° of reaction	**Promoter** (eq)	**Donor** (eq)	**Acceptor** (eq)	**Reaction conditions**
A	TMSOTf (1)	β -Me-GalBn* (1)	Pentatriacontan-18-ol (3)	$CHCl_3$, 2 h, 60°C
B	TMSOTf (1)	β -Me-GalBn* (1)	Pentatriacontan-18-ol (3)	Toluene, 2 h, 140°C, fractioned distillation
C	TMSOTf (1)	β -Me-GalBn* (1)	Pentatriacontan-18-ol (3)	$CHCl_3$, 2 h, 60°C, fractioned distillation
D	TMSOTf (1)	β-Me-GalBn * (1)	Pentatriacontan-18-ol (3)	DCE, 20 min, 100°C (MW)
E	TMSOTf (1)	β -Me-GalBn* (1)	Pentatriacontan-18-ol (3)	$CHCl_3$, 20 min, 100°C (MW)
F	TMSOTf (1)	β -Me-GalBn* (1)	Pentatriacontan-18-ol (3)	$CHCl_3$, 20 min, 130°C (MW)
G	TMSOTf (1)	β -Me-GalBn* (1)	Pentatriacontan-18-ol (3)	$CHCl_3$, 30 min, 130°C (MW)
H	TMSOTf (1)	β -Me-GalBn* (1)	Pentatriacontan-18-ol (3)	$CHCl_3$, 40 min, 130°C (MW)
I	TMSOTf (1)	β -Me-GalBn* (1)	Pentatriacontan-18-ol (3)	$CHCl_3$, 20 min, 170°C (MW)

7.4 Results and discussion

A. Glycosylation using trichloroacetimidate glycosides as donors

All the glycosylation reactions performed with trichloroacetimidate method both under conventional and microwave heating were not successful. The reaction D (table 1S), conducted in Biotage Initiator EXP8 reactor and obtained with the best yield (10 %, α/β ratio 2:1), is shown in the scheme 9.

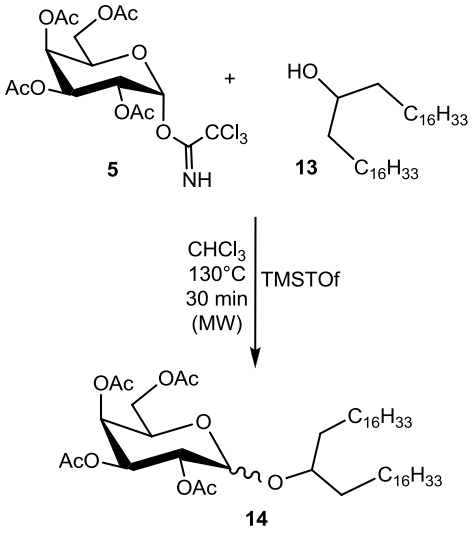

Scheme 9: Glycosylation using trichloroacetimidate method under MW.

The experiments, carried out with this approach, gave rise to the following issues:

a) A formation of 1,2-orthoester coupling product was noticed: the *in situ* generation of a cyclic dioxolenium intermediate (scheme 10) is able to induce nucleophilic attack of the acceptor from the less hindered side of the anomeric position ('Path a'), but an undesired 'Path b' is possible, leading to the formation of 1,2-orthoester coupling product;

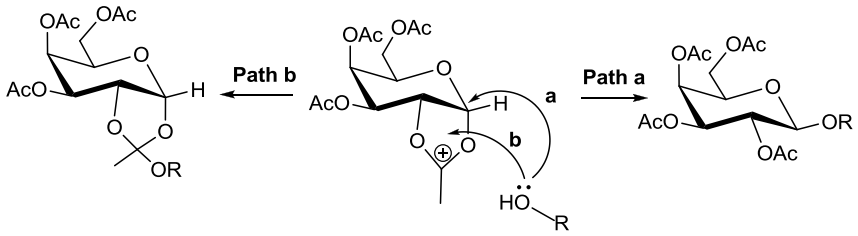

Scheme 10: Mechanism of Glycosylation.

b) With the increases of temperature and reaction time, the formation of α-product seems favored.;

c) The use of $CHCl_3$, free from ethanol traces, is necessary because in some reactions a formation of ethyl glycosides was observed;

d) With the increase of the temperature (130°C-170°C), the alcohol undergoes a process of dehydration and there is a loss of acetyl protecting groups from the sugar.

B. Glycosylation using methyl glycosides as donors

The synthesis of 'model A compound' (**15**) was successful, getting results comparable with the findings reported in Shimizu et al.

The reactions conducted under conventional heating gave the following yields:

- 32 % of α/β anomeric mixture in the ratio 1:1 for the reaction carried out for 1 h;

- 56 % of α/β anomeric mixture in the ratio 1.5:1 for the reaction carried out for 4 h.

While the microwave-assisted attempts gave the following yields:

- 69 % of α/β anomeric mixture in the ratio 2:1 for the reactions performed at 100°C, 8 min in closed vessel (30 W) (scheme 11)

- 40% of α/β anomeric mixture in the ratio 3.5:1 for the reactions performed at 100°C, 8 min under reflux (30 W).

Final results pointed out that using a conventional heating the yields (32%, α/β ratio 1:1; after 4 h the yield increased to 50 %) are lower than those obtained under microwave irradiation (69 % in 8 min).

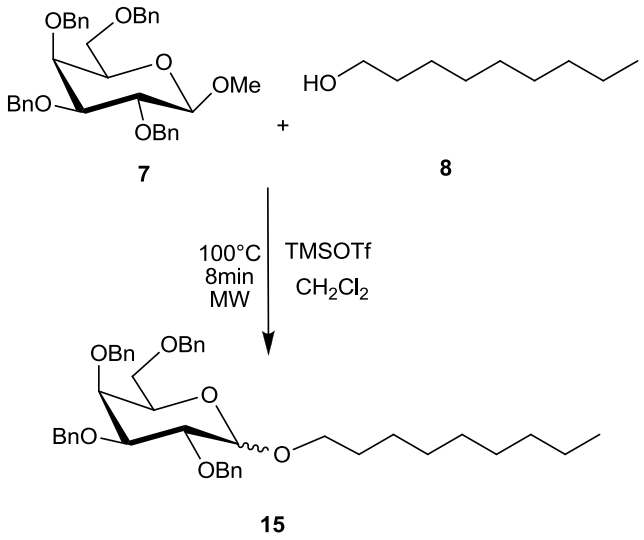

Scheme 11: Glycosilation obtained with high yield (69 %) using methyl galactopyranoside as donor and 1-nonanol as acceptor under microwave irradiation.

Once achieved these good results, the synthesis of 18-*O*-(2,3,4,6-tetra-*O*-benzyl-β-D-galactopyranosyl)-pentatriacontanol (**16**) was performed.

In the above reactions a glycosylation of 1-nonanol with a galactopyranoside unit was carried out. It is important to notice that the reaction has 1-nonanol, short chain alcohol, as acceptor and the activation

has a dependency on the length of the alkyl chain, besides the fact that the hydroxyl protecting groups on donors also affect deeply.

Moreover the products of the glycosylation obtained with this approach are a mixture of α- and β- glycosylated compounds; while the synthesis of the compound **1** requires a preferential β-stereoselectivity. Since the main task is currently the outcome of glycosylation, it was decided to start with this generic approach in which a methyl 2,3,4,6-tetra-*O*-benzyl-β-D-galactopyranoside reacts with a long alcohol chain. In the case of success of this reaction, (in order to get a β-stereoselectivity) a protecting group at O-2 of the sugar, able to promote the β anomeric configuration, should be inserted.

In spite of the lack of stereoselectivity, the reduction of time reaction and high yields make advantageous the use of microwaves in glycosylation reactions.

The first attempt of glycosylation using pentatricontan-18 ol as acceptor was performed under conventional heating, following the same procedure carried out for the synthesis of 'model A compound' (**15**). Since the scarce solubility of pentatriacontan-18-ol in DCM, it was decided to test other solvent conditions. The chloroform at 60°C is the unique solvent system in which the secondary long chain alcohol is totally dissolved. Thus, succeeding attempts of glycosilation were performed in $CHCl_3$.

Making the reaction in $CHCl_3$ at 60°C for 2 h (Scheme 12), only the yield of 4.6% (α/β ratio 1:1) was achieved.

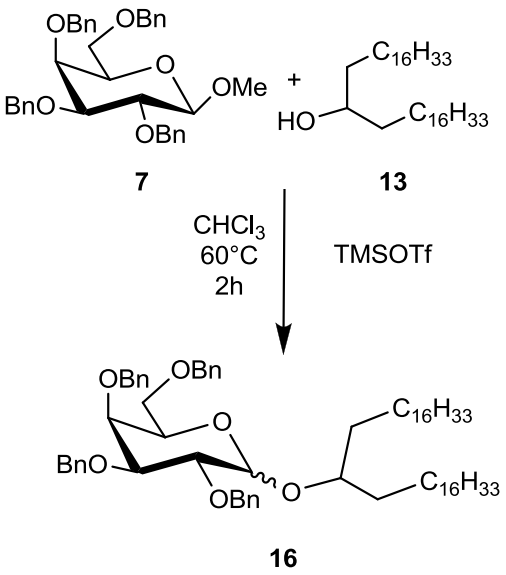

Scheme 12: Glycosylation using methyl galactopyranoside as donor and pentatriacontan-18-ol as acceptor under conventional heating.

The reactions were also carried out under microwave irradiation. The reaction E (table 3S and scheme 13), performed in $CHCl_3$ at 100°C for 20 minutes, gave the best yield (14%, α/β ratio 2.5:1).

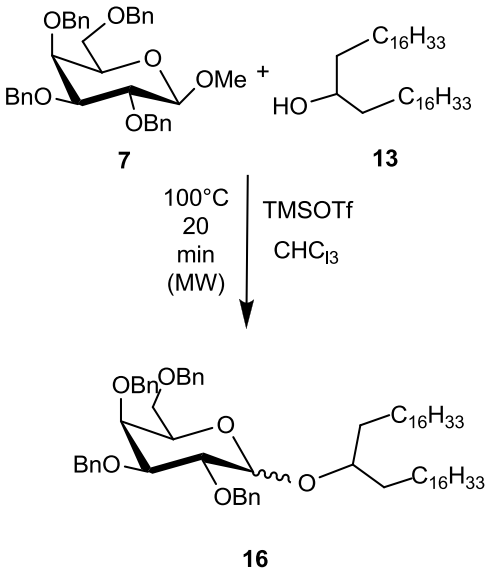

Scheme 13: Glycosylation using methyl galactopyranoside as donor and pentatriacontan-18-ol as acceptor under microwave heating.

These results may depend on many reasons.

First of all the main problem depends on the characteristics of the acceptor (pentatriacontan-18-ol):

- The length of the alkyl chains (C_{35}), which form a steric impediment, makes the alcoholic function less reactive.

- The choice of solvent reaction is strongly restricted because of the low solubility of this alcohol in common organic solvents. Pentatriacontan-18-ol is totally dissolved only in chloroform at 60°C.

Furthermore, since the methyl 2,3,4,6-tetra-*O*-benzyl-*α*-D-galactopyranoside was obtained with high percentages, it was possible to derive that this type of reaction is an equilibrium reaction in which the MeOH, the "outgoing" group, reacts with the donor: for example, in the reaction E (scheme 13 and table 3S) 13% of methyl 2,3,4,6-tetra-*O*-benzyl-*α*-D-galactopyranoside was obtained.

In order to remove MeOH from the equilibrium, the reaction was performed using a fractioned distillation system. The same reaction conditions above described were applied, but toluene instead of $CHCl_3$ was used as solvent because of the boiling point. In fact, chloroform and methanol have similar boiling points (61 °C and 64.7 °C respectively), while that of toluene is much higher (110.6 °C). In this way it might possible to remove MeOH from the equilibrium reaction, without reaching toluene boiling point. Unfortunately, the results of this procedure were not successful and the yields were not higher than 2.6 %.

In addition, under microwave irradiation, the increase of the temperature (130°C-170°C) led to the dehydratation of the acceptor (**13**) and so the availability of the nucleophilic agent in the reaction environment is reduced. However, it is worthy of note the increase in reaction yields and the reduction in reaction time for all microwave-assisted glycosilations.

7.5 Conclusion

In order to optimize the yield of the crucial step of β-glycosylation for the synthesis of compound **1**, two alternative approaches were applied:

- Glycosylation using trichloroacetimidate glycosides as donors;
- Glycosylation using methyl glycosides as donors.

In a process of glycosylation, the nucleophilic attack on the anomeric carbon is favored when the nucleophilic agent is highly reactive and not sterically cluttered.

When the acceptor is a primary alcohol with short alkyl chain the reactions are successful (see the attempts carried out using nonan-1ol as acceptor, 7.4.2 section). Indeed, the main problem of the synthesis of 18-*O*-(β-D-galactopyranosyl)-pentatriacontanol is the length of the alkyl chain of the acceptor and its scarce reactivity. Pentatriacontan-18-ol is a secondary alcohol which can't be dissolved in common organic solvents and is sterically cluttered, weighing upon its reactivity. In order to improve its dissolution, and consequently its availability in the reaction, several solvents at different temperatures were tested. Only the chloroform at 60°C is able to dissolve totally the pentatriacontan-18-ol.

Moreover with Shimizu method, the starting donor in anomeric mixture always reform. The leaving group (MeOH) reacts again with oxocarbenium cation intermediates, leading to methyl 2,3,4,6-tetra-*O*-benzyl-*α/β*-D-galactopyranoside. The MeOH has a reactivity higher than pentatriacontan-18-ol because it is not sterically cluttered and so its nucleophilic attack is favored. Although the use of a fractioned distillation system, no improvements were observed.

Among the several attempts, conducted both under conventional heating and microwave irradiation, the best yield (14 %), obtained so far, was achieved using methyl glycoside as donor under microwave irradiation.

It is important to emphasize that the reactions performed with the help of microwave gave yields higher than those carried out by conventional heating. Besides the higher yield, the advantage of microwaves is also in reduced reaction times: in 20 minutes a reaction was obtained with a yield about three times larger than a reaction performed in 2 hours under conventional heating.

However, optimization of microwave parameter is necessary because the results suggest that high temperature (130°C-170°C) could be the cause of the alcohol dehydration.

In addition, since a loss of acetyl groups was observed in the reaction conducted with the trichloroacetimidate method under microwave heating, it would be worth to investigate the use of acetyl as protecting groups in the microwave-assisted synthesis.

Therefore, in order to achieve an efficient synthetic method to get simplexide and its analogues, further studies are necessary to increase the yields of β-glycosylation.

In the meantime, deacetylation and/or debenzylation of 18-*O*-(β-D-2,3,4,6-tetra-*O*-acetylgalactopyranosyl)-pentatriacontanol (**14**) and/or 18-*O*-(β-D-2,3,4,6-tetra-*O*-benzylgalactopyranosyl)-pentatriacontanol (**16**) respectively, will be carried out in order to get 18-*O*-(β-D-galactopyranosyl)-pentatriacontanol (**1**). This analogue of simplexide will be tested on human blood monocytes and results will be compared with those of natural simplexide.

7.6 Experimental Section

ESI MS experiments were performed on a Applied Biosystem API 2000 triple-quadrupole mass spectrometer. The spectra were recorded by infusion into the ESI source using MeOH as the solvent. The spectra were recorded by infusion into the ESI source using MeOH as solvent. NMR spectra were determined on Varian UnityInova spectrometers at 500 MHz; chemical shifts were referenced to the residual solvent signal ($CDCl_3$: $\delta_H = 7.26$, $\delta_C = 77.0$).

For an accurate measurement of the coupling constants, the one-dimensional ^1H NMR spectra were transformed at 64K points (digital resolution: 0.09 Hz). Homonuclear ^1H connectivities were determined by a COSY experiment. The single-quantum heteronuclear correlation (HSQC) and multiple-bond heteronuclear correlation (HMBC) spectra were adjusted, respectively, for an average $^1J_{CH}$ of 142 Hz and a $^{2,3}J_{CH}$ of 8.3 Hz. High performance liquid chromatographies (HPLC) were performed on a Varian Prostar 210 apparatus equipped with an Varian 350 refractive index detector.

The reactions were monitored using TLC (Kiesel-gel 60 F_{254}), revealed with sodium molybdate and cerium sulfate in solution.

The microwave-assisted reactions were performed in automated single mode microwave reactor (400 W), Biotage Initiator EXP 8, which experiments were done in closed vessels (2-5 ml); and in CEM Discover LabMate reactor, which experiments were also performed at air pressure.

7.6.1 Synthetic procedures

A. 2,3,4,6-tetra-*O*-acetyl-α-Galactosetrichloroacetimidate (5)

508.4 mg of D-galactose (**2**) were acetylated with acetic anhydride (5 ml) and pyridine (5ml) at room temperature for 12 hours. The weight, calculated after vacuum drying, was 1.1 g (yield 99%).

783.5 mg of 1,2,3,4,6-*O*-pentacetylgalactose (**3**) (2 mmol) were subjected to hydrolysis with hydrazine acetate (221.2 mg, 2.4 mmol) in DMF (11.5 ml) to release anomeric carbon selectively. The reaction, argon saturated, was carried out for 4 h at room temperature. Then the reaction was partitioned between distillated water and ethyl acetate. The organic layers were pooled, treated with anhydrous sodium sulfate, filtered and concentrated under vacuum. The weight was 453.9 mg (yield 65%).

55.8 mg of 2,3,4,6-*O*-tetracetylgalactose (**4**) (0.16 mmol) was converted into 2,3,4,6-*O*-tetraacetyl-α-Galactosetrichloroacetimidate (**5**), the glycosil donor successively used in the reaction of β-glycosilation. The reaction was carried out using trichloroacetonitrile (160.4 μL, 1.6 mmol) and cesium carbonate (65.8 mg, 0.176 mmol) in dichloromethane (25 ml). After reacting for 2 h at room temperature, the reaction mixture was filtered with diethyl ether on a celite-silica septum (yield 70 %).

B. Methyl 2,3,4,6-tetra-*O*-benzyl-β-D-galactopyranoside (7): β-methyl-D-galactopyranoside (**6**) (541.2 mg, 2.8 mmol) was dissolved in DMF (22 ml) and successively sodium hydride and benzyl bromide (12.5 mmol, 1.5 ml) were added at 0°C. After the total H_2 removal, the reaction mixture was

stirred overnight at room temperature. Distillated water was added and 3 extractions with AcOEt were carried out in a separation funnel. The organic layers were pooled, treated with anhydrous sodium sulfate, filtered and concentrated under vacuum.

The crude reaction (4.1 g) was purified on a SiO_2 column (eluents: *n*-hexane and ethyl acetate), getting the pure methyl 2,3,4,6-tetra-*O*-benzyl-β-D-galactopyranoside (80 %).

C. 1-nonanol (8): 500 μL of 1-nonanal (2.7 mmol) in CH_2Cl_2/MeOH 5:1 (8.5 ml) were subjected to reduction with $NaBH_4$ (408 mg, 10.8 mmol), added to the solution at 0°C. After 2 h at room temperature, the reaction was quenched with H_2SO_4 2.5 M until reaching acid pH. A partition between distillated water and dichloromethane was done, and the organic layers were treated with anhydrous sodium sulfate, filtered and concentrated under vacuum (yield 76 %).

D. Pentatriacontan-18-ol (13): a catalytic amount of iodine was added to 372 mg of magnesium metal and Bunsen burner heating was applied in order to evaporate iodine. By means of a funnel, 1-bromoheptadecane (**11**) (1.5 g, 5 mmol) dissolved in 2.6 ml of diethyl ether was added.

The reaction mixture, argon saturated, was stirred under reflux at 40°C. After 3 hours, 1-octadecanal (**10**) (665 mg, 2.5 mmol) dissolved in diethyl ether, was added in situ. The oil bath was removed in 2 hours and the reaction mixture was stirred overnight at room temperature. In order to

quench the reaction, 7 ml of HCl 2N were added. Afterwards the addition of a sodium chloride solution, 3 extractions in a separation funnel were carried out using diethyl ether as organic solvent. The organic layers were pooled, treated with anhydrous sodium sulfate, filtered and concentrated under vacuum.

Pure pentatriacontan-18-ol was obtained by means of a sort of crystallization: the crude reaction was solubilized in 30 ml of *n*-hexane/AcOEt 95:5 and the formation of a precipitate was observed. ^{1}H and ^{13}C NMR of precipitate and supernatant allowed to assume that the precipitate contain only the secondary alcohol (**13**) (yield 65%).

E. 18-*O*-(β-D-2,3,4,6-tetra-*O*-acetylgalactopyranosyl)-pentatriacontanol (14)- Conventional heating: 70.4 mg of 2,3,4,6-tetraacetyl-α-galactosetrichloroacetimidate (**5**) (0.14 mmol) was dissolved in 2.5 ml of $CHCl_3$; 25.5 μL of TMSOTf (0.14 mmol) and, successively, 201.3 mg of pentatriacontan-18-ol (**13**) (0.43 mmol) were added to the solution. The reaction, argon saturated, was refluxed for 2 h at 65°C.

The reaction mixture was partitioned between a solution of water, $NaHCO_3$ saturated, and dichloromethane. The organic layers were pooled, treated with anhydrous sodium sulfate, filtered and concentrated under vacuum. Then the reaction mixture was chromatographed by HPLC using as solvent *n*-hexane/AcOEt 8:2.

F. 18-*O*-(β-D-2,3,4,6-tetra-*O*-acetylgalactopyranosyl)-pentatriacontanol (14)-microwave irradiation (reaction D, table 1S): 11.5 mg of 2,3,4,6-tetraacetyl-α-galactosetrichloroacetimidate (**5**) (0.023 mmol) was dissolved in 500μL of $CHCl_3$ and transferred in a closed vessel (5 ml).

4.2 μL of TMSOTf (0.023 mmol) and, successively, 35 mg of pentatriacontan-18-ol (**13**) (0.069 mmol) were dissolved in 3 ml of $CHCl_3$. The reaction mixture was stirred and irradiated for 30 minutes, at 130 °C in a Biotage Initiator EXP 8 microwave reactor. A power of 400 W was needed to get a temperature of 130°C. The crude reaction (42.9 mg) was HPLC-chromatographed using a normal-phase column (*n*-hexane-AcOEt 8:2), giving 1.3 mg of 18-*O*-(α-D-2,3,4,6-tetra-*O*-acetylgalactopyranosyl)-pentatriacontanol and 0.7 mg of 18-*O*-(β-D-2,3,4,6-tetra-*O*-acetylgalactopyranosyl)-pentatriacontanol (total yields 10 %).

The other attempts conducted with trichloroacetimidate method were carried out using the same procedure described above, but changing the temperature and time conditions as reported in the table 1S.

^{1}H NMR (500MHz $CDCl_3$) δ 5.37 (1H, d, *J* = 2.9 Hz, H-4″), 5.18 (1H, dd, *J* = 10.4 e 8.1 Hz, H-2″), 5.01 (1H, dd, *J* = 10.4 e 3.4 Hz, H-3″), 4.47 (1H, d, *J* = 7.9 Hz, H-1″), 4.13 (1H, m, H-6″a e H-6″b), 3.87 (1H, t, *J* = 6.6 Hz, H-5″), 3.52 (1H, m, H-1), 2.15 (3H, s, acetyl proton), 2.04 (3H, s, acetyl proton), 2.03 (3H, s, acetyl proton), 1.98 (3H, s, acetyl proton), 1.42 (4H, m, 2H-17 and 2H-19), 1.24 (60H, m, alkyl chain proton), 0.88 (6H, t, J = 6.6 Hz, 3H-17 and 3H-18′).

G. 1-*O*-(β-D-2,3,4,6-tetra-*O*-benzylgalactopyranosyl)-nonanol (15) - conventional heating: methyl 2,3,4,6-tetra-*O*-benzyl-β-D-galactopyranoside (**7**) (116.3 mg, 0.21 mmol,), 1-nonanol (**8**) (93.2 mg, 0.63mmol) and TMSOTf (38 μg, 0.21 mmol) in DCM were stirred under reflux at 35°C for 1 h. A water solution of $NaHCO_3$ was added and three extractions with CH_2Cl_2 were done in a separation funnel. The organic layers were pooled, treated with anhydrous sodium sulfate, filtered and concentrated under vacuum.

The crude reaction was HPLC-chromatographed using a normal-phase column (*n*-hexane-AcOEt 8:2): the α and β anomers of 1-*O*-(D-2,3,4,6-tetra-*O*-benzylgalactopyranosyl)-nonanol (**15**) were obtained in the ratio 1:1 (yield: 32%).

^{1}H NMR (500 MHz $CDCl_3$) δ 7.38-7.24 (20 H, m, aromatic protons), 4.94 – 4.61 (2 H, d, *J* = 11.7 Hz, benzyl methylenes), 4.92 – 4.75 (2 H, d, *J* = 11.7 Hz, benzyl methylenes), 4.72 – 4.70 (2 H, d, *J* = 11.7 Hz, benzyl methylenes), 4.45 – 4.40 (2 H, d, *J* = 11.7 Hz, benzyl methylenes), 4.34 (1 H, d, *J* = 7.8 Hz,, H-1'), 3.93 (1 H, m, H-1a), 3.88 (1 H, Br.s, H-4'), 3.80 (1 H, t, *J* = 8.8, H-2'), 3.60 – 3.56 (2 H, m, H-6'a H-6'b), 3.52 (1 H, m, H-3'), 3.51 (1 H, m, H-5'), 3.49 (1 H, m, H-1b), 1.28 – 1.21 (4 H, m, H-2 e H-8), 0.87 (3 H, t, *J* = 6.97 Hz, CH_3); ^{13}C NMR (500 MHz $CDCl_3$) δ 74.5 – 73.0 (C, C-1 benzyl), 128.5-127.8 (CH, benzenes), 104.0 (CH, C-1'), 82.2 (CH, C-3'), 79.6 (CH, C-2'), 73.7 (CH, C-4'), 73.5 (CH, C-5'), 68.9 (CH, C-6'), 68.3 (CH_2, C-1), 61.9 (CH, C-3), 29.7 (CH_2, C-5), 29.4 (CH_2, alkyl chain), 25.2 (CH_2, C-6), 14.1 (CH_3, C-9).

H- 1-*O*-(β-D-2,3,4,6-tetra-*O*-benzylgalactopyranosyl)-nonanol (15) - microwave irradiation: methyl 2,3,4,6-tetra-*O*-benzyl-β-D-galactopyranoside (**7**) (107.4 mg, 0.19 mmol,), 1-nonanol (**8**) (82.6 mg, 0.57 mmol) and TMSOTf (36.1 μg, 0.19 mmol) in DCM were mixed in a closed vessel, previously argon saturated. The reaction mixture was irradiated for 8 min at 100 °C (30 W) in a CEM Discovery LabMate microwave reactor.

In the end, a ripartition in a separation funnel was carried out using a water solution of $NaHCO_3$ and CH_2Cl_2. The organic layers were pooled, treated with anhydrous sodium sulfate, filtered and concentrated under vacuum.

The crude reaction was HPLC-chromatographed using a normal-phase column (*n*-heaxne-AcOEt 8:2): the α and β anomers of 1-*O*-(D-2,3,4,6-tetra-*O*-benzylgalactopyranosyl)-nonanol (**15**) were obtained in the ratio 2:1 (yield 69%).

I. 18-*O*-(β-D-2,3,4,6-tetra-*O*-benzylgalactopyranosyl)-pentatriacontanol (16) - conventional heating: methyl 2,3,4,6-tetra-*O*-benzyl-β-D-galactopyranoside (**7**) (54 mg, 0.097 mmol,), pentatriacontan-18-ol (**13**) (147.8 mg, 0.291 mmol) and TMSOTf (17.6 μg, 0.097 mmol) in $CHCl_3$ were stirred at 60°C for 2 h under argon.

At the end of reaction, solution of $NaHCO_3$ was added and three extractions with CH_2Cl_2 were done in a separation funnel. The organic layers were pooled, treated with anhydrous sodium sulfate, filtered and concentrated under vacuum.

The crude reaction (290 mg) was HPLC-chromatographed using a normal-phase column (*n*-heaxne-AcOEt 9:1) and a fraction containing both α and β products was subjected to analytical HPLC (*n*-esano/AcOEt 97:3). 2.2 mg of 18-*O*-(β-D-2,3,4,6-tetra-*O*-benzylgalactopyranosyl)-pentatriacontanol and 2.4 mg 18-*O*-(α-D-2,3,4,6-tetra-*O*-benzylgalactopyranosyl)-pentatriacontanol were obtained (yield 4.6 %, α/β ratio 1:1).

For the other attempts carried out with Shimizu method, the reaction conditions above described were used but a system of distillation was introduced in order to remove MeOH. The reaction performed in toluene at 120-140 °C gave 1.4 % of 18-*O*-(β-D-2,3,4,6-tetra-*O*-benzylgalactopyranosyl)-pentatriacontanol and 1.9 % of 18-*O*-(α-D-2,3,4,6-tetra-*O*-benzylgalactopyranosyl)-pentatriacontanol. Instead the reaction done in $CHCl_3$ gave 1.0 % of 18-*O*-(β-D-2,3,4,6-tetra-*O*-benzylgalactopyranosyl)-pentatriacontanol and 1.3 % of 18-*O*-(α-D-2,3,4,6-tetra-*O*-benzylgalactopyranosyl)-pentatriacontanol.

^{1}H NMR (500 MHz $CDCl_3$): δ 7.34-7.24 (20 H, m, aromatic protons), 4.92-4.74 (2 H, d, *J* = 11.1 Hz, benzyl methylenes), 4.74-4.7 (2 H, d, *J* = 11.1 Hz, benzyl methylenes), 4.62-6.60 (2 H, d, *J* = 11.8 Hz, benzyl methylenes), 4.43-4.39 (2 H, d, *J* = 11.8 Hz, benzyl methylenes), 4.37 (1 H, dd, J=7.8 and 1.88 Hz, H-1″), 3.86 (1 H, br.s., H-4″), 3.76 (1 H, ddd, J=9.7, 7.8 and 1.88 Hz, H-2″), 3.6 (1 H, br.s., H-1), 3.56 (2 H, m, H-6″a and H-6″b), 3.5 (1 H, m, H-3″), 3.49 (1 H, m, H-5″), 1.57 (2 H, m, H-2′), 1.5 (2 H, m, H-2), 0.88-0.87 (6 H, t, 7.1, CH3); ^{13}C NMR (500 MHz $CDCl_3$): δ 103 (CH, C-1″), 82.5 (CH, C-3″), 80.1 (CH, C-1), 79.6 (CH, C-2″), 73.6 (CH, C-4″),

73.2 (CH, C-5″), 69.0 (CH_2, C-6″), 34.5 (CH_2, C-2′), 33.9 (CH_2, C-2), 14.1-10.9 (CH_3, C-17 and C-18′).

L. 18-*O*-(β-D-2,3,4,6-tetra-*O*-benzylgalactopyranosyl)-pentatriacontanol (16) - microwave irradiation: methyl 2,3,4,6-tetra-*O*-benzyl-β-D-galactopyranoside (**7**) (10.9 mg, 0.019 mmol), TMSOTf (3.4 μg, 0.019 mmol) and then pentatriacontan-18-ol (**13**) (29.3 mg, 0.057 mmol) were put in a closed vessel (2-5ml), saturated with argon, in 3.5 ml of $CHCl_3$. The reaction mixture was stirred and irradiated for 20 minutes, at 100 °C in a Biotage Initiator EXP 8 microwave reactor. A power of 400 W was necessary to reach the temperature of 100°C (Figure 7.8).

In the end of reaction, solution of $NaHCO_3$ was added and three extractions with CH_2Cl_2 were done in a separation funnel. The organic layers were pooled, treated with anhydrous $MgSO_4$, filtered and concentrated under vacuum. The crude reaction was HPLC-chromatographed using a normal-phase column (*n*-hexane-AcOEt 9:1) and a fraction containing both α and β products was subjected to analytical HPLC (*n*-hexane/AcOEt 97:3). 2 mg of α-anomer and 0.8 mg of β-anomer were obtained (yields 14 %).

The other attempts conducted with Shimizu Method were carried out using the same procedure described above, changing the temperature and time conditions as reported in the table 3S.

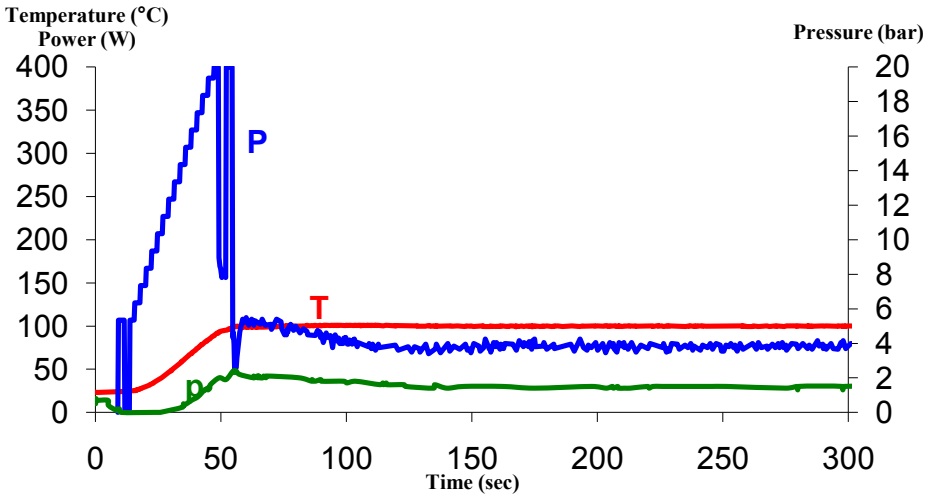

Figure 7.8: Power (P, blue), pressure (p, green) and temperature (T, red) trends during the reaction performed at 100°C for 20 min in Biotage Initiator EXP 8 microwave reactor

7.7 NMR data

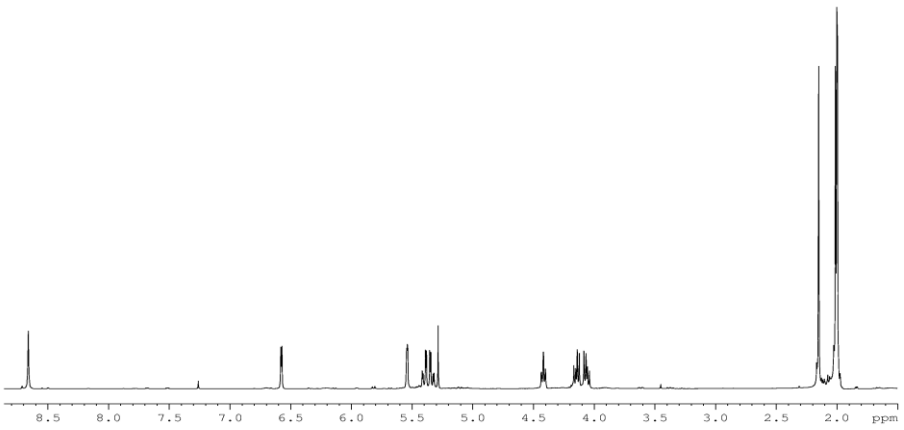

^{1}H NMR spectrum (400 MHz, $CDCl_3$) of compound **5**

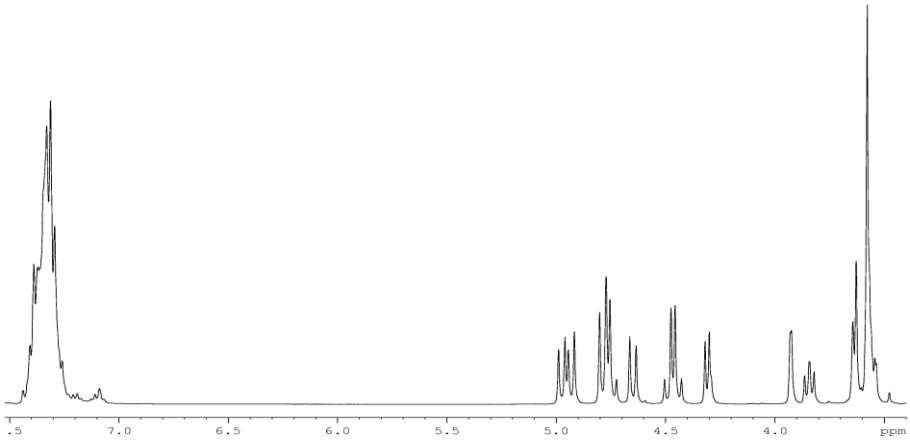

1H NMR spectrum (400 MHz, $CDCl_3$) of compound **7**

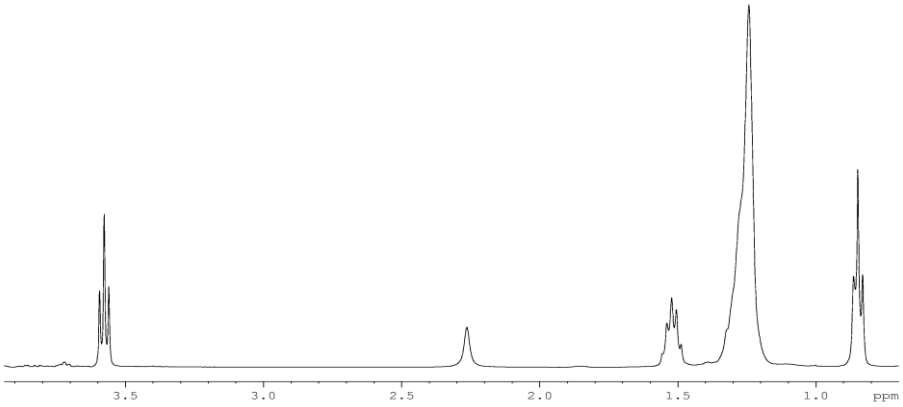

^{1}H NMR spectrum (400 MHz, $CDCl_3$) of compound **8**

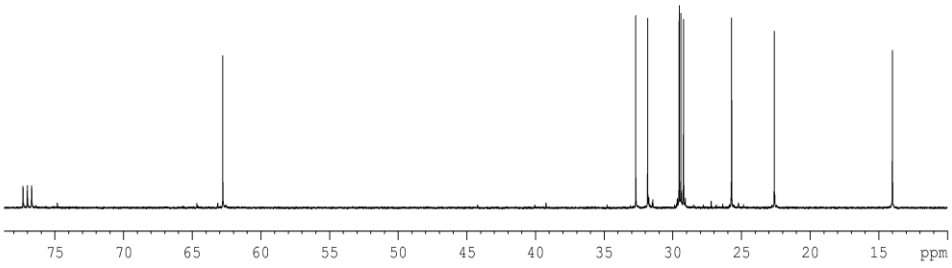

^{13}C NMR spectrum (175 MHz, $CDCl_3$) of compound **8**

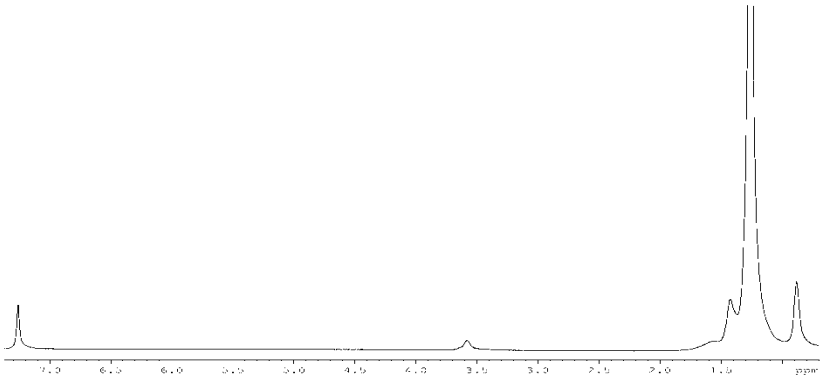

^{1}H NMR spectrum (400 MHz, $CDCl_3$) of compound **13**

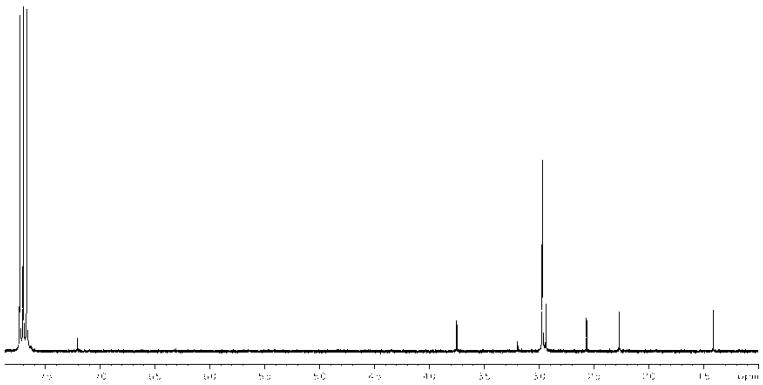

^{13}C NMR spectrum (175 MHz, $CDCl_3$) of compound **13**

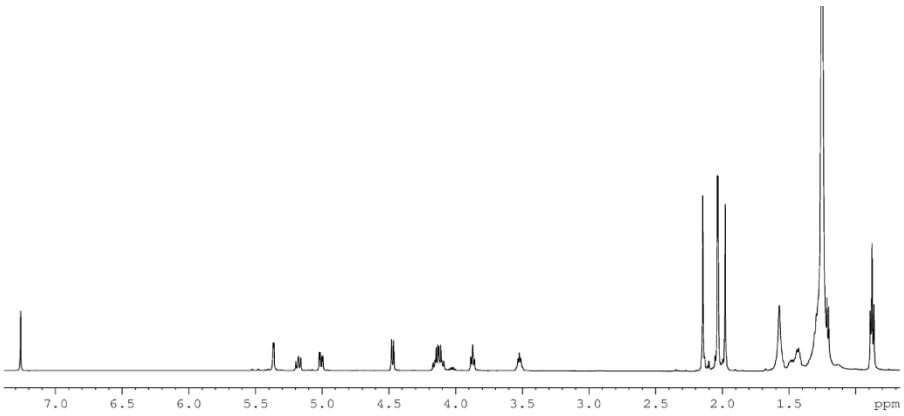

^{1}H NMR spectrum (400 MHz, $CDCl_3$) of compound **14** (β-anomer)

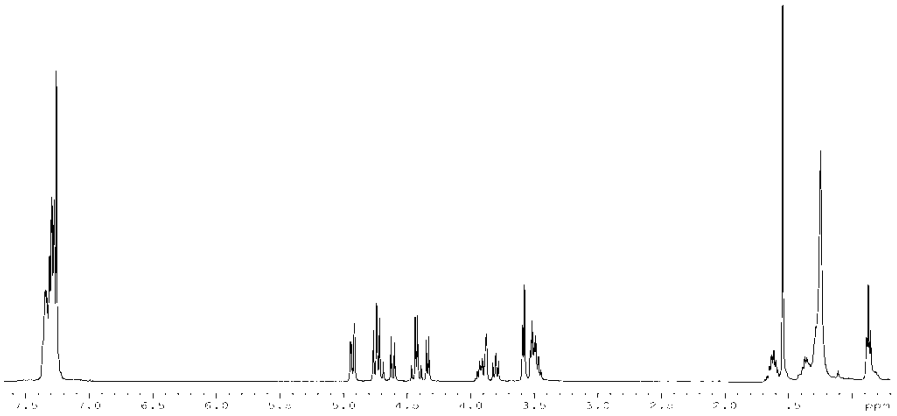

^{1}H NMR spectrum (400 MHz, $CDCl_3$) of compound **15**

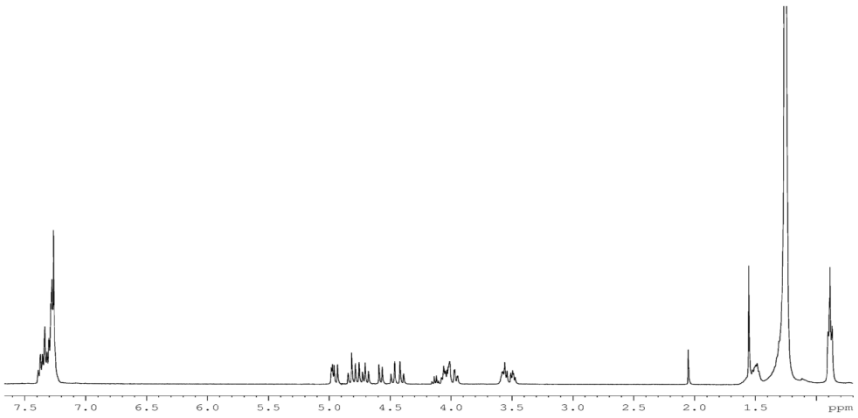

^{1}H NMR spectrum (500 MHz, $CDCl_3$) of compound **16** (α-anomer)

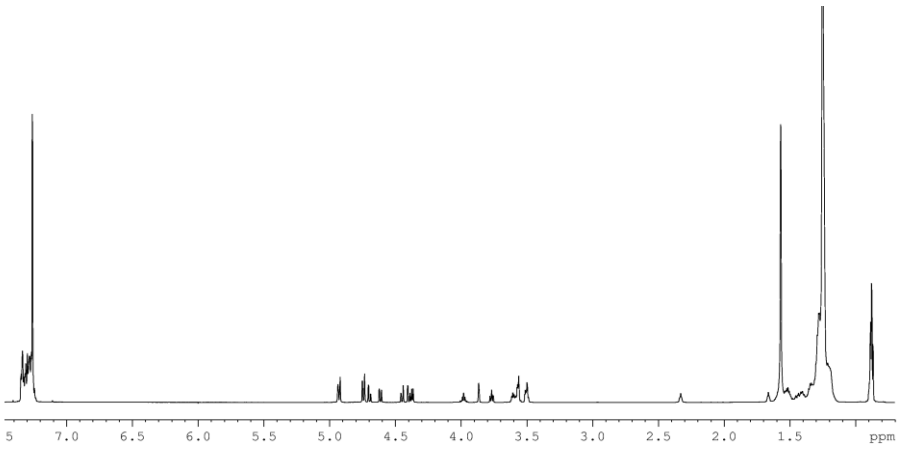

^{1}H NMR spectrum (500 MHz, $CDCl_3$) of compound **16** (β-anomer)

Scientific collaborations and contributions

The work of this thesis was possible thanks to the following collaborations and contributions:

- Dr. Fiorentina Roviezzo, Luana De Gruttola and Professor Giuseppe Cirino, Dipartimento di Farmacologia Sperimentale, Faculty of Pharmacy, University of Naples Federico II (Italy), for the evaluation of the anti-inflammatory activity of tedanol isolated from the sponge *Tedania ignis*.
- Dr. Elisa Panza and Professor Angela Ianaro, Dipartimento di Farmacologia Sperimentale, Faculty of Pharmacy, University of Naples Federico II (Italy), for the investigation of inhibitory effects on iNOS of tedarene A and B from *Tedania ignis*.
- Dr. Delphine Lamoral-Theys and Professor Robert Kiss, Laboratoire de Toxicologie and Laboratoire de Chimie Analytique Toxicologie et de Chimie Physique Appliquée, Institut de Pharmacie, Université Libre de Bruxelles (Belgium), for the evaluation of the anticancer activity of diterpene isonitriles isolated from the sponge *Pseudaxinella flava.*
- Professor Oliver C. Kappe, Organic and Bioorganic Chemistry, Institute of Chemistry, Karl-Franzens University of Graz, (Austria), for microwave assisted reactions performed during my training period at Christian Doppler Laboratory For Microwave Chemistry

(CDLMC), Institute of Chemistry, Karl-Franzens University of Graz, (Austria).

Acknowledgments

I would like to thank the following people, whose contribution in assorted ways to the research deserves special mention:

- Professor Alfonso Mangoni, for his advice and brilliant ideas which gave me valuable guidance throughout the work.
- Professor Valeria Costantino, for her constant contribution and involvement with enthusiasm in the projects carried out.
- Roberta Teta and Pina Chianese, for their support and the great time spent together.
- All my fellow workers at the Department of Chemistry of Natural Products: Gerardo Della Sala, Adriana Romano, Thomas Hochmut, Paolo Luciano, Concetta Imperatore, Rocco Vitalone, Fernando Scala, Masteria Yunovilsa Putra, Emma Dello Iacovo, Luciana Tartaglione, Laura Grauso, Valentina Sepe, Carmen Festa.
- All the Master Thesis students, in particular Fabiana Filace and Teresa Vitale, which became real friends.
- A special thank is due to my parents and my sister, who have always motivated me and share with me the challenges of the life.
- Last but not least, I want to thank Francesco: you are a special person who encourages and supports me with great patient. You always give me the strength to face challenges.

Sincerely,

Cristina Perinu